PURE THERMAL DIFFUSION

Thesis for the Degree of Ph. D.
MICHIGAN STATE UNIVERSITY
TERRY GRANT ANDERSON
1968

This is to certify that the

thesis entitled

PURE THERMAL DIFFUSION

presented by

TERRY GRANT ANDERSON

has been accepted towards fulfillment
of the requirements for

PH.D degree in Chemistry

Frederick H. Horne
Major professor

Date September 9, 1968

O-169

ABSTRACT

PURE THERMAL DIFFUSION

by Terry Grant Anderson

The time-dependent theory of pure thermal diffusion in binary fluid mixtures is obtained, and experiments on the carbon tetrachloride-cyclohexane system are reported. The theory takes full account of the temperature and composition dependences of the thermal diffusion factor, thermal conductivity, mutual diffusion coefficient, and density. The second order partial differential equations which describe simultaneous transport of heat and mass are solved approximately by means of series expansion methods in both time and space. Inclusion of the effects of time-dependent temperature and center of mass velocity gradients during the warming up period yields unambiguous identification of zero time. Inclusion of the variability of the coefficients makes it possible to evaluate the effects of the usual assumption of constant coefficients. A laser wavefront shearing interferometer is used for in situ measurements of refractive index gradients. Improved cell design and careful temperature control have eliminated the effects of convection, previously the chief source of difficulty in pure thermal diffusion experiments. Measurements made during both the approach to the steady state (demixing) and the diffusional decay from the steady state following removal of the temperature gradient(remixing) are analyzed with the help of computerized curve fitting programs. Ex-

periments at four different mean temperatures and over the entire composition range yield, with a precision of about 1%, $\alpha_1 = -1.83 + 0.18x_1 + 0.01(T - 25)$, $10^5 D = 1.29 + 0.19x_1 + 0.26(T - 25)$, where α_1 is the thermal diffusion factor, D is the mutual diffusion coefficient in $cm^2\ sec^{-1}$, x_1 is the mole fraction of CCl_4, and T is the temperature in degrees C. The thermal diffusion factors at 25° agree with the flow cell results of Turner, Butler, and Story (Trans. Faraday Soc. 63, 1906 (1967)), and the mutual diffusion coefficients at 25° and 35° agree well with the results of Kulkarni, Allen, and Lyons (J. Phys. Chem. 69, 2491 (1965)). The temperature dependence of these parameters has not previously been available. New results are also reported for the temperature dependence of the refractive index of the pure components. It now appears that pure thermal diffusion can be a reliable experimental method when adequately described and carefully executed.

PURE THERMAL DIFFUSION

By

Terry Grant Anderson

A THESIS

Submitted to
Michigan State University
in partial fulfillment of the requirements
for the degree of

DOCTOR OF PHILOSOPHY

Department of Chemistry

1968

To Janie

I am gr

ppreciation to

he completion o

Richard Menke of

who helped immea

and parts of the

Michigan State U

who constructed

Kirk, who wrote

was extremely us

I am gra

for the facilitie

to the Departmen

equipment and co

in the form of a

Science Foundatio

1314, purchased

for a Research As

I wish es

those computer pr

data handling and

ACKNOWLEDGMENTS

I am grateful for this opportunity to express my appreciation to those who played such important roles in the completion of this work: Mr. Russell Geyer and Mr. Richard Menke of the Chemistry Department Machine Shop, who helped immeasurably with the construction of the cell and parts of the interferometer; Mr. Frank Galbavi of the Michigan State University Glass Fabrication Laboratory, who constructed the glass sample chamber; and Mr. Dwayne Knirk, who wrote a computer program for data plotting which was extremely useful.

I am grateful also to: Michigan State University for the facilities provided and for a one-year fellowship; to the Department of Chemistry, which purchased permanent equipment and computer time and provided financial support in the form of a Teaching Assistantship; and to the National Science Foundation, which, through its grant number NSF GP 05254, purchased specialized equipment and provided funds for a Research Assistantship.

I wish especially to thank my colleague John Bartelt, whose computer programs MULTREG and MINIMIZE certainly eased data handling and yielded more information than would

otherwise have

hours of enligh

to both the the

work.

I can

to Dr. F. H. Ho

work so challen

hours of labor,

Finally

helped in innum

and whose under

available.

otherwise have been obtained, and with whom I enjoyed many hours of enlightening discussions which contributed greatly to both the theoretical and experimental aspects of this work.

I can only begin to convey my sincere appreciation to Dr. F. H. Horne for his participation, which made the work so challenging, and for his encouragement and countless hours of labor, which helped make it so rewarding.

Finally, I am deeply grateful to my wife JaneAnn, who helped in innumerable ways, who endured my difficult times, and whose understanding and encouragement were always available.

TABLE OF CONTENTS

Table

2a. Approxim
parameter
25° C, w

2b. Relative
the flux

T_m = 25°
steady s

2c. Levels o

5a. Lot anal
bottle 1

5b. Lot anal
bottle 1

5c. Sample w

5d. Densitie

5e. Pure comp

5f. Composit
index fo
at 20° C

5g. Ordinary
CCl_4 - C
et al., 1

5h. Thermal d
results f

5i. Measureme
B5, t = 7

5j. Fringe po

5k. Sample la
of a pure

6a. Summary o

6b. Experimen

LIST OF TABLES

Figure

3.1 Compos
z for
w_1^o (CC
dT/dz

3.2 Center
as a f
C_6H_{12},
differ
synthe

4.1 Water
Overal

4.2 Assembl
positi

4.3 Helium-

4.4 Path o
shearin

4.5 Interfe
and Pol

5.1 Plot of
(circle
order p

5.2 Plot of
z = 0 a
(circle
curve.
impropе

6.1 Experim
factor
functio
at 25°

LIST OF FIGURES

Figure

6.2 Experime
factor f
function
at 25° C
previous

6.3 Experime
factor a
at three

6.4 Experime
for CCl_4
applied
$x_1^o = 0.5$

6.5 Experime
coefficie
function

6.6 Experime
coefficie
function
comparis

6.7 Experime
coefficie
function
composit

Appendix

LIST OF APPENDICES

A. The Phenomen

Thermal
due to a temper
of studying the
arrangement. I
arate the compo
nary, or mutual

Thermog
takes use of th
stable convecti
taining a horiz
thod (Turner
through a horiz
gradient causes
the fluid, and a
the fluid into p
differences. In
two chambers equ
mixture to be st
tube or a membr

CHAPTER I

INTRODUCTION

e Phenomenon

Thermal diffusion is diffusion which takes place a temperature gradient. There are several methods dying the phenomenon, each with its own experimental ement. In all cases, thermal diffusion acts to sep- the components of a mixture and is opposed by ordi- or mutual, diffusion.

Thermogravitational thermal diffusion (Horne, 1962) se of the earth's gravitational field to set up convective fluid flow in a vertical apparatus con- a horizontal temperature gradient. The flow cell (Turner et al., 1967) utilizes forced laminar flow a horizontal channel. A vertical temperature t causes a partial separation of the components of id, and a horizontal knife edge is used to divide id into portions for measurement of composition nces. In a third method (Dicave and Emery, 1968), bers equipped with stirring devices contain the to be studied and are separated by a porous glass a membrane. When the chambers are maintained at

ferent temperatures, thermal diffusion takes place be-
en them, and a composition difference develops.

A fourth method, pure thermal diffusion, is con-
ually the simplest. Here, the fluid mixture is con-
ed between two horizontal flat metal plates attached
eservoirs for individual temperature control. When a
ical temperature difference is applied in such a way
the densest portion of the fluid is closest to the
er of the earth (i.e., when the fluid is heated from
except when its density increases with increasing
erature) thermal diffusion occurs. Thermal diffusive
ing continues, opposed by the remixing tendency of
ary diffusion, until a steady state is reached in
the two effects balance each other, and a steady
cal composition gradient is obtained.

Given the appropriate mathematical description of
ystem, one can calculate experimental values for the
al diffusion transport parameters by measuring the
p of the composition gradient, its steady state value,
decay to zero following removal of the temperature
ence in a remixing experiment (Gustafsson et al.,

Thermal diffusion has been studied for many years.
ew article by Grove (1959) lists over 900 references.
heless, the phenomenological theory of pure thermal

sion (Ludwig, 1856), or the Soret effect (Soret, 1879),
een inadequate in many cases.

ivation

Thermal diffusion has a wide range of applications.
thermal transport in living systems is certainly of
st to biologists. Some chemically indistinguishable
es and isomers can be separated efficiently by means
ined thermal diffusion techniques (Mulliken, 1922).
tical mechanicians interested in fundamental knowledge
liquid state require accurate experimental values of
rt parameters in order to judge the validity or range
r theories (see, for example, Bearman and Horne,

The most complete phenomenological theory of pure
diffusion previously available (Bierlein, 1955),
adequate in many cases, is limited in the follow-
. (1) Transport parameters are treated as constants,
, for instance, that the temperature gradient is
throughout the fluid. (2) The composition depen-
density, or the "forgotten effect" (de Groot et
), is neglected. (3) "Warming up effects" (Agar,
nsequences of the fact that the temperature
builds up in the fluid not instantaneously but
asurable period of time, are neglected. No allow-
de for the possibility of convective transfer
mass during the warming up period.

Our primary purpose here is to obtain a phenomeno-
al theory of pure thermal diffusion which is not sub-
to the above restrictions and which, hopefully, will
re the discrepancies which now exist in the literature
homaes, 1951; Horne, 1962; Turner et al., 1967;
ein, 1966) between the reported values of thermal
ion coefficients obtained from the different experi-
methods. In addition, we hope to explain the dif-
e reported (Dicave and Emery, 1968) between ordinary
ion coefficients measured during a nonisothermal
ng experiment and those measured during isothermal
ng after a steady state has been reached.

The second purpose of this work is to show that
rect application of an adequate phenomenological
of pure thermal diffusion to well designed experi-
an lead (for the first time) to reliable results
re thermal diffusion. Hopefully, this technique
be used for any number of systems to obtain un-
s results more easily than from the more complicated,
l understood methods.

Our third purpose, implied above, is to present
values of thermal diffusion parameters for the
trachloride-cyclohexane system as a function of
re and composition. By so doing, we shall demon-
e significance of our theory and provide the first
sive data for the temperature dependence of thermal
parameters.

lan of the Thesis

In the following treatment we make full use of the ions of hydrodynamics and nonequilibrium thermodynamics scribing the simultaneous transport of heat and mass in id system undergoing pure thermal diffusion. We solve esulting set of partial differential equations for the f a two component fluid by means of a series expansion which retains explicitly the temperature and composi- ependences of the thermal diffusion factor, ordinary ion coefficient, thermal conductivity, and density. o include time dependent boundary temperatures and the ility of convective transport.

The results of the theoretical section are used in ting values for the thermal diffusion factor and the y diffusion coefficient for mixtures of carbon tetra- e and cyclohexane over the entire range of initial tions. Both classical demixing and isothermal remix- eriments are described. A sensitive laser wavefront interferometer used to measure very small refrac- ex gradients in volatile liquids is also discussed. the results of our experiments with the CCl_4 - stem are presented together with a discussion of imental uncertainty and a comparison of our results ious results.

CHAPTER II

EQUATIONS OF TRANSPORT

troduction

In this chapter we present the differential equa- which describe macroscopic transport phenomena. alized equations for pure thermal diffusion and their priate initial and boundary conditions are then pre- d. We consider only continuous, isotropic, nonpolar- fluids in which no chemical reactions occur and are subject to no external forces other than the ational field. For a more detailed discussion of uations which follow see, for example, works by (1966), Kirkwood and Crawford (1952), de Groot and 1962), and Fitts (1962).

tions of Hydrodynamics

For a fluid containing ν components there are ν dent equations of continuity of mass:

$$(d\rho/dt) + \rho\nabla\cdot\underset{\sim}{u} = 0 , \tag{2.1}$$

$$\rho(dw_\alpha/dt) + \nabla\cdot\underset{\sim}{j}_\alpha = 0$$
$$\alpha = 1,\ldots,\nu - 1 , \tag{2.2}$$

e ρ is the local fluid density, t is time, $\underset{\sim}{u}$ is the
er of mass, or barycentric, velocity, and w_α and $\underset{\sim}{j}_\alpha$
respectively the mass fraction and diffusion flux of
onent α. The barycentric velocity $\underset{\sim}{u}$ is defined by

$$\underset{\sim}{u} = \sum_{\alpha=1}^{\nu} w_\alpha \underset{\sim}{u}_\alpha \ , \tag{2.3}$$

e $\underset{\sim}{u}_\alpha$ is the velocity of component α with respect to a
atory reference frame. The diffusion flux $\underset{\sim}{j}_\alpha$ is de-
l by

$$\underset{\sim}{j}_\alpha = \rho_\alpha(\underset{\sim}{u}_\alpha - \underset{\sim}{u}), \ \alpha = 1,\ldots,\nu \ , \tag{2.4}$$

$\rho_\alpha = w_\alpha \rho$. The diffusion fluxes are not all indepen-

$$\sum_{\alpha=1}^{\nu} \underset{\sim}{j}_\alpha = 0 \ . \tag{2.5}$$

antial time derivatives d/dt are related to local time
tives $\partial/\partial t$ by

$$d/dt = (\partial/\partial t) + \underset{\sim}{u}\cdot\nabla \ . \tag{2.6}$$

erator "del" is defined by

$$\nabla \equiv \underset{\sim}{i}\frac{\partial}{\partial x} + \underset{\sim}{j}\frac{\partial}{\partial y} + \underset{\sim}{k}\frac{\partial}{\partial z} \ , \tag{2.7}$$

, $\underset{\sim}{j}$, and $\underset{\sim}{k}$, are the unit vectors of a three dimen-
Cartesian coordinate system.

The equation of motion of the fluid is

$$\rho(d\underset{\sim}{u}/dt) - \nabla\cdot\underset{\approx}{\sigma} = \rho\underset{\sim}{g} \ , \tag{2.8}$$

is the gravitational field, and where $\underset{\approx}{\sigma}$ is the

s tensor, given approximately by the linear phenomeno-
al relation

$$\underset{\approx}{\sigma} = - \left[p + \left(\frac{2}{3} \eta - \varphi \right) \left(\nabla \cdot \underset{\sim}{u} \right) \right] \underset{\approx}{1} + 2\eta \ \text{sym} \ \nabla \underset{\sim}{u} \ . \qquad (2.9)$$

(2.9) p is the pressure, sym $\nabla \underset{\sim}{u}$ is the symmetric
f the tensor $\nabla \underset{\sim}{u}$, and η and φ are the coefficients
ar viscosity and bulk viscosity, respectively. Com-
on of Eqs. (2.8) and (2.9) yields the Navier-Stokes
on:

$$t) + \nabla \left[\left(\frac{2}{3} \eta - \varphi \right) \left(\nabla \cdot \underset{\sim}{u} \right) \right] - 2\nabla \cdot \eta \ \text{sym} \ \nabla \underset{\sim}{u} = \rho \underset{\sim}{g} - \nabla p \ . \qquad (2.10)$$

The general equation of continuity of total energy

$$(\partial \rho \overline{E}_T / \partial t) + \nabla \cdot \underset{\sim}{J}_{E_T} = 0 \ , \qquad (2.11)$$

E_T is the total flux of total energy, and where the
nergy $\overline{E}_T$ is the sum of the internal energy $\overline{E}$ and the
inetic energy of the center of mass:

$$\overline{E}_T = \overline{U} + W_1 + \sum_{\alpha=1}^{\nu} \frac{1}{2} w_\alpha u_\alpha^2 \ . \qquad (2.12)$$

(2.12) we have further separated $\overline{E}$ into a thermal
nd an external potential part, where W_1 is defined

$$\underset{\sim}{g} = - \nabla W_1 \qquad (2.13)$$

lso that

$$u_\alpha^2 = \underset{\sim}{u}_\alpha \cdot \underset{\sim}{u}_\alpha \quad . \tag{2.14}$$

The equation of energy transport can be expressed,
he negligible terms or order j_α^2 are ignored, as

$$\rho(d\overline{E}/dt) + \nabla \cdot \underset{\sim}{j}_E = \underset{\approx}{\sigma} : \nabla \underset{\sim}{u} - \rho \underset{\sim}{u} \cdot \underset{\sim}{g} \ , \tag{2.15}$$

$_E$ is the internal energy flux not due to bulk flow:

$$\underset{\sim}{j}_E \equiv \underset{\sim}{J}_E - \rho \underset{\sim}{u} \overline{E} + \underset{\sim}{u} \cdot \underset{\approx}{\sigma} \ . \tag{2.16}$$

tions of Nonequilibrium
modynamics

We can recast the equations of the preceding section
re convenient form by making use of some of the re-
f nonequilibrium thermodynamics. In order to use
such as temperature and entropy which are defined
namically only for equilibrium states, i.e., for
simultaneously in mechanical equilibrium, thermal
ium, and chemical equilibrium (see Bartelt, 1968),
cessary to postulate their existence in systems not
ibrium. That postulate is (Fitts, 1962):

Postulate 1

For a system in which irreversible processes
taking place, all thermodynamic functions of
exist for each macroscopic volume element
e system. These thermodynamic quantities
he nonequilibrium system are the same func-
of the local state variables as the corres-
ng equilibrium thermodynamic quantities.

Unfortunately, the historical and universal name of postulate is "the Postulate of Local Equilibrium." In , local equilibrium is not postulated. Instead, we are ulating that it is permissible to use the properties relationships defined in equilibrium thermodynamics rmostatics). An alternative approach is to construct nitio a nonequilibrium thermodynamic theory in which opy, temperature, etc. are defined in context. This ach has been developed by the practitioners of con- m mechanics (Truesdell and Toupin, 1960; Coleman and 1963; and Müller, 1968), and its relationship to the tional postulatory extension of thermostatics is cur- y under investigation (Bartelt). It appears that the operational equations result from both approaches, fferences between the approaches are therefore of sequence for our present work. For simplicity of tion, we adopt the traditional postulatory approach. tulate 1, we may use the Gibbs equation for $d\overline{E}$

$$d\overline{E} = Td\overline{S} - pd\overline{V} + \sum_{\alpha=1}^{\nu} \mu_\alpha dw_\alpha + dW_1 \ , \qquad (2.17)$$

e Gibbs-Duhem equation,

$$\overline{S}\nabla T - \overline{V}\nabla p + \sum_{\alpha=1}^{\nu} w_\alpha \nabla \mu_\alpha + \underset{\sim}{g} = 0 \ , \qquad (2.18)$$

' is the temperature, p is the pressure, $\overline{E}$, $\overline{S}$, and respectively, the specific energy, specific entropy,

e specific volume, and μ_α is the chemical potential,
s units, of component α. Each of the total specific
dynamic functions is a weighted sum of the partial
ic functions; for example,

$$\overline{E} = \sum_{\alpha=1}^{\nu} w_\alpha \overline{E}_\alpha \ , \tag{2.19}$$

$$\overline{E}_\alpha = (\partial \overline{E}/\partial w_\alpha)_{\overline{S},\overline{V},W_1,w_{\beta\neq\alpha}} \ . \tag{2.20}$$

Application of the chain rule for differentiation
$p,w_\alpha,W_1)$ yields

$$/dt) = (\overline{c}_p - pV\ )(dT/dt) - (TV\beta - pV\beta')(dp/dt)$$

$$+ \sum_{\alpha=1}^{\nu-1} (\overline{E}_\alpha - \overline{E}_\nu)(dw_\alpha/dt) - \underset{\sim}{u}\cdot\underset{\sim}{g} \ , \tag{2.21}$$

is the specific heat capacity at constant pressure
tant external fields, β is thermal expansivity,

$$\beta \equiv \overline{V}^{-1}(\partial \overline{V}/\partial T)_{p,w_\alpha,W_1} \ , \tag{2.22}$$

othermal compressibility,

$$\beta' \equiv -\overline{V}^{-1}(\partial \overline{V}/\partial p)_{T,w_\alpha,W_1} \ , \tag{2.23}$$

partial specific internal energy. Application
ain rule for differentiation to the equation of
$\rho(T,p,w_\alpha)$ gives a similar relation,

$$\rho\beta \frac{dT}{dt} + \rho\beta' \frac{dp}{dt} - \rho^2 \sum_{\alpha=1}^{\nu-1} (\overline{V}_\alpha - \overline{V}_\nu) \frac{dw_\alpha}{dt} \ . \tag{2.24}$$

ergy transport equation (2.15) can be restated by
tuting Eqs. (2.1), (2.2), (2.20), and (2.24) into
.15):

$$\frac{dT}{dt} - T\beta \frac{dp}{dt} = \phi_1 - \nabla\cdot\underset{\sim}{q} - \sum_{\alpha=1}^{\nu-1} \underset{\sim}{j}_\alpha\cdot\nabla(\bar{H}_\alpha - \bar{H}_\nu) \ , \qquad (2.25)$$

ϕ_1 is the entropy source term for bulk flow,

$$\phi_1 \equiv (\underset{\approx}{\sigma} + p\underset{\approx}{1}):\nabla\underset{\sim}{u} \ , \qquad (2.26)$$

he heat flux,

$$\underset{\sim}{q} \equiv \underset{\sim}{j}_E - \sum_{\alpha=1}^{\nu} \underset{\sim}{j}_\alpha\bar{H}_\alpha \ , \qquad (2.27)$$

is partial specific enthalpy.

One observes empirically that for nonisothermal
the heat flux is proportional to the temperature
t (Fourier's Law). Similarly, in an isothermal
the diffusion flux is proportional to the composi-
adient (Fick's Law). The generalization of these
ions, as well as an extension to include cross
a such as thermal diffusion, is expressed by the
ostulate of nonequilibrium thermodynamics, that of
henomenological equations (Fitts, 1962):

Postulate 2

"The fluxes $\underset{\sim}{J}_\alpha$ are linear, homogeneous functions of
es $\underset{\sim}{Y}_\alpha$. That is,

$$\underset{\sim}{J}_\alpha = \sum_{\beta=1}^{\nu} L_{\alpha\beta}\underset{\sim}{Y}_\beta \ ." \qquad (2.28)$$

rces are "driving forces" for the fluxes; for example,
the driving force for the heat flux in a single com-
fluid. The phenomenological coefficients $L_{\alpha\beta}$ are
ndent of the forces. The diagonal coefficients $L_{\alpha\alpha}$
conjugate fluxes and forces, while the off-diagonal
ts $L_{\alpha\beta}(\alpha \neq \beta)$ give rise to cross phenomena. Although
oice of fluxes and forces is to some extent arbitrary,
guidelines are provided by the Second Law and by
ial order (de Groot, 1962; Fitts, 1962; Bartelt,
We shall use the set most convenient for our pur-
We have already used Postulate 2 in writing Eq.
Postulate 2 is demonstrably invalid for many ex-
ntal situations, notably those in which chemical
ons are occurring and those in which viscous dissi-
is significant. It seems to be quite satisfactory,
:, for situations in which only heat and matter fluxes
portant, such as thermal diffusion. The range of
y of Postulate 2 is delineated in the continuum
cs approach mentioned earlier.

As forces conjugate to the fluxes of heat and matter,
se $\nabla \ell n\ T$ and $\nabla_T(\mu_\beta - \mu_\nu)$, $\beta = 1,\ldots, \nu - 1$, where

$$\nabla_T \mu_\beta \equiv \nabla\mu_\beta + \bar{S}_\beta \nabla T, \quad \beta = 1,\ldots,\nu \ . \tag{2.29}$$

ılate 2,

$$-\underset{\sim}{q} = \Omega_{00}\nabla \ell n\ T + \sum_{\beta=1}^{\nu-1} \Omega_{0\beta}\nabla_T(\mu_\beta - \mu_\nu) \tag{2.30}$$

$$= \Omega_{\alpha 0} \nabla \ell n\ T + \sum_{\beta=1}^{\nu-1} \Omega_{\alpha\beta} \nabla_T (\mu_\beta - \mu_\nu) \quad \alpha = 1,\ldots,\nu - 1 \ , \tag{2.31}$$

the Ω's are the phenomenological coefficients.

As a consequence of Eq. (2.5) we have

$$\sum_{\alpha=1}^{\nu} \Omega_{\alpha\beta} = 0 \ , \ \beta = 0,1,\ldots,\nu \ . \tag{2.32}$$

due to the requirement of positive definite entropy
ction (see Appendix A) we have

$$\sum_{\alpha=1}^{\nu} \Omega_{\alpha\beta} = 0 \ , \ \alpha = 0,1,\ldots,\nu \ . \tag{2.33}$$

An expression for the gradient of the chemical
tial, which appears in Eqs. (2.30) and (2.31) can be
ned from thermostatics and the chain rule for
entiation:

$$\nabla \mu_\beta = - \overline{S}_\beta \nabla T + \overline{V}_\beta \nabla p + \sum_{\alpha=1}^{\nu-1} \mu_{\beta\alpha} \nabla w_\alpha - \underset{\sim}{g} \ , \tag{2.34}$$

$$\mu_{\beta\alpha} \equiv (\partial \mu_\beta / \partial w_\alpha)_{T,p,\underset{\sim}{g},w_{\beta\neq\alpha}} \ . \tag{2.35}$$

ation of Eqs. (2.29) - (2.34) gives the following
sion for the fluxes:

$$\Omega_{\alpha 0} \nabla \ell n\ T + \sum_{\beta=1}^{\nu-1} \Omega_{\alpha\beta} (\overline{V}_\beta - \overline{V}_\nu) \nabla p + \sum_{\beta=1}^{\nu-1} \sum_{\beta=1}^{\nu-1} \Omega_{\alpha\beta} (\mu_{\beta\alpha}$$

$- \mu_{\beta\nu}) \nabla w_\gamma \ , \ \alpha = 0,1,\ldots,\nu - 1 \ , \text{ where } \underset{\sim}{j}_0 \equiv \underset{\sim}{q} \ .$

(2.36)

The equations for the fluxes can be written in the ving compact notation:

$$- \underset{\sim}{j}_\alpha = \sum_{\gamma=0}^{\nu+1} D_{\alpha\gamma} \underset{\sim}{F}_\gamma \ , \ \alpha = 0,1,\ldots,\nu - 1 \ , \qquad (2.37)$$

$$D_{\alpha 0} = \Omega_{\alpha 0}$$

$$D_{\alpha\gamma} = \sum_{\beta=1}^{\nu-1} \Omega_{\alpha\beta}(\mu_{\beta\gamma} - \mu_{\nu\gamma}) \ , \ \gamma = 1,\ldots,\nu - 1$$

$$D_{\alpha\nu} = \sum_{\beta=1}^{\nu} \Omega_{\alpha\beta}\overline{\nabla}_\beta$$

$$,\nu+1 = - \sum_{\beta=1}^{\nu} \Omega_{\alpha\beta} = 0$$

$$\underset{\sim}{F}_0 = \nabla \ \ell n \ T$$

$$\underset{\sim}{F}_\gamma = \nabla w_\gamma \ , \ \gamma = 1,\ldots,\nu - 1$$

$$\underset{\sim}{F}_\nu = \nabla p$$

$$\underset{\sim}{F}_{\nu+1} = - \nabla w_1$$

We make the following associations with traditional ental transport parameters:

D_{00} is related to thermal conductivity;

$D_{\alpha 0}$, $\alpha = 1,\ldots,\nu - 1$, are related to thermal diffusion coefficients;

$D_{\alpha\gamma}$, $\alpha = 1,\ldots,\nu - 1$, are related to mutual diffusion coefficients;

4) $D_{0\gamma}$, $\alpha = 1,\ldots,\nu - 1$, are related to Dufour coefficients;

5) $D_{\alpha\nu}$, $\alpha = 0,\ldots,\nu - 1$, are related to sedimentation;

) $D_{\alpha,\nu+1} = 0$, $\alpha = 0,1,\ldots,\nu - 1$.

We now have a complete set of $4(\nu + 1)$ transport ons: (2.1), (2.2), (2.10), (2.25), and (2.37). The ons can be solved for the $4(\nu + 1)$ quantities: ature, pressure, $\nu - 1$ compositions, three components center of mass velocity, and the three components of the ν mass fluxes. At this point our description system is complete and valid for any number of com-. Before proceeding to the solutions, however, we restrict our consideration to binary fluid mixtures , whence Eqs. (2.1), (2.2), (2.10), (2.25), and become:

$$(d\rho/dt) + \rho\nabla\cdot\underset{\sim}{u} = 0$$

$$\rho(dw_1/dt) + \nabla\cdot\underset{\sim}{j}_i = 0$$

$$\rho(d\underset{\sim}{u}/dt) - \nabla\cdot\underset{\approx}{\sigma} = \rho\underset{\sim}{g}$$

$$\rho\bar{c}_p \frac{dT}{dt} - T\beta \frac{dp}{dt} = \phi_1 - \nabla\cdot\underset{\sim}{j}_0 - \underset{\sim}{j}_1\cdot\nabla(\bar{H}_1 - \bar{H}_2)$$

$$-\underset{\sim}{j}_\alpha = \sum_{\gamma=0}^{3} D_{\alpha\gamma}\underset{\sim}{F}_\gamma \ , \ \alpha = 0,1 \ , \qquad (2.39)$$

$$D_{\alpha 0} = \Omega_{\alpha 0}$$

$$D_{\alpha 1} = \Omega_{\alpha 1}\mu_{11}/w_2$$

$$D_{\alpha 2} = \Omega_{\alpha 1}(\overline{V}_1 - \overline{V}_2)$$

$$D_{\alpha 3} = 0$$

$$\underset{\sim}{F}_0 = \nabla \ell n\ T$$

$$\underset{\sim}{F}_1 = \nabla w_1$$

$$\underset{\sim}{F}_2 = \nabla p$$

$$\underset{\sim}{F}_3 = -\nabla W_1 \ . \qquad (2.40)$$

erimental Transport Parameters

When the only external force is gravitational, a librium system containing ν components may undergo) types of transport processes in addition to vis- enomena. For a binary system, the six types are ee contributions to the heat flux $\underset{\sim}{j}_0$ and the three utions to the mass flux $\underset{\sim}{j}_1$ resulting from the gra- of temperature, composition, and pressure.

We make the following associations between the ological coefficients and the traditional experi- ransport parameters D, α_1, Q_1^*, κ_i, and s_1 which pectively, the mutual diffusion coefficient, the diffusion factor of component 1, the heat of trans- component 1, the initial thermal conductivity of ure (when $\partial w_1/\partial z = 0$), and the sedimentation co- of component 1:

$$D_{00} = \Omega_{00} = T\kappa_i$$

$$D_{01} = \Omega_{01}\mu_{11}/w_2 = \rho D Q_1^*$$

$$D_{10} = \Omega_{10} = -\rho D \alpha_1 w_1 w_2$$

$$D_{11} = \Omega_{11}\mu_{11}/w_2 = \rho D$$

$$\Omega_{11} = \rho D s_1 \ . \qquad (2.41)$$

onsequence of Eqs. (2.32) and (2.33), the six pheno-
an be expressed in terms of four independent coef-
ts.

The experimental mutual diffusion coefficient D is
d by Fick's law for isothermal, isobaric mutual dif-
in the absence of external fields,

$$-\underset{\sim}{j}_1^V = D\nabla c_1 \qquad (2.42)$$

$\underset{\sim}{j}_1^V$ is the diffusion flux relative to the velocity of
nter of volume, and c_1 is the concentration of com-
l expressed in units of moles per cubic centimeter.
ivalent form of Fick's law in terms of mass fraction
nter of mass velocity is

$$-\underset{\sim}{j}_1 = \rho D \nabla w_1 \ . \qquad (2.43)$$

The thermal diffusion factor α_1 is defined by con-
g the steady state of a pure thermal diffusion ex-
t in the absence of pressure gradients and external

$$-\underset{\sim}{j}_1 = 0 = \nabla w_1 - \alpha_1 w_1 w_2 \nabla \ln T \ . \qquad (2.44)$$

ommon thermal diffusion parameters may be expressed
the relations

$$\alpha_1 = - TD_{T,1}/D \ , \tag{2.45}$$

$$\alpha_1 = - T\sigma_1 \ , \tag{2.46}$$

$_{T,1}$ is the thermal diffusion coefficient of component
σ_1 is the Soret coefficient of that component (Soret,
It follows from Eq. (2.5) and the independence of
ces that $\sigma_2 = - \alpha_1$. The composition gradient of
nt 1 has the same sign as the temperature if α_1 is
e.

Alternative expressions for the diffusion flux can
ten by using the relations (2.45) and (2.46):

$$= \rho D\nabla w_1 + \rho D_{T,1} w_1 w_2 \nabla T + \rho D Q_1^* (\bar{V}_1 - \bar{V}_2) w_2 \mu_{11}^{-1} \nabla p \tag{2.47}$$

$$= \rho D[\nabla w_1 + \sigma_1 w_1 w_2 \nabla T + Q_1^* (\bar{V}_1 - \bar{V}_2) w_2 \mu_{11}^{-1} \nabla p] \tag{2.48}$$

(2.47) emphasizes the existence of the two phenomena
sion and thermal diffusion, while Eq. (2.48) con-
y allows removal of a common factor from the three

For an isothermal binary system the heat of trans-
is defined by

$$\underline{q} = Q_1^* \underline{j}_1 \ . \tag{2.49}$$

's from Eqs. (2.38) and (2.41) that

$$D_{01} = \rho D Q_1^* \quad . \tag{2.50}$$

phenomenon which involves a heat flux due to a composi-
gradient in an isothermal system in the absence of
rnal fields is the Dufour effect (Dufour, 1873), which
be considered the inverse of thermal diffusion. For
ids the heat of transport Q_1^* is very small, and reports
easurements are still subject to question (Rastogi and
n, 1965). We discuss the magnitude of Q_1^* as well as
rical values of the other transport parameters later in
chapter.

The thermal conductivity coefficient κ_i, measured
he beginning of a pure thermal diffusion experiment
re the composition gradient develops is given by Fourier's
of heat conduction,

$$-\underset{\sim}{q} = \kappa_i \nabla T \quad . \tag{2.51}$$

attempt to measure the thermal conductivity of a mixture
pplying a temperature difference necessarily results in
development of a composition gradient (unless $\alpha_1 = 0$),
here is consequently an additional contribution to the
flux due to the heat of transport. Thus the effective
al conductivity is the sum of two parts, one of which
ds on κ_i and ∇T and the other on Q_1^* and ∇w_1. At the
y state of a pure thermal diffusion experiment in the
ce of external fields we have

$$\nabla w_1 = \alpha_1 T^{-1} w_1 w_2 \nabla T \quad . \tag{2.44}$$

llows that at the steady state

$$- \underset{\sim}{q} = \kappa_f \nabla T \ , \tag{2.52}$$

$$\kappa_f = \kappa_i + \rho D Q_1^* \alpha_1 w_1 w_2 / T \ . \tag{2.53}$$

could measure the difference between the thermal
ctivity of the mixture initially and that at the
y state, we could calculate Q_1^* directly. That dif-
ce, however, appears to be smaller than the experi-
l uncertainties which arise while attempting to
re it with present equipment (see Table 2a).

The sedimentation coefficient s_1 is defined by
dering the steady state of an isothermal experiment
ch the gravitational field is the only external

$$- \underset{\sim}{j}_1 = 0 = \nabla w_1 + s_1 (\overline{V}_1 - \overline{V}_2) \nabla p \ , \tag{2.54}$$

$$s_1 = w_2 / \mu_{11} \ . \tag{2.55}$$

The fluxes in Eq. (2.39) may now be rewritten en-
in terms of experimental transport parameters:

$$- \underset{\sim}{q} = \kappa_i \nabla T + \rho D Q_1^* \nabla w_1 + \rho D Q_1^* s_1 (\overline{V}_1 - \overline{V}_2) \nabla p$$

$$_1 = - \rho D x_1 w_1 w_2 T^{-1} \nabla T + \rho D \nabla w_1 + \rho D s_1 (\overline{V}_1 - \overline{V}_2) \nabla p \ . \tag{2.56}$$

Before proceeding to a solution to the equations of
nsport, we examine the relative magnitudes of the pheno-
a occurring simultaneously inside an experimental cell.
Table 2a are presented estimates or typical values of
eral important parameters for the system CCl_4 - C_6H_{12} at
C when $w_1 = w_2 = 0.5$. In calculating a value for s_1 we
e used the relation for the specific chemical potential:

$$\mu_1(T,p,x,) = \mu_1^*(T,p) + \frac{RT}{M_1} \ell n \ (f_1 x_1) \ , \qquad (2.57)$$

re f_1 is the activity coefficient of component 1 and
$_1p)$ is the chemical potential of component 1 in the
ndard state defined by

$$\mu_1^* = \lim_{x_1 \to 1} \mu_1 \ . \qquad (2.58)$$

rder to obtain an approximate value for s_1 we take
1. In the earth's gravitational field, the steady
e composition gradient which would develop due to
mentation is:

$$\frac{\partial w_1}{\partial z} = - \ 0.8 \times 10^{-6} \ cm^{-1} \ .$$

The relative contributions of the gradients of
erature, pressure, and composition can be estimated by
Eqs. (2.57) and inserting reasonable values for all
ie quantities which appear. Consider the steady state
pure thermal diffusion experiment for CCl_4 - C_6H_{12},
$T_m = 25°C$ and $w_1^o = 0.5$. If we use the numerical

e 2a.--Approximate values of transport parameters for CCl_4 - C_6H_{12} at 25°C, $w_1 = 0.5$.

tity	Reference	Value
	a	1.4×10^{-5} cm^2 sec^{-1}
	b	4×10^{-8} cm^2 sec^{-1} deg^{-1}
	b	6×10^{-3} deg^{-1}
	b	-1.7
	c	2.4×10^{-4} cal cm^{-1} sec^{-1} deg^{-1}
κ_i	c	5×10^{-8} cal cm^{-1} sec^{-1} deg^{-1}
	c	6. cal g^{-1}
	Eq. (2.55)	-3.2×10^{-6} cm^{-1}
	d	1.1 g cm^{-3}
$\bar{v}_2$	d	-0.66 cm^3 g^{-1}
	e	0.2 cal deg^{-1} g^{-1}

[a]Kulkarni, et al., 1965.

[b]Turner, et al., 1967; Beyerlein, (in press).

[c]Horne, 1967.

[d]Wood and Gray, 1952.

[e]Hodgman, 1962.

lues in Table 2a and specify a temperature gradient of 5 g cm^{-1}, then the six terms of interest have the values ven in Table 2b, where we have also used

$$\nabla p = - \rho \underset{\sim}{g} , \tag{2.59}$$

ch follows from Eq. (2.8) at the steady state and tially. Since sedimentation effects are observable ther initially nor in the steady state, and since there no reason to expect observable departure from Eq. (2.59) any time, we henceforth neglect pressure effects. (See le 2b.)

le 2b.--Relative contributions of forces to the fluxes; CCl_4 - C_6H_{12}, $w_1^o = 0.5$, $T_m = 25°C$, $\frac{dT}{dz} = 5$ deg cm^{-1}, steady state.

	Temperature	Composition	Pressure	Units
	1×10^{-3}	7×10^{-9}	8×10^{-11}	$\frac{cal}{cm^2\ sec}$
z	$+1.2 \times 10^{-7}$	-1.2×10^{-7}	1×10^{-10}	$\frac{g}{cm^2\ sec}$

ther experimental situations, such as thermal diffusion centrifuge or in a flow cell apparatus, the influence e pressure gradient must be re-examined.

Since we have no practical interest in the pressure, riginal $4(\nu + 1)$ independent equations have been

ed to eleven. Furthermore, by inserting the expres-
(2.57) for the fluxes into the three continuity
ons (2.1), (2.2), and (2.25) we effectively reduce
mber of dependent variables to five: temperature,
ition, and the three components of the center of mass
ty. In order to solve the set of differential equa-
we must specify an initial condition and two boundary
ions for each of the five unknowns.

ndary Conditions for Pure
rmal Diffusion

Pure thermal diffusion requires that a vertical
ture gradient be maintained across a layer of fluid
s not undergoing any type of forced motion. More-
he sign of the temperature gradient must be such
e denser portion of the fluid is closer to the cen-
the earth than the less dense portion. For ordinary
this just means that the top must be warmer than the
There are exceptions, however. For example, water
s freezing point would be studied with the top cooler
e bottom.

If the temperature gradient is purely vertical and
nly external force is the gravitational field, there
o non-vertical components of any of the forces, and
ntly the fluxes have no horizontal components. Al-
t is plausible that the center of mass velocity also

horizontal components, the existence of vertical gra-
of temperature, composition and pressure is not suffi-
to prove that $u_x = u_y = 0$. Instead, we have at best
vertical density gradient gives (see Eq. (2.1))

$$\frac{1}{\rho}\frac{\partial \rho}{\partial t} + \frac{\partial u_x}{\partial x} + \frac{\partial u_y}{\partial y} = -\frac{1}{\rho}\frac{\partial \rho u_z}{\partial z}\,, \qquad (2.60)$$

hich the steady state relation follows:

$$\nabla \cdot \underset{\sim}{u} = -u_z \frac{\partial\, \ell n\, \rho}{\partial z}\,. \qquad (2.61)$$

s point we make the additional assumption that all
is vertical and that $u_x = u_y = 0$. The possibility
zontal components of $\underset{\sim}{u}$ has been considered by Bartelt
but is beyond the scope of this work.

We denote by "ideal" the boundary conditions which
in a purely one dimensional system. The possibility
zontal components of the fluxes or forces arises
sofar as the actual experimental boundary conditions
ideal. Since it is possible to eliminate effectively
sence of spurious thermal gradients by proper cell
and temperature control, we confine our interest to
undergoing vertical motion only.

The three quantities which remain as unknowns are
erature, the composition, and the vertical component
ocal center of mass velocity, each of which is a
of vertical position and time. We choose the three

ations describing the interrelations between the three
ctions to be the equations of continuity of mass (2.1),
fraction (2.2), and energy (2.25). In one dimension,
equations remaining are:

$$(d\rho/dt) + \rho(\partial u_z/\partial z) = 0 \qquad (2.62)$$

$$\rho(dw_1/dt) + (\partial j_{1z}/\partial z) = 0 \qquad (2.63)$$

$$\rho\bar{c}_p \frac{dT}{dt} = \phi_1 - \left(\frac{\partial q_z}{\partial z}\right) = j_{1z} \frac{\partial}{\partial z} (\bar{H}_1 - \bar{H}_2) \ , \qquad (2.64)$$

$$- j_{iz} = \rho D \left(\frac{\partial w_1}{\partial z} - \frac{\alpha_1}{T} w_1 w_2 \frac{\partial T}{\partial z}\right) , \qquad (2.65)$$

$$- q_z = \kappa_i \frac{\partial T}{\partial z} + \rho D Q_1^* \frac{\partial w_1}{\partial z} \ . \qquad (2.66)$$

The domain of the independent variables t and z is
emi-infinite strip defined by

$$- \frac{a}{2} \leq z \leq \frac{a}{2} \ ; \ t \geq 0 \ , \qquad (2.67)$$

a is the cell height. The earth's radius vector points
e direction of increasing z. The choice of the center
e call for z = 0 follows from the odd spatial symmetry
which the temperature and composition profiles develop.
since we use Taylor series expansions in z about the
of the cell, it is convenient to choose that point to
e origin.

Although it is possible to begin a pure thermal dif-
on experiment with an arbitrary set of initial conditions,
acilitate comparison with experiment, we choose the ini-
state (t = 0) to be an equilibrium one in which the
rature and composition of the fluid are uniform and the
r of mass velocity is zero. Thus we have:

$$T(z,0) = T_m$$

$$w_1(z,0) = w_1^o$$

$$u_z(z,0) = 0 \; ; \; -\frac{a}{2} < z < \frac{a}{2} \; , \qquad (2.68)$$

T_m is any chosen temperature, and w_1^o is the chosen
ing composition.

The temperatures maintained at the upper and lower
plates constitute the two boundary conditions for T,
the impermeability of the boundaries provides the
ing conditions. The complete set of boundary condi-
is expressed as follows for t > 0:

$$T(a/2,t) = \phi_h(t)$$
$$T(-a/2,t) = \phi_c(t) \qquad (2.69)$$

$$j_{1z}(a/2,t) = 0$$
$$j_{1z}(-a/2,t) = 0 \qquad (2.70)$$

$$u_z(a/2,t) = 0$$
$$u_z(-a/2,t) = 0 \; . \qquad (2.71)$$

In Eqs. (2.70) the functions $\phi_h(t)$ and $\phi_c(t)$ express fact that a certain period of time is required to change boundary temperatures. Both quantities are functions of reservoir volume, water flow rate, metal plate material thickness, and temperature difference. Consequently are best determined empirically.

The pure thermal diffusion problem has now been fully ented in terms of three differential equations (2.62), 3), and (2.64); three initial conditions (2.68); and e sets of boundary conditions (2.69), (2.70), and (2.71), the fluxes given by Eqs. (2.65) and (2.66). The various s of approximations usually made in going from first ciples to complete solutions are discussed in the fol- g section.

mplifying Assumptions

We distinguish between three levels of assumptions nly made in obtaining working solutions to the equa- of transport. First are those assumptions inherent nequilibrium thermodynamics and hydrodynamics such as which allow us to use equilibrium properties, linear nenological relations for the fluxes, and continuum mechanics. These assumptions are fundamental and as re necessary starting points which must be retained.

Second are assumptions of a more technical nature restrict our attention to certain types of systems, ich can be realized experimentally and do not, in

nciple, introduce error. In this group are the assump-
ns of a two component fluid, purely vertical motion,
:ial ideality of boundary temperatures, absence of ex-
nal fields other than gravity, and the insignificance of
ssure gradients. Since it is possible experimentally to
eve the requirements imposed by these assumptions, it
o our advantage to incorporate them into the phenomeno-
cal theory, the net effect being a simplification of
differential equations.

Third are assumptions which have been made in all
ious descriptions of pure thermal diffusion, but which
demonstrably incorrect and can lead to significant
rs in the description of the phenomenon. This group
udes the assumptions of time-independent boundary
eratures; uniform temperature gradient; no convective
sport; and constant diffusion coefficients, thermal
usion factors, and density. The three types of assump-
, viz., (1) necessary, (2) unnecessary but desirable,
3) unnecessary and undesirable are summarized in Table

In the next chapter we discuss in more detail the
ptions of the third group and the solutions to the
port equations which one obtains both with and without
assumptions. Our goal is to obtain a description of
thermal diffusion subject only to a minimum number of
ptions.

le 2c.--Levels of Assumptions.

essary	Unnecessary but Desirable	Unnecessary and Undesirable
inuous uid	Binary system	Linear temperature distribution
	Vertical motion	
ulate 1	Spatially uniform boundary temperatures	Temperature independent of time
ulate 2		Constant ρ, D, α_1, κ_i
	No external fields except gravity	Zero convective velocity
	Sedimentation negligible	$\phi_1 = 0$, Eq. (2.26)
		$j_{1z} \frac{\partial}{\partial z} (\overline{H}_1 - \overline{H}_2) = 0$

CHAPTER III

SOLUTIONS

Previous Solutions

Previous phenomenological theories of pure thermal fusion (see, for example, deGroot, 1945; Bierlein, 1955) been obtained only after the following simplifications made.

1. The temperature distribution does not vary with . Although not experimentally realizable, this assump- has been made in the past with the explanation that initial period of time during which the temperature is ging is so much smaller than the time required to com- e an experiment that it may be ignored. Since the im- d discontinuity in the temperature gradient cannot be ved experimentally, there has been an uncertainty in definition of "zero time." The "warming up period" s at the start of an experiment and lasts until no er changes are observable in the temperature distribu- Its length, of course, depends on the apparatus used, ypically may be three to seven minutes. The relaxation θ for pure thermal diffusion increases with the square

e cell height. For most mixtures of carbon tetrachloride yclohexane near room temperature, for example, $\theta = 120$ nutes when the cell height a is expressed in units of meters. Consequently, for a cell height of one or two meters, which is not uncommon, the warming up period may significant portion of the total time for an experiment. gar (1960) has considered the warming up period. He by shifting the time axis in order to compensate for me during which the temperature gradient does not have eady state value. His subsequent treatment was other- nmodified and required that

$$dT/dz = \Delta T/a \tag{3.1}$$

l values of time, where ΔT is the temperature difference.

2. The temperature distribution is a linear function vertical position in the cell. This assumption is ob- not true while the temperature profile is changing me. Moreover, it is true for the steady temperature ution only if the thermal conductivity κ_i is a con- ndependent of temperature and composition and if the ution of the heat of transport is not considered.

3. The center of mass velocity u_z is zero. It fol- om Eq. (2.1) that only if the velocity is nonzero may nge in the density occur. Since density certainly from point to point, a consistent theory requires that onzero. Actually, both u_z and its effect on the com- n distribution are usually very small. Nevertheless,

s desirable to retain the velocity as a variable so that effects can be discussed quantitatively.

4. The density ρ is independent of the temperature. assumption (see deGroot, 1945) results in a great simcation of the differential equation (2.63). Although composition dependence of density, "the forgotten effect" root, et al., 1942), usually has only a small influence he composition distribution in a pure thermal diffusion riment, it cannot be ignored if one wants to be consis- because both optical and gravimetric techniques depend ensity changes due to composition changes. It is also rable to retain the "forgotten effect" in order to be to discuss quantitatively its effect.

6. The mutual diffusion coefficient D is independent mperature. This assumption also simplifies Eq. (2.63) s not generally valid. A change in D of about one perper degree is not unusual (Longsworth, 1957), nor are iments with twenty degree temperature differences oot, 1945). Hence, a complete treatment must allow for variations.

7. The mutual diffusion coefficient D is independent mposition. The remarks of paragraph 6 apply here as Note, however, that the range of compositions ened in a pure thermal diffusion experiment is much er (about 1000 times) than the temperature range. Conitly, we anticipate a much smaller effect due to the sition dependence of D.

8. The function α_1/T is independent of temperature. marks of paragraph 6 again apply. For mixtures of tetrachloride and cyclohexane near room temperature, ample, the function α_1/T decreases about five percent gree.

9. The thermal diffusion factor α_1 is independent position. The remarks of paragraph 7 apply, with $w_1)_T = 0.18$ at 25°C, while α_1 is about -1.75 (see r VI).

10. The product w_1w_2 in Eq. (2.65) can be replaced This assumption of deGroot (1945) limited his ent to very dilute solutions, and is obviously not te.

11. The product w_1w_2 in Eq. (2.65) can be replaced leading terms of the Taylor series expansion about nt w_1^o:

$$w_1w_2 = w_1^o w_2^o + (1 - 2w_1^o)(w_1 - w_1^o) . \qquad (3.2)$$

n (1955) used this "tangential approximation" to ze the term in Eq. (2.65) which contains the pro- w_2, a parabola. The function can be approximated y point w_1^o by its Taylor series expansion at that

$$= w_1^o w_2^o + (1 - 2w_1^o)(w_1 - w_1^o) - 2(w_1 - w_1^o)^2 . \qquad (3.3)$$

pure thermal diffusion experiments, the maximum value
$- w_1^o$) is on the order of 10^{-3}, so that neglect of the
d term in Eq. (3.3) is justified. The use of Eq. (3.2)
ivalent to replacing a small segment of the curve in
ighborhood of w_1^o by the tangent to the curve at that

12. The entropy source term ϕ_1 in Eq. (2.64) does not
oute significantly to the temperature distribution.
ssumption is reasonable, since ϕ_1 is due to bulk flow,
is very small in a pure thermal diffusion experiment.
dimension we have, approximately,

$$\phi_1 = \left(\frac{4}{3}\eta + \varphi\right)\left(\frac{\partial u_z}{\partial z}\right)^2 \quad . \tag{3.4}$$

v below that for systems of interest the maximum value
$_z/\partial z)$ is about 10^{-6} sec^{-1}, making ϕ_1 very small indeed.

13. The term $-j_{1z}\frac{\partial}{\partial z}(\bar{H}_1 - \bar{H}_2)$ in Eq. (2.64) can be
l. For mixtures of carbon tetrachloride and cyclo-
with dT/dz = 5 deg/cm, that term, which is zero
.ly and zero at the steady state, has a maximum value
it $5 \times 10^{-8}\frac{\partial}{\partial T}(\bar{H}_1 - \bar{H}_2)$. This can be ignored when
d with the term $u_z \rho \bar{c}_p (\partial T/\partial z)$ which is itself very

We now consider the most complete solutions pre-
available for the functions T, u_z, and w_1 for a
ermal diffusion experiment. The theoretical

ɾiption under consideration is that of Bierlein (1955)
ı follows from all of the assumptions listed except
ɛrs 4 and 10.

Assumptions 1, 2, 12, and 13 result in a tempera-
distribution of the form

$$T(z) = T_m + \frac{\Delta T}{2}\frac{z}{a} , \tag{3.4}$$

no mention of time dependence. The center of mass
ity is simply stated in the third assumption:

$$u_z = 0 , \tag{3.5}$$

ll values of z and t.

The remaining assumptions (5 - 9) simplify the
ion of continuity of mass fraction:

$$\frac{\partial w_1}{\partial t} = D\left\{\frac{\partial^2 w_1}{\partial z^2} + \frac{\Delta T}{a}\left[\left(\frac{\partial\, \ell n\, \rho}{\partial T}\right)_{w_1} - \frac{\alpha_1}{T_m}(1 - 2w_1^o)\right]\frac{\partial w_1}{\partial z}\right.$$

$$\left. - \frac{\alpha_1}{T_m}\left(\frac{\Delta T}{a}\right)^2\left(\frac{\partial\, \ell n\, \rho}{\partial T}\right)_{w_1}\left[w_1^o w_2^o + (1 - 2w_1^o)(w_1 - w_1^o)\right]\right\} . \tag{3.6}$$

ation of the separation of variables technique to
ove equation and imposition of the above-mentioned
l and boundary conditions results (see Appendix B)
following solution, designated w_1^* in order to dis-
sh it from a later expression for w_1:

$$w_1^*(z,t) = w_1^o + \alpha_1 w_1^o w_2^o \frac{\Delta T}{T_m}\left(\frac{z}{a} + \frac{2}{\pi^3} S\right) , \tag{3.7}$$

re

$$S = \sum_{k=1}^{\infty} k^{-3} V_k W_k \exp\left(-k^2 t/\theta - pz/a - p/2\right) , \quad (3.8)$$

$$V_k = 1 - (1)^k \exp(P) , \quad (3.9a)$$

$$P = \frac{1}{2}\left[\Delta T \left(\frac{\partial \ell n\, \rho}{\partial T}\right)_{w_1} - \frac{\alpha_1}{T_m} \Delta T (1 - 2w_1^{\circ})\right] , \quad (3.9b)$$

$$W_k = B \sin \zeta + k\pi \cos \zeta , \quad (3.9c)$$

$$\zeta = k\pi \left(\frac{z}{a} + \frac{1}{2}\right) , \quad (3.10)$$

$$\theta = a^2/(\pi^2 D) , \quad (3.11)$$

$$p = - \alpha_1 \Delta T/T_m , \quad (3.12)$$

$$2B = \Delta T \left(\frac{\partial \ell n\, \rho}{\partial T}\right)_{w_1} + \frac{\alpha_1}{T_m} \Delta T (1 - 2w_1^{\circ}) . \quad (3.13)$$

re 3.1 shows the general shape of $w_1^*(z,t)$. The conver-
e properties of the infinite series are of interest and
be discussed below.

Although the above expressions (3.4), (3.5), and
for the temperature distribution, center of mass
ity, and composition distribution have been used to
late thermal diffusion factors for a large number of
ms reported in the literature (see, for example,
fsson et al., 1965; Meyerhoff and Nachtigall, 1962)

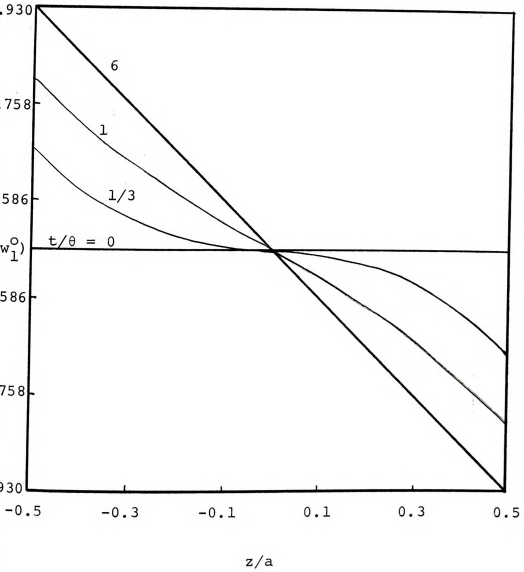

Figure 3.1--Composition w_1^* as a function of z for t/θ = 0.33, 1.0, 2.0, 6.0; w_1^o (CCl_4) = 0.5, dT/dz = 5 deg cm^{-1}.

of them is ever exact. Moreover, the degree of in-
ness has not previously been examined quantitatively.

There are several shortcomings of the above solu-
. First, the steady temperature profile in the fluid
t exactly linear. Variations in thermal conductivity
duce a slight curvature. Also, for several minutes
the temperature difference is first applied to the
and while the temperature profile is being built up,
variation exists in the local temperature gradients.
gradients near the metal plates may accelerate the
ng, or smaller gradients near the middle of the cell
pede it. Semi-empirical corrections involving a
shift in the time scale to take account of warming
ects have been suggested (Agar, 1960), but no rigorous
ent has been published. The exclusion of the possi-
of convective motion and the restrictions to systems
constant transport parameters are additional short-
s with which we concern ourselves in the following
n.

Solutions

In order to keep our treatment very general and to
the most complete description of the pure thermal
on phenomenon, we make only the last three of the
isted assumptions of the third type. The use of
gential approximation (11) and the neglect of ϕ_1

and $j_{1z} \frac{\partial}{\partial z} (\overline{H}_1 - \overline{H}_2)$(13) are certainly justified. We
ct that any error introduced at this point will be much
ler than the limits of experimental measurability.

To avoid a cumbersome simultaneous solution of three
ial differential equations, we adopt a scheme which de-
s on the fact that the calculation of an experimental
e for the thermal diffusion factor α_1 is most strongly
uenced by the accuracy with which the composition gra-
is known, next on that for the temperature gradient,
inally, to a lesser extent, on that for the velocity.
tice also that the composition gradient depends mostly
e temperature gradient and only partly on the velocity.
emperature gradient is a function mainly of the thermal
ctivity of the fluid and some apparatus parameters.
ly, the velocity is quite small and can be determined
ciently well from existing expressions for the tempera-
and composition. Hence, we can work backwards, first
ng the velocity, and then using it to obtain an improved
on for the temperature. The final step involves the
both u_z and T to determine the solution for the com-
on. The simultaneous solutions can be approached by
tion of the three-step cycle until self-consistency
ained.

ter of Mass Velocity

In a uniform fluid mixture at equilibrium, such as
quid in a pure thermal diffusion cell at its initial

(ignoring sedimentation), the center of mass of the
is located at the geometric center of the cell.
arly, the center of mass of each small volume element
ies the geometric center of that volume element. How-
at the steady state of a pure thermal diffusion ex-
ent a vertical density gradient exists, and the center
ss of each volume element is displaced vertically
ward) from the geometric center. This displacement
e center of mass during some time interval gives rise
e vertical component of the center of mass velocity
ich is nonzero as long as the density changes with

It should be noted that the velocity with which we
ncerned results from an uneven expansion and contrac-
f the fluid as the temperature and composition change.
not due to any sort of forced flow.

In order to obtain a mathematical expression for u_z
the equation of continuity of mass:

$$(d\rho/dt) + \rho(\partial u_z/\partial z) = 0 \ . \qquad (2.62)$$

edimentation is ignored, the chain rule for differen-
of the density gives

$$\left(\frac{d\rho}{dt}\right) = \left(\frac{\partial\rho}{\partial T}\right)_{w_1}\left(\frac{dT}{dt}\right) + \left(\frac{\partial\rho}{\partial w_1}\right)_T\left(\frac{dw_1}{dt}\right) \qquad (3.14)$$

ining Eqs. (2.62) and (3.14) with the balance equa-
or energy (2.64) and mass fraction (2.63), we can

e time as a variable and obtain a differential equa-
z only:

$$\frac{\partial u_z}{\partial z} = - \frac{\beta}{\rho \bar{c}_p} \left(\frac{\partial q_z}{\partial z} \right) + \frac{1}{\rho} \left(\frac{\partial \ell n \ \rho}{\partial w_1} \right)_T \left(\frac{\partial j_{1z}}{\partial z} \right) . \quad (3.15)$$

dary condition is simply

$$u_z \left(\left| \frac{a}{2} \right|, t \right) = 0 . \quad (3.16)$$

dependence of the velocity is still contained in
essions for the fluxes. If these were known exactly
d integrate Eq. (3.15) directly to find an expres-
u_z. However, because of the simultaneous nature
roblem j_{1z} and q_z can be known completely only when
own. Nevertheless, we can learn a good deal about
city by using the approximate expressions for the
tained when $w_1(z,t)$ is taken to be Bierlin's (1955)
Eq. (3.7), and $T(z,t)$ is the temperature in a solid
tant thermal conductivity (see $T^*(z,t)$ in Appendix C).
s a test, the following hypothetical system was

$CCl_4 - C_6H_{12}$, $w_1^o = 0.5$,

$T_m = 25°C$, $\Delta T = 4°C$,

cell height = 0.741 cm ,

$\alpha_1 = - 1.72$,

$\kappa_i = 2.45 \times 10^{-4}$ cal deg^{-1} sec^{-1} cm^{-1} .

ration of the resulting expression for $(\partial u_z/\partial z)$ is
htforward, but extremely messy. In order to obtain
rical solution more easily, we used a finite differ-
ntegrating technique (Ralston and Wilf, 1960) and a
l Data Corporation 3600 digital computer. The dis-
age of the numerical method is that no analytical
on for u_z is obtained. For purposes of illustration,
r, the calculated velocity at the center of the cell
wn as a function of time by the solid curve in Figure

The velocity is very small in magnitude (less than
$^{-7}$ cm. sec^{-1}) and is short lived. The whole effect
disappears when the thermal steady state $(\partial T/\partial t = 0)$
ched. The spatial distribution of the velocity at
e must be representable by a function which vanishes
the top and bottom boundaries of the cell.

In order to facilitate the use of the velocity as
ion and to avoid having to perform a finite differ-
tegration each time, we have used the boundary,
, and steady state conditions on u_z as well as the
ce of spatial and temporal extrema (see Figure 3.2)
in a synthetic expression for $u_z(z,t)$. Figure 3.2
s that the time part of u_z is some sort of Morse-type
n. In fact, we found that the function

$$z,t) = \frac{4u_{00}}{a^2}\left[z^2 - \left(\frac{a}{2}\right)^2\right]e^{-\frac{t\,\ell n2}{t_0}}\left(1 - e^{-\frac{t\,\ell n2}{t_0}}\right), \tag{3.17}$$

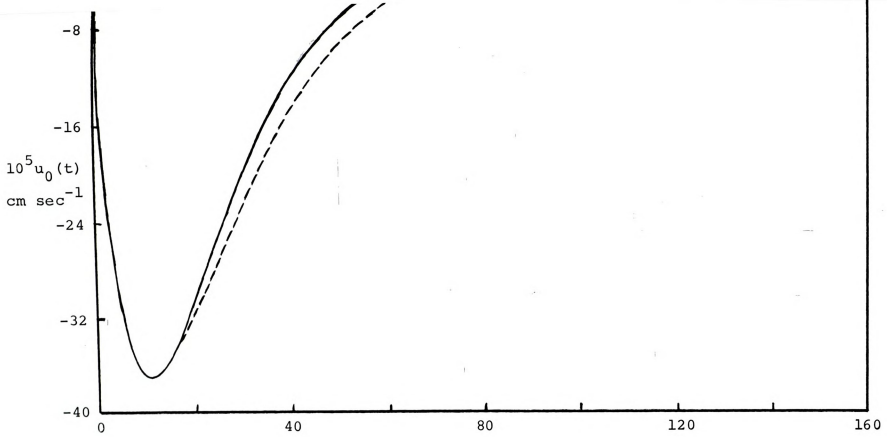

Figure 3.2--Center of mass velocity at z = 0 as a function of time for CCl_4 - C_6H_{12}, $\Delta T/a$ = 5 deg cm^{-1}; finite difference solution (----) and synthetic function (——).

the finite difference solution very well. The dotted
in Figure 3.2 is a plot of Eq. (3.17) for the example
when u_{00} and t_0 are obtained from the finite difference
ion. The difference between the two methods for express-
$_z(z,t)$ is very small, and no significant additional error
be introduced if the more convenient formula (3.17) is
Equation (3.17) is only an approximation, and we use
ly to estimate the contribution of terms which are quite
ortant. It satisfies the conservation equations for
and energy, but it does not satisfy the equation of
, (presumably because we have taken $\phi_1 = 0$ and $\Delta p = -\rho g$).
on (3.17) may be regarded as the leading term of the
olution. For experimental situations in which verti-
nvection is important, such as approximations of
l diffusion in living systems, a more refined analysis
be required. Equation (3.17) suffices to indicate that
e present experiments the maximum value of u_z is about
m sec^{-1}, and the maximum occurs at about 15 seconds
the beginning of the experiment. Convection thus
essentially no contribution to the measured value of
t note that this is a conclusion rather than an
tion.

perature Distribution

All previous theories of pure thermal diffusion are
on the assumption that the temperature gradient inside
id can be expressed by the constant $\Delta T/a$ independent

ime and position. However, in an experiment some mea-
ble time period is required before a steady temperature
ient is established in the fluid. Even if the plate
eratures could be changed instantaneously, the heat
uction process would still result in a time lag. The
tional contribution of time dependent plate temperatures
lts in a warming up period which may not be insignifi-
as previously assumed, when compared with the relaxa-
time θ for diffusion. In our experiments, described
, the warming up period of six minutes was about ten
ent of the relaxation time θ for a cell height of 0.741
Thermal diffusion studies are also being made with
smaller cell heights (see, for example, Meyerhoff and
igall, 1962), and since for CCl_4 - C_6H_{12} mixtures near
$\theta = 120\ a^2$ minutes, a cell height of less than 0.25 cm
θ comparable to the length of the warming up period.
ver, once a steady temperature distribution is estab-
d, it is not perfectly linear because of variations in
al conductivity.

Rather than ignore both the time and space dependences
e temperature gradient, we obtain an explicit formula
includes them, and which can be used in solving the
ential equation for the composition distribution.
ng in chronological order, we confine our attention
to the temperature distribution during the warming
iod.

Time Dependent Temperature Distribution

According to the assumptions which we are making, (11), nd (13), the equation of energy transport (2.64) can ten as

$$\rho \bar{c}_p \left(\frac{\partial T}{\partial t} + u_z \frac{\partial T}{\partial z} \right) = - \frac{\partial q_z}{\partial z} \qquad (3.18)$$

$_z$ is given by Eq. (2.66) and the auxiliary conditions (2.68) and (2.69).

Since our main interest at this point is the time nce of temperature, we can tolerate the very small ntroduced by assuming that Q_1^* and $(\partial w_1/\partial z)$ are known t the thermal conductivity κ_i is constant. Except term containing the velocity, Eq. (3.18) is anal- o the problem of one dimensional heat conduction in . An additional complication is the presence of dependent boundary conditions. As usual an infinite series solution is expected. The following method Duhamel's integral formula (see Bartels and l, 1942), is a convenient one for treating the in- ous equation with time dependent boundary conditions. Some of our early work with numerical solutions of 8) indicated that during the warming up period the ure can be well represented by the sum of two func- ne representing temperature changes due only to duction (as in a solid), and the other representing ributions of the heat transfer by convection and

on. It is, of course, not unreasonable to neglect
ve heat transfer in our apparatus.
Accordingly, we write

$$T(z,t) = T^*(z,t) + bu_z(z,t) \frac{\partial T^*}{\partial z}(z,t) , \qquad (3.19)$$

*(z,t) is the solution to

$$\rho \bar{c}_p \frac{\partial T^*}{\partial t} = \kappa_i \frac{\partial^2 T^*}{\partial z^2} , \qquad (3.20)$$

blem of heat conduction in a solid of uniform thermal
ivity with time dependent boundary temperatures, and
constant whose value is to be determined.
Equation (3.19) takes account of the following

When the velocity is zero the temperature is just what it would be in a solid with the appropriate thermal conductivity, density, and heat capacity. When the temperature gradient ($\partial T^*/\partial z$) is zero the velocity causes no measurable change in the temperature distribution.

The velocity has a larger effect on the temperature distribution when the temperature gradient is large. The effect of the velocity on the temperature distribution depends on the sign and magnitude of the velocity.

An explicit expression for the constant b can be by combining Eqs. (3.18), (3.19), and (3.20)(see

C). Since b does not depend on z or t, it is con-
to evaluate all quantities at $t = t_0$ and $z = 0$.
noring terms of order u_z^2 with respect to terms of
, we obtain

$$b = - \frac{a^2 \rho \bar{c}_p}{8 \kappa_i} \tag{3.21}$$

Hence, the temperature during the warming up period
from Eqs. (3.19) and (3.21):

$$(z,t) = T^*(z,t) - \frac{a^2 \rho \bar{c}_p}{8 \kappa_i} u_z(z,t) \frac{\partial T^*}{\partial z}(z,t) \ . \tag{3.22}$$

(3.22) satisfies our intuitive requirements for
erature, it satisfies the differential equation
nd it satisfies the initial, boundary, and steady
nditions. Therefore, to describe the temperature
he warming up period we have only to find an ex-
for T^*, the conductive part of the temperature
isfies Eqs. (2.68), (2.69), and (3.20).
uhamel's integral formula (Bartels and Churchill,
vides a means for solving the heat conduction
ith time dependent boundary conditions. Param-
on breaks the time domain into a number of small
. Within each interval the boundary conditions
ant and depend on the parameter λ. Let $F(z,t,\lambda)$
lution of the same problem except that the boundary
s $\phi_c(t)$ and $\phi_h(t)$ have been replaced by $\phi_c(\lambda)$ and

their values at time λ. Then the solution to Eqs. (2.68), , and (2.70) is

$$T^*(z,t) = T_m + \int_0^t \frac{\partial}{\partial t} F(z,\lambda,t-\lambda)d\lambda \ . \qquad (3.23)$$

w in Appendix D that

$$T^*(z,t) = r_1(z,t) + r_2(z,t) \ , \qquad (3.24)$$

$$= \frac{4T_m}{\pi} \sum_{n=0}^{\infty} (2n+1)^{-1} \sin\left[(2n+1)\pi\left(\frac{z}{a}+\frac{1}{2}\right)\right] \exp\left[\frac{-\pi^2\kappa_i}{\rho\bar{c}_p}\frac{(2n+1)^2 t}{a^2}\right],$$

$$= \frac{2\kappa_i\pi}{\rho\bar{c}_p a^2} \sum_{n=1}^{\infty} n \sin\left[n\pi\left(\frac{z}{a}+\frac{1}{2}\right)\right] I \exp\left[\frac{-\kappa_i\pi^2 n^2 t}{a^2}\right],$$

$$= \int_0^t e^{\kappa_i n^2\pi^2\lambda/a^2\rho\bar{c}_p}\left[\phi_c(\lambda) - (-1)^n \phi_h(\lambda)\right]d\lambda \ .$$

ypical experiment we may have, for example,

$$\phi_h(t) = T_m + \frac{\Delta T}{2}\left(1 - e^{-t/t_h}\right) \ , \qquad (3.24a)$$

$$\phi_c(t) = T_m - \frac{\Delta T}{2}\left(1 - e^{-t/t_c}\right) \ ,$$

$_h$ and t_c are some experimental relaxation times. In se we can write

$$I = I_c - (-1)^n I_h \ , \qquad (3.24b)$$

$$\frac{1}{K}\left(T_m - \frac{\Delta T}{2}\right)(e^{Kt} - 1) + \frac{t_c}{Kt_c - 1}\left[e^{t(K - 1/t_c)} - 1\right],$$

$$\frac{1}{K}\left(T_m + \frac{\Delta T}{2}\right)(e^{Kt} - 1) + \frac{t_h}{Kt_h - 1}\left[e^{t(K - 1/t_h)} - 1\right],$$

$$\kappa_i n^2 \pi^3 / (a^2 \rho \bar{c}_p) .$$

The expression which we now have for the tempera-
f the fluid in a pure thermal diffusion cell is
e during the warming up period, which for us is
ly six to eight minutes, when we are more interested
time dependence of temperature than in its precise
distribution and can tolerate the use of a constant
conductivity. After this initial period and while
all of the thermal diffusion occurs, the temperature
t remains constant, within the limits of experimental
bility, but it is in most cases not perfectly linear.
ntity κ_i varies both with temperature and with
tion.

Steady Temperature Distribution

According to the discussion following Eq. (2.51),
ctive thermal conductivity of the fluid initially
from that when a composition gradient exists. The
ion is that the temperature distribution continues
e slightly until the steady state of thermal dif-
s reached. In practice, however, the effective

al conductivity is indistinguishable from κ_i, which we
henceforth as κ. After the warming up period Eq.
becomes simply

$$\frac{d}{dz}\left[\kappa(z)\ \frac{dT}{dz}\right] = 0 \ , \tag{3.25}$$

κ varies from point to point in the cell. The boundary
ions after the warming up period are

$$\begin{aligned} T(a/2) &= T_h \\ T(-a/2) &= T_c \end{aligned} \tag{3.26}$$

Equation (3.25) can be integrated by means of a
bation technique. Since κ varies only slightly with
may write the expansion

$$\kappa = \kappa_0(1 + \varepsilon k_1 z + \varepsilon_2 k_2 z^2 + \ldots + \varepsilon^n k_n z^n + \ldots) \ , \tag{3.27}$$

$k_n = (\kappa_o n!)^{-1}(d^n\kappa/dz^n)_0$, n = 1,2,..., can be found
s of the chain rule. The zero subscript means the
y is evaluated at z = 0, and ε is an ordering param-
ich allows us to keep track of the spatial dependence
ature and composition dependence) of the thermal con-
ty. Note that ε is merely an index which does not
The solution for the temperature has the form

$$T = T_0 + \varepsilon T_1 + \varepsilon^2 T_2 + \ldots \ , \tag{3.28}$$

ere the subscripts refer to the order of the per-
on. The integration is straightforward (see Appendix
to terms of order ε^2, yields

$$T(z) = T_m + \frac{\Delta T}{a}\left\{z + \varepsilon k_1\left(\frac{a^2}{8} - \frac{z^2}{2}\right)\right.$$
$$\left. + \varepsilon^2(k_2 - k_1^2)\left(\frac{a^2 z}{12} - \frac{z^3}{3}\right) + O(\varepsilon^3)\right. . \quad (3.29)$$

terms are not necessary because they involve third atives of κ, which are unmeasurable, and products of and second derivatives of κ, which are extremely

Discussion

It is convenient both at the thermal steady state ring the approach to it to use a function $f(z,t)$ which es the departure of the temperature gradient from the nt value $\Delta T/a$ and expresses its time dependence. The on $f(z,t)$ is defined by

$$\frac{\partial T}{\partial z}(z,t) \equiv \frac{\Delta T}{a} + f(z,t) . \quad (3.30)$$

The portion of the temperature gradient which is in is just what has previously been ignored. Note that is not, in general, negligible when compared to $\Delta T/a$. 0, for example, $f(z,t) = -\Delta T/a$. Inclusion of $f(z,t)$ remainder of our theoretical treatment automatically account of warming up effects and deviations from a t steady gradient and leaves no uncertainty about mixing begins or what to take as "zero time." Our ents begin precisely at the instant the temperatures metal plates begin to change, not when the tempera- adient is fully established.

As expected, the temperature gradient builds up slowly
cally during four to six minutes) near the center of
ell; consequently, the diffusion flux in that region
ehind what it would have been if there were no warming
riod. Near the metal plates, however, transient large
ents develop, causing an acceleration of the diffusion
n those regions for a short time.

Agar (1960) has suggested a semiempirical correction
ese effects. According to him we need not be concerned
acceleration of the flux is balanced by the decelera-
lsewhere. If the two effects do not balance, however,
net effect can be negated by shifting the time axis in
propriate direction in order to pretend that an unper-
amount of diffusion has been going on for some slightly
r or longer time. For example, when the boundary
ature are given by

$$T(a/2,t) = T_m + \frac{\Delta T}{a}\left(1 - e^{-t/\tau}\right)$$
$$T(-a/2,t) = T_m - \frac{\Delta T}{a}\left(1 - e^{-t/\tau}\right), \qquad (3.31)$$

experiment with $CCl_4 - C_6H_{12}$, $w_1^o = 0.5$, $T_m = 25°C$,
°C, a = 0.741 cm, τ = 46 sec, the time shift t* is
y

$$t^* = \left(\tau - \frac{D}{12K}\right) \qquad (3.32)$$

is the function $\kappa/\rho\bar{c}_p$. Choosing

$$\kappa = 2.4 \times 10^{-4} \text{ cal cm}^{-1} \text{ sec}^{-1} \text{ deg}^{-1}$$

$$\rho = 1.1 \text{ g cm}^{-3}$$

$$\bar{c}_p = 0.2 \text{ cal deg}^{-1} \text{ g}^{-1} ,$$

ind

$$t^* = 46 \text{ sec.}$$

No such manipulations are necessary with our method ccounting for warming up effects, which is automatic unambiguous.

The function $f(z,t)$ is also important after a steady erature distribution is attained. Nonlinearities due to ations in thermal conductivity which have previously been ected appear explicitly, and their effects on any measure- s are readily calculable.

The temperature distribution has now been fully acterized. The external information on which it depends sts of the thermal conductivity of the fluid and the dependence of the boundary temperatures.

Our descriptions of the center of mass velocity and emperature will next be used to obtain an expression he composition of the mixture as a function of position ime.

mposition Distribution

Steady State

Because it is a great deal simpler and because its ion can serve as a test for the large-time limit of

mplete solution, the steady state case will be con-
d first. The steady state is defined by the vanishing
local time derivatives. It follows from Eq. (2.62)
e impermeability of the cell boundaries that $u_z = 0$
steady state. Equation (2.63) then implies that

$$\frac{\partial}{\partial z} j_{iz} = 0 , \tag{3.33}$$

nce j_{1z} is zero at the boundaries, it must be zero
here. Consequently, we have from Eq. (2.65) that at
eady state

$$\left(\frac{dw_1}{dz}\right) = \frac{\alpha_1}{T}\left(\frac{dT}{dz}\right) w_1 w_2 . \tag{3.34}$$

propriate boundary condition for Eq. (3.34) follows
qs. (2.70):

$$\frac{1}{a}\int_{-a/2}^{a/2} w_1(z)dz = w_1^o . \tag{3.35}$$

The steady state solutions of both Bierlein and
t can be obtained by integrating Eq. (3.34) with

$$\frac{\alpha_1}{T} w_1 w_2 = \text{constant} , \tag{3.36}$$

$$\frac{dT}{dz} = \frac{\Delta T}{a} . \tag{3.37}$$

sult in that case is simply

$$w_1(z) = w_1^o + \frac{\alpha_1}{T_m} w_1^o(1 - w_1^o)\frac{\Delta T}{a} , \tag{3.38}$$

is readily calculated from the steady state composi-
radient:

$$\alpha_1 = \frac{(dw_1/dz)_{ss}\ T_m a}{\Delta T\ w_1^o(1 - w_1^o)} \ . \tag{3.39}$$

eady state solution is obtained by integrating Eq.
without making the simplifications given by Eqs.
and (3.37). Since (dT/dz) and ($\alpha_1 w_1 w_2/T$) are rarely
nts, we make use of the following expansions:

$$\alpha_1 w_1 w_2/T = S(z) \ , \tag{3.40}$$

$$(dT/dz) = \frac{\Delta T}{a} + f(z) \ , \tag{3.41}$$

$$S(z) = \sum_{n=0}^{\infty} \varepsilon^n \delta_n z^n \ . \tag{3.42}$$

By Eq. (3.29),

$$\frac{\Delta T}{a}\left[-\varepsilon k_1 z + \varepsilon^2 (k_2 - k_1^2)\left(\frac{a^2}{12} - z^2\right) + O(\varepsilon^3)\right] \ . \tag{3.43}$$

lows that

$$\delta_n = \frac{1}{n!}\left(\frac{d^n S}{dz^n}\right)_0 , \quad n = 0,1,\ldots, \tag{3.44}$$

at

$$f(z) = \sum_{n=1}^{2} \varepsilon^n f_n + O(\varepsilon^3) , \tag{3.45}$$

$$f_1 = - k_1 z \tag{3.45a}$$

$$f_2 = (k_2 - k_1^2)\left(\frac{a^2}{12} - z^2\right) \ . \tag{3.45b}$$

The method of integration is discussed in Appendix F. lution to Eq. (3.34) through terms of order ε^2 is

$$\overset{o}{1} + \frac{\Delta T}{a}\left\{\left[\delta_o z + \varepsilon(\delta_1 - k_1\delta_o)\left(\frac{z^2}{2} - \frac{a^2}{24}\right)\right]\right.$$

$$\left.\varepsilon^2\left[\delta_o(k_2 - k_1^2)\left(\frac{a^2 z}{12} - \frac{z^3}{3} - \frac{a^3}{48}\right) - (\delta_1 k_1 + \delta_2)\frac{z^3}{3}\right]\right\} + O(\varepsilon^3)$$

Equation (3.46) shows explicitly the influence on mposition distribution of variations in (dT/dz) and $_2$/T). Deviations from a linear temperature distri- are accounted for by the quantities k_1 and k_2. The ties δ_1 and δ_2 express the temperature and composition ences of $(\alpha_1 w_1 w_2/T)$. Comparison of Eqs. (3.38) and gives immediately the difference between our steady solution and the previous one:

$$- \varepsilon(\delta_1 - k_1\delta_o)\left(\frac{z^2}{2} - \frac{a^2}{24}\right) + \varepsilon^2\left[\delta_o(k_2 - k_1^2)\left(\frac{a^2 z}{12} - \frac{z^3}{3} - \frac{a^3}{48}\right)\right.$$

$$\left.(\delta_1 k_1 + \delta_2)\frac{z^3}{3}\right]\Big\} + O(\varepsilon^3) \quad . \qquad (3.46a)$$

ation for calculating α_1 from the measured steady composition gradient will be presented in Section F s chapter.

Approach to Steady State

In deriving the corrections which arise due to g up effects, variable coefficients, etc., we use the on G(z,t), which is defined to be the difference be- the true composition $w_1(z,t)$ and the simplified

ssion given by Eq. (3.7) which we shall denote hereafter
(z,t):

$$w_1(z,t) = w_1^*(z,t) + G(z,t) \ . \qquad (3.47)$$

The equation of continuity of mass fraction remains

$$\rho(dw_1/dt) = - (\partial j_{iz}/\partial z) \ , \qquad (2.64)$$

now

$$\rho D\left\{\left[\frac{\partial w_1^*}{\partial z} + \frac{\partial G}{\partial z} - \frac{\alpha_1}{T}\frac{\partial T}{\partial z}\right] w_1^o(1 - w_1^o) + (1 - 2w_1^o)(w_1^* + G - w_1^o)\right\} \ . \qquad (3.48)$$

unction G(z,t) must obey a differential equation of the

$$\frac{\partial G}{\partial t} = P_1(z,t)\frac{\partial^2 G}{\partial z^2} + P_2(z,t)\frac{\partial G}{\partial z} + P_3(z,t)G + P_4 \ , \qquad (3.49)$$

$$,t) = D \ ,$$

$$,t) = - D\alpha_1 \frac{\partial \ \ell n \ T}{\partial z}(1 - 2w_1^o) + \frac{\partial D}{\partial z} + D\frac{\partial \ \ell n \ \rho}{\partial z} - u_z \ ,$$

$$,t) = - \frac{1}{\rho}(1 - 2w_1^o)\frac{\partial}{\partial z}\left(\rho D\alpha_1 \frac{\partial \ \ell n \ T}{\partial z}\right),$$

$$,t) = D\left\{\frac{\partial^2 w_1^*}{\partial z^2} - \alpha_1(1 - 2w_1^o)\frac{\partial w_1^*}{\partial z}\frac{\partial \ \ell n \ T}{\partial z} - [w_1^o(1 - w_1^o) + (1 - 2w_1^o)(w_1^* - w_1^o)]\frac{\partial}{\partial z}\left(\alpha_1 \frac{\partial \ \ell n \ T}{\partial z}\right)\right\} + \left\{\frac{\partial w_1^*}{\partial z} - \alpha_1 \frac{\partial \ \ell n \ T}{\partial z}[w_1^o(1 - w_1^o) + (1 - 2w_1^o)(w_1^* - w_1^o)]\right\}$$

$$\frac{1}{\rho}\frac{\partial}{\partial z}(\rho D) - \frac{\partial w_1^*}{\partial t} - u_z \frac{\partial w_1^*}{\partial z} \ . \qquad (3.50)$$

The functions $P_j(z,t)$, $(j = 1,\ldots,4)$ are completely known functions of z and t since all of the quantities appearing in them can be determined without knowing G. The initial and boundary conditions are

$$\lim_{t\to 0} G(z,t) = 0 \ , \ -\frac{a}{2} < z < \frac{a}{2} \ , \tag{3.51}$$

and

$$\lim_{z\to \pm a/2} j_{1z} = 0 \ , \ t > 0 \ , \tag{3.52}$$

or

$$\int_{-a/2}^{a/2} G(z,t)dz = 0 \ , \ t > 0 \ . \tag{3.53}$$

The coefficients $P_j(z,t)$, $(j = 1,\ldots,4)$, are obviously the sources of all the corrections to $w_1^*(z,t)$ with which we are concerned. Because of the factors $P_j(z,t)$, Eq. (3.49) cannot be simplified by separation of variables. Moreover, the factors $P_j(z,t)$ are complicated functions (some parts are infinite Fourier series), and we have found no satisfactory integrating factors for simplifying Eq. (3.49). Integral transform methods are not usable because the spatial boundary conditions are two-point and finite. The only approach left is that of Frobenius. By Fuch's Theorem (Johnson and Johnson, 1965, p. 47) the z-dependence of G is given by

$$G = \sum_{k=0}^{\infty} g_k(t) z^k \ , \tag{3.54}$$

if the functions P_2/P_1 and P_3/P_1 analytic (expandable in

Taylor's series) about $z = 0$. By inspection, these functions possess no singularities in any neighborhood of $z = 0$, and Eq. (3.54) is indeed the solution of Eq. (3.49).

The time-dependent coefficients $g(t)$ in Eq. (3.54) are completely determined by: (1) the form of the original differential equation (3.49); (2) the expansions for the coefficients $P_j(z,t)$,

$$P_j(z,t) = \sum_{k=0}^{\infty} P_{jk}(t) z^k \quad , \quad j = 1,\ldots,4 \; ; \tag{3.55}$$

and (3) the auxiliary conditions on G, Eqs. (3.51)-(3.53). Differentiation of Eq. (3.54), followed by substitution into Eq. (3.49) and use of Eq. (3.55), gives immediately the relationships between the desired coefficients $g_k(t)$ and the known coefficients $P_{jk}(t)$.

As with any Frobenius-type method (see Irving and Mullineux, 1959), the preliminary result is a transformation of the problem from a single partial differential equation to a set of simultaneous ordinary differential equations in t for the coefficients $g_k(t)$. In this case Eq. (3.49) becomes

$$\begin{aligned} &\sum_{k=0}^{\infty} \dot{g}_k z^k - \sum_{n=0}^{\infty} P_{1,n} z^n \sum_{k=0}^{\infty} k(k-1) g_k z^{k-2} \\ &- \sum_{n=0}^{\infty} P_{2,n} z^n \sum_{k=0}^{\infty} k g_k z^{k-1} \\ &- \sum_{n=0}^{\infty} P_{3,n} z^n \sum_{k=0}^{\infty} g_k z^k \\ &- \sum_{n=0}^{\infty} P_{4,n} z^n = 0 \; , \end{aligned} \tag{3.56}$$

where

$$\dot{g}_k \equiv (dg_k/dt) \ . \tag{3.57}$$

Since the functions $\{z^n\}$ are linearly independent and form a complete set, and since the infinite series converge for $-a/2 < z < a/2$, the coefficient of each power of z must be independently equal to zero. The resulting set of ordinary differential equations can be expressed compactly by

$$\dot{\underset{\sim}{B}} = A\underset{\sim}{B} + \underset{\sim}{C} \ , \tag{3.58}$$

where $\underset{\sim}{B}$ is the column vector whose elements are $g_k (k = 0,1,...)$; $\underset{\sim}{C}$ is a column vector whose elements are

$$c_k = p_{4,k} \ , \ (k = 0,1,...) \ ; \tag{3.59}$$

and A is a matrix whose elements $a_{ij} (i,j = 1,2,...)$ are related to the coefficients $p_{1,n}$, $p_{2,n}$, and $p_{3,n} (n = 0,1,...)$. A portion of the matrix is given by

$$a_{i1} = p_{3,i-1}$$

$$a_{i2} = p_{2,i-1} + p_{3,1-2}$$

$$a_{i3} = 2p_{1,i-1} + 2p_{2,i-2} + p_{3,i-3}$$

$$a_{i4} = 6p_{1,i-2} + 3p_{2,i-3} + p_{3,i-4}$$

$$a_{ik} = (k-1)(k-2)p_{1,i-k+2} + (k-1)p_{2,i-k+1} + p_{3,i-k} \ , \tag{3.60}$$

where $p_{ij} = 0$, if i or j is less than zero.

By making use of the initial conditions

$$g_k(0) = 0 \ , \ k = 0,1,\ldots, \tag{3.61}$$

one can solve the set of differential equations (3.58) for any number of coefficients $g_k(k = 0,1,\ldots,N)$ in terms of two constants of integration which must be evaluated from the boundary conditions (3.52) and (3.53).

For the purpose of measuring a thermal diffusion factor α_1 we do not need a complete solution for all of the g_k's. In fact, because our experimental method measures the gradient of refractive index (which is directly related to the composition gradient) and because we have used series expansions about the center of the cell where z = 0, all that is required is the quantity

$$(\partial G/\partial z)_{z=0} = g_1(t) \ . \tag{3.62}$$

In obtaining an expression for $g_1(t)$ we are justified in bringing to bear all of the information we have about the function G, including the steady state solution, which must be approached asymptotically as t becomes infinite. One of the expressions which $g_1(t)$ must satisfy follows from Eqs. (3.59)-(3.60):

$$\dot{g}_0 = p_{3,0}g_0 + p_{2,0}g_1 + {}^2p_{1,0}g_2 + p_{4,0} \ . \tag{3.63}$$

Since we expect no anomolous behavior at z = 0 due to unusual temperature gradients we write

$$g_0 = F_0(1 - e^{-t/\theta}) \ , \tag{3.64}$$

where F_0 is an amplitude factor corresponding to the steady state value of g_0. It is not unreasonable to expect that g_0 is well behaved since our measurements (discussed below) suggest that for $t \geq \theta/3$, properties such as the refractive index gradient and the composition gradient near the center of the cell change smoothly and monotonically as a simple exponential function of time and do not exhibit the more unusual behavior observed near the metal plates.

Since we are interested only in the first derivative of G and not in G itself, only one constant of integration, say $g_2(t)$, can be eliminated by means of the boundary condition (3.53), which gives

$$g_2(t) = -\frac{24}{a^2} g_0(t) \quad . \tag{3.65}$$

The remaining constant F_0 must be obtained from a condition on $g_1(t)$ for some extreme (0 or ∞) value of time.

The expression for $g_1(t)$ which one gets by rearranging Eq. (3.63) is indeterminate in the limit as t approaches zero. (Note that this situation would not arise if the whole system of equations (3.58) were solved simultaneously.) Consequently, we use the alternative condition,

$$\lim_{t\to\infty} g_1(t) = g_1(\text{steady state}) \quad , \tag{3.66}$$

which is known from Eq. (3.46a). The second order perturbation solution (including terms of order ε^2) is

$$g_1(\text{st. st.}) = \frac{\Delta T}{a} \delta_0 (k_2 - k_1^2) \frac{a^2}{12} + \mathcal{O}(\varepsilon^3) \quad , \tag{3.67}$$

where δ_0, k_1, and k_2 are given by Eqs. (3.44) and (3.45) respectively. Equation (3.46a) indicates that at the steady state G depends quite strongly on δ_1, the term expressing the temperature and composition dependences of the thermal diffusion factor. The first derivative of G at the center of the cell, as shown by Eq. (3.67), does not, to terms of order ε^3, depend on δ_1. Our choice of the center of the cell as a point about which to expand variable coefficients has resulted in this unexpected simplification. The simplification is certainly a reasonable one, since we recall that in practice the temperature gradient at z = 0 is also unaffected by linear variations in the thermal conductivity. Note in what follows, however, that the time-dependent expression for $g_1(t)$ does depend on δ_1 and other factors that do not appear in Eq. (3.67). On combining Eqs. (3.63)-(3.66) we find

$$g_1(t) = \frac{F_0}{p_{2,0}(t)}\left[\theta^{-1}e^{-t/\theta} + (1 - e^{-t/\theta})\left(\frac{48p_{1,0}(t)}{a^2} - p_{3,0}(t)\right)\right] - \frac{p_{4,0}(t)}{p_{2,0}(t)}, \tag{3.68}$$

where

$$48F_0 = a^2 g_1(\text{st. st.})\left(\frac{\partial\ \ell n\ D}{\partial z}\right)_{\substack{z=0\\t=\infty}} - a^2 w_1^o(1 - w_1^o)\left[\frac{\partial}{\partial z}\alpha_1\left(\frac{\partial\ \ell n\ T}{\partial z}\right)\right]_{\substack{z=0\\t=\infty}} \tag{3.69}$$

and $g_1(\text{st. st.})$ is given by Eq. (3.67).

Our final expression for the composition gradient at the center of the cell is

$$(\partial w_1/\partial z)_0 = (\partial w_1^*/\partial z)_0 + g_1(t) \ , \qquad (3.70)$$

where $w_1^*(z,t)$ is given by Eq. (3.7) and $g_1(t)$ is given by Eq. (3.68). Inspection of Eqs. (3.67-3.69) and (3.50) shows that g_1 is primarily the result of inclusion of variable coefficients and secondarily a result of inclusion of warming up effects. The warming up part is of virtually no consequence after the steady temperature distribution is established, but it is, of course, all-important during the first few minutes. In order to calculate thermal diffusion factors by extrapolating to zero time, a popular practice, it is necessary in principle to use for the composition gradient Eq. (3.70) rather than the z-derivative of Eq. (3.7) alone. Since we have derived equations which fully characterize the experiment for all times, we may calculate thermal diffusion factors from measurements at any time. In particular, we may select those times for which the equations are the simplest. Working equations are presented in the next section.

F. Working Equations

The basic equation with which one can calculate α_1 from measurements of the composition gradient is

$$\left(\frac{\partial w_1}{\partial z}\right)_0 = \left(\frac{\partial w_1^*}{\partial z}\right)_0 + g_1(t) \ , \ t \geq 0 \ , \qquad (3.70)$$

which is valid both during the approach to and at the steady state. The quantity on the left hand side if what is measured (directly or indirectly). The first quantity on the right hand side is a known function of α_1, and the quantity $g_1(t)$ is a correction term which is also known. Upon rearranging Eq. (3.70) and transforming to refractive index gradients instead of directly measured composition gradients, we find

$$\alpha_1 = \frac{T_m(N(t) - g_1(t))}{H(t)} , \tag{3.71}$$

where T_m is the mean temperature of the fluid,

$$N(t) = \frac{\left(\frac{\partial n}{\partial z}\right)_0 - \left(\frac{\partial n}{\partial T}\right)_{w_1}\left(\frac{\partial T}{\partial z}\right)_0}{(\partial n/\partial w_1)_T} , \tag{3.72}$$

$g_1(t)$ is given by Eq. (3.68), and from Eq. (3.7),

$$H(t) = \Delta T w_1^o(1 - w_1^o)\left[\frac{1}{a} + \frac{2}{\pi^3}\sum_{k=1}^{\infty}\frac{V_k}{k^3} e^{-k^2 t/\theta}\left(\frac{dW_k}{dz} - \frac{p}{a} W_k\right)\right]. \tag{3.73}$$

When $(\partial n/\partial T)_{w_1}$, $(\partial n/\partial w_1)_T$, and $(\partial T/\partial z)_0$ are known, one can use Eq. (3.71) to calculate α_1 from measured values of the refractive index gradient for either steady state or non-steady state experiments. Clearly, similar equations hold for any other choice of measurement, such as electrical conductivity or capacitance. All that is required is the gradient of the property being observed and information about its temperature and composition dependences.

G. Composition Distribution During Remixing

By "remixing experiment" we mean one whose initial state is identical with the steady state of the corresponding demixing experiment. In practice one conducts the two experiments in succession with the same system. To initiate remixing one removes the temperature difference. The temperature gradient decays to zero during the next few minutes, and for a period of length 6θ the composition gradient decays to zero by means of ordinary diffusion. Although no thermal diffusion takes place, the thermal diffusion factor α_1 can still be measured since it determines the magnitude and direction of the original composition gradient.

During remixing the velocity is the same as that given in Eq. (3.17) except for the sign of u_{00}.

The temperature gradient is still given by Eq. (3.30) where now f is determined as in section D except that the final condition is

$$\lim_{t\to\infty} T(z) = T_m \ , \tag{3.74}$$

and the boundary conditions are

$$T(-a/2) = \phi_c(t) \ ,$$

$$T(a/2) = \phi_h(t) \ , \tag{3.75}$$

where now $\phi_c(t)$ and $\phi_h(t)$ are not the same as in Eq. (2.69). In particular, different flow rates and heat capacities between the baths used in the two types of experiments lead

to different relaxation times t_h and t_c. Also, both $\phi_c(t)$ and $\phi_h(t)$ must approach T_m as t increases. The solution for the temperature, however, still has the form of Eq. (C.17) except that $\phi_h(t)$ and $\phi_c(t)$ are given by

$$\phi_c(t) = T_m - \frac{\Delta T}{2} e^{-t/t_c} ,$$

$$\phi_h(t) = T_m + \frac{\Delta T}{2} e^{-t/t_h} , \qquad (3.76)$$

and

$$r_1 = \frac{4}{\pi}\left(T_m + \frac{\Delta T}{a} z\right) \sum_{n=0}^{\infty} \frac{1}{(2n+1)} \sin\left[(2n+1)\pi\left(\frac{z}{a}+\frac{1}{2}\right)\right] e^{-\frac{k(n+1)\pi^2 t}{a^2}} . \qquad (3.77)$$

The solution for the composition gradient at the center of the cell is obtained in the same way as for demixing experiments except for the final condition:

$$\lim_{t\to\infty} w_1(z,t) = w_1^o . \qquad (3.78)$$

At z = 0 we have again

$$\left(\frac{\partial w_1}{\partial z}\right)_0 = \left(\frac{\partial w_1^*}{\partial z}\right)_0 + g_1(t) , \qquad (3.70)$$

where now

$$\left(\frac{\partial w_1^*}{\partial z}\right)_0 = \frac{\alpha_1}{T_m} w_1^o(1 - w_1^o) T_m \frac{2}{\pi^3} \sum_{k=1}^{\infty} \frac{V_k}{k^3} \exp(-k^2 t/\theta - p/2)\left\{\frac{dW_k}{dz} - \frac{p}{a} W_k\right\} , \qquad (3.79)$$

$$\lim_{t\to\infty} g_1(t) = 0 \ , \tag{3.80}$$

and

$$\lim_{t\to 0} g_1(t) = g_1(\text{st. st.}) \ . \tag{3.81}$$

As in the case of Eq. (3.68), we find

$$g_1(t) = \frac{F_0}{p_{2,0}(t)} \left[\theta^{-1}\left(1 - e^{-t/\theta}\right) + e^{-t/\theta}\left(\frac{48 p_{1,0}(t)}{a^2} - p_{3,0}(t)\right)\right] - \frac{p_{4,0}(t)}{p_{2,0}(t)} \ ,$$

where

$$48F_0 = a^2 g_1(\text{st. st.}) \left(\frac{\partial \ \ell n\ \rho D}{\partial z}\right)_{\substack{z=0 \\ t=0}} - a^2 w_1^o (1 - w_1^o) \left[\frac{\partial}{\partial z}\left(\alpha_1 \frac{\partial \ \ell n\ T}{\partial z}\right)\right]_{\substack{z=0 \\ t=0}} \ . \tag{3.82}$$

Analogous expressions follow for the working equations:

$$\alpha_1 = \frac{T_m(N(t) - g_1(t))}{H(t)} \ , \tag{3.83}$$

where $N(t)$ and $H(t)$ have the same form as in Eqs. (3.72) and (3.73), but $(\partial T/\partial z)_0$ is appropriately modified in Eq. (3.72), and

$$H(t) = \Delta T w_1^o (1 - w_1^o) \frac{2}{\pi^3} \sum_{k=1}^{\infty} \frac{V_k}{k^3} \exp\ (-k^2 t/\theta - p/2)(W_k' - p/a\ W_k) \ . \tag{3.84}$$

One determines α_1 in the same way as described above. The significant difference between the two methods is that no temperature gradient exists during most of the remixing. Consequently, there is no possibility of inducing convection by poor control of boundary temperatures. Moreover, after the first few minutes N(t) simplifies to

$$N(t) = \frac{(\partial n/\partial z)_0}{(\partial n/\partial w_1)_T} . \qquad (3.85)$$

There is an extra advantage of the remixing method when an optical technique is used for in situ measurements of the refractive index gradient. Changes in $(\partial n/\partial z)_0$ due to fluctuations in metal plate temperatures do not appear because there is no heat conduction through the fluid. All observed phenomena are due to composition changes only. As we shall show in Chapters V and VI, literature values of the composition dependence of refractive index are much more reliable than literature values of temperature dependence.

H. Calculation of the Ordinary Diffusion Coefficient

At least one measurement of $(\partial n/\partial z)_0$ must be available to compute α_1 from either of Eqs. (3.71) and (3.83). When several values of $(\partial n/\partial z)_0$ are available at various times, they can be used in estimating the precision of the measurements. Also, when two or more values of $(\partial n/\partial z)_0$ are obtained at different times, they can be used to

calculate not only α_1, but also a second parameter, such as the relaxation time θ. Then, since the cell height a is known, the ordinary diffusion coefficient of the mixture can be calculated from

$$D = \frac{a^2}{\pi^2 \theta} . \tag{3.86}$$

Of course, only measurements during the approach to the steady state will exhibit the characteristic time dependence necessary to calculate θ.

In principle, with sufficiently refined auxiliary equipment, we could also determine many other parameters such as thermal conductivity, heat of transport, temperature and composition dependences of transport coefficients, etc. Even with our relatively simple equipment, we calculate from our equations the following properties: thermal diffusion factors plus their temperature and composition dependences, ordinary diffusion coefficients plus their temperature and composition dependences, and the temperature dependence of refractive index.

I. Discussion

For the first time we have a phenomenological theory of pure thermal diffusion which takes complete account of transport parameters which vary with temperature and composition, warming up effects, non-linear temperature distribution, and transient convective transport. The results

of this chapter can be used to predict the effect on the composition distribution resulting from a temperature distribution which varies slightly with position or with time (even an oscillating temperature difference).

Alternatively, experiments can now be interpreted more accurately, and calculated values of α_1 should be more reliable. The experimental time scale is clearly defined and leads to no ambiguous curve fitting or extrapolation to zero time. Because of our particular way of expressing the composition as

$$w_1 = w_1^* + G \ ,$$

comparison of results calculated from our theory with those from the best previous theory is very easy: simply set G equal to zero in the latter case. In Eqs. (3.71) and (3.83) set $g_1(t) = 0$, and $(\partial T/\partial z)_0 = \Delta T/a$.

At the end of Chapter II we discussed three levels of approximations and stated our intention to derive a theory based on a minimum number of them. The "necessary" assumptions concerning the applicability of hydrodynamics and nonequilibrium thermodynamics have been retained as have the "unnecessary but desirable" assumptions which can be realized experimentally. Of the thirteen simplifying assumptions classed "unnecessary and undesirable" we have eliminated all but the last three. We feel justified in retaining the following approximations:

(1) $w_1 w_2 = w_1^o(1 - w_1^o) + (1 - 2w_1^o)(w_1 - w_1^o)$. This linearizes the differential equation and makes it tractable.

(2) The entropy source term ϕ_1 in the energy transport equation (2.64) is negligible.

(3) The term $- j_{iz} \frac{\partial}{\partial z}(\overline{H}_1 - \overline{H}_2)$ in Eq. (2.64) may be ignored.

We have also justified two unclassified assumptions, viz., the absence of pressure effects (sedimentation) and the negligibility of the heat of transport Q_1^*. For systems in which the gradients of temperature, pressure, composition, and velocity are as small as they are for our experiments, these simplifications certainly introduce no detectable error.

CHAPTER IV

EXPERIMENTAL APPARATUS

A. Introduction

There are three fundamental components of any pure thermal diffusion system: an appropriate sample container; a means of controlling the boundary temperatures; and a method for detecting small changes in composition.

The first component, the cell, is much simpler for pure thermal diffusion than for any of the other methods. It requires no forced flow mechanism, no membrane or porous plate, and no stirring device. The cell dimensions are not as critical as they are in the case of a thermogravitational thermal diffusion column. In addition, a flat plate is generally easier to machine to a desired tolerance than is a narrow annulus. Moreover, expansion and contraction of the metal parts due to temperature changes cannot change critical dimensions since the plate separation depends only on the thickness of a piece of glass. For that reason also, the height of the cell is easily changed. A thermogravitational column lacks flexibility in that respect.

The only criteria affecting the choice of cell dimensions are convenience and sensitivity of the detection

system. The relaxation time for the thermal diffusion process, unlike that for the thermogravitational apparatus, does not depend directly on the composition or the temperature difference and is given (to within 0.01%) by

$$\theta = a^2/\pi^2 D \tag{4.1}$$

where a is the cell height and D is the ordinary (mutual) diffusion coefficient of the mixture. For carbon tetrachloride-cyclohexane mixtures at the temperatures and concentrations of interest, say 25°C and $w_1 = 0.5$, D is about 1.4×10^{-5} $cm^2 sec^{-1}$. Consequently,

$$\theta \simeq 120\ a^2 \text{ min} \tag{4.2}$$

Since the demixing is 99.75% complete when $t = 6\theta$, and since, for experimental convenience, we wish to complete both demixing and remixing experiments in a 12 to 14 hour period, it follows that we should require

$$a \simeq 0.75 \text{ cm.} \tag{4.3}$$

The length of the cell must be small enough so that a uniform temperature can be maintained, yet great enough so that the optical path through the liquid is sufficient for the desired sensitivity of the interferometer. After measuring the dimensions of the interferometer components and estimating the magnitude of the expected refractive index gradient, we concluded that a cell length of eight centimeters was suitable.

Another pronounced difference between thermogravitational and pure thermal diffusion exists in the importance

of temperature control. In the former case the amount of composition separation does not depend on the magnitude of the temperature difference, but in the latter the temperature distribution in the liquid is extremely important. In fact temperature control is the most troublesome part of pure thermal diffusion experiments.

Large fluctuations at ΔT and drifting of T_h and T_c both result in changes in the diffusion flux. An additional problem occurs when an optical method is used to detect composition changes. A very slight change in the temperature gradient can produce a change in the refractive index gradient nearly as great as that due to all of the thermal diffusion which has taken place. Consequently it is very important to maintain a constant temperature gradient as long as measurements of composition changes are being made. Our water circulation system was carefully designed to minimize temperature fluctuations.

Although optical analysis of composition changes introduce the problem mentioned in the preceding paragraph, the advantages outweigh the disadvantages. Conductometric methods are restricted to electrolyte solutions and necessarily result in a great deal of spatial averaging of compositions. Moreover, the imposed electric field constitutes another force which should be included in the phenomenological relations.

Another method which has been used involves withdrawing an aliquot of the sample liquid at some predetermined

time from some known position and then determining the average composition of the aliquot either chemically, conductometrically, or refractometrically. This method has the obvious disadvantage of disturbing the system and can provide at most a single reliable measurement for each experiment. Due to the time and work needed to carry out each experiment, we easily ruled out such sampling.

Optical interferometric techniques have the decided advantage of providing an extremely large number of data while not disturbing the system in any significant way. Both electrolytes and nonelectrolytes can be studied, although dilute salt solutions require greater sensitivity. Interferometers suitable for diffusion studies utilize the composition dependence of the refractive index of the liquid. Our particular instrument was designed to measure the gradient of the refractive index, which completely determines the composition gradient if the temperature distribution is known. The wavefront shearing interferometer is at least as sensitive as any of the other types which have been used, and it has the advantage of being simpler to use. Our addition of the laser as a light source resulted in increased intensity and improved accuracy.

With this general idea of the apparatus in mind, we turn to a more comprehensive discussion of each of the components.

B. The Cell

Of primary importance in a pure thermal diffusion experiment is the cell. More than just a container, it must satisfy a long list of requirements. It must:

1. have horizontal boundaries consisting of metal plates whose temperatures can be well controlled,
2. have glass walls to permit in situ optical analysis,
3. be fillable and sealable in some way which excludes a vapor phase,
4. contain volatile liquids without permitting evaporation or leakage,
5. be able to be accurately levelled,
6. have reproducible geometry,
7. be free of disturbing vibrations,
8. have uniform temperature distribution over the metal plates,
9. provide efficient heat transfer through the liquid,
10. have a reproducible and measurable warming up time,
11. not permit formation of impurities by means of chemical reactions between the sample liquid, the sealant, and the metal,
12. be much larger in horizontal extent than in depth so that any anomalous behavior at the side walls or corners is negligible,
13. provide proper control of boundary temperature so that convective remixing does not occur,

14. have reservoirs for circulating water with large heat capacity to minimize temperature fluctuations,
15. be easily dismantled, cleaned, and reassembled.

Four preliminary designs were tested and found to be unsatisfactory with respect to the requirements of either temperature control, sealing, or inertness. We found that copper catalyzes the formation of oxides in aqueous solutions. Consequently all metal parts contacting the sample liquid were silver plated. The upper and lower plates were of copper, 6 in. × 6 in. × 1/4 in. Two filling tubes of 1/8 in. o.d. copper were soldered into holes in the upper plate 1/2 in. apart before the plates were machined flat. All of the copper pieces were then coated with 0.001 in. of silver deposited electrolytically (for $10 by Sarver Mfg. of Lansing, Michigan).

Heating and cooling reservoirs were made from 8 in. × 8 in. × 1.5 in. magnesium blocks. The metal was chosen for its machinability, its availability, and because by rapidly exchanging heat with the circulating water it can help to damp temperature fluctuations. Channels were cut into the magnesium to form the reservoirs and to direct the flow of circulating water over the metal plates in such a way that spatial variations in the plate temperature were minimized. (See Fig. 4.1.) Each reservoir was supplied with one inlet and two outlet ports (3/8 in. dia.) in order to maintain a symmetric flow pattern.

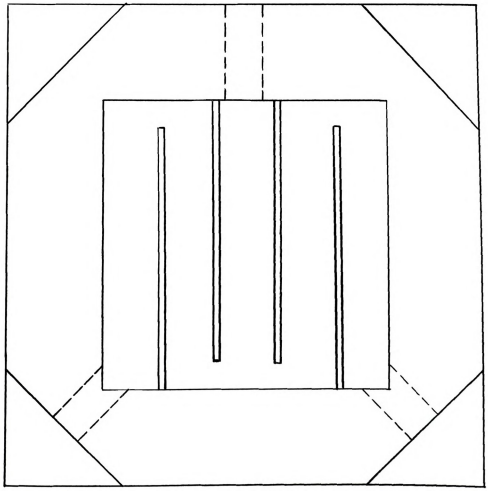

Figure 4.1--Water deflecting channels in reservoir. Overall dimensions 8 in. × 8 in.

Each of the metal plates was secured to a reservoir with twelve brass machine screws (size 10-24) which passed through countersunk holes in the plates and into tapped holes in the magnesium block. The space between the plate and its reservoir was filled with a gasket (1/16 in. "Vellumoid") which was coated on both sides with "Lubriseal" stopcock grease. The resulting seal was completely effective in preventing any leakage of the circulating water. Each reservoir had a capacity of about 300 ml.

The vertical walls of the sample chamber were made of 3/8 in. thick Pyrex optical glass. Pyrex was chosen because its low thermal expansivity insures (1) that it will not crack when subjected to temperature gradients; (2) that there will be no change in cell volume when the temperature changes; and (3) that the thickness of the glass walls does not vary with the temperature. Four bars of width 8 mm, two 8.6 cm long and two 6.3 cm long, were cut from a single plate of optical glass 3/8 in. thick. The four were positioned to form a rectangle with inside dimensions 6 × 8.3 cm. The alignment of opposite walls was made precisely parallel by means of coincidental back-reflection of a helium-neon laser beam.

When properly aligned, the four pieces of glass were joined together with a two-part epoxy resin cement (Sears, "filled," gray in color). Earlier trials with a colorless epoxy always resulted in a breakdown of the

adhesive properties after several hours exposure to water or CCl_4 - C_6H_{12} mixtures. The colorless epoxy did not dissolve, but it became hard and brittle and would not adhere to the glass. The filled epoxy, however, was entirely satisfactory, remaining inert and securely bonded to the glass after 1000 hours of use.

Construction of the sample chamber was completed by grinding the upper and lower surfaces of the glass assembly with carborundum until those two surfaces were uniformly flat and parallel to within 0.0005 cm (a sheet of paper 0.0005 cm in thickness could not be passed between the plate and a flat guage block held in contact with it. The height of the glass walls after grinding and polishing was 0.7410 cm ± 0.0005 cm (by actual measurement with a micrometer).

The material chosen for the sealant between the glass and the metal plates was a very viscous fluorosilicone (Dow Corning "FS" stopcock sealant) which formed a leakproof seal and did not dissolve in or react with the liquids used.

Assembly of the cell was accomplished in the following way. The upper reservoir was inverted (metal plate up) and the glass wall assembly, to which a thin layer of sealant had been applied with a syringe, was placed on the metal plate in such a way that the long axis of the cell was parallel to the optical axis of the interferometer

system, and the two small filling holes just appeared inside one corner of the glass. Sealant was then applied to the top surface of the glass cell wall assembly, and the upper reservoir, with glass attached, was returned to position and lowered over four guide bolts until the glass contacted the lower metal plate. The entire unit was held together when four brass nuts (size 12-20) were applied to the four guide bolts which passed up through the upper reservoir housing.

Four large holes in the corner of the bottom magnesium block fitted onto four upright 1/2 in. diameter threaded steel rods, each 18 in. in length. Steel nuts held the cell assembly to the threaded rods while allowing for height adjustment and levelling. The rods in turn were anchored to a steel I-beam 8 in. wide by 10 in. high and 15 ft long which was itself bolted to two 55-gallon drums filled with concrete. The entire structure, which weighed about 3000 lbs, was separated from the floor by 3/4 in. cushions of dense foam rubber and 1 in. thick plywood boards under the barrels of cement.

To aid in filling the cell, the mounting was designed so that the cell assembly could be tilted about 25 degrees from the horizontal along a diagonal axis. (See Fig. 4.2.) Thus the two filling holes in the top plate occupied the highest corner of the sample chamber. While the cell was being filled by means of a syringe, all of

Figure 4.2.--Assembled cell in tilted position for filling.

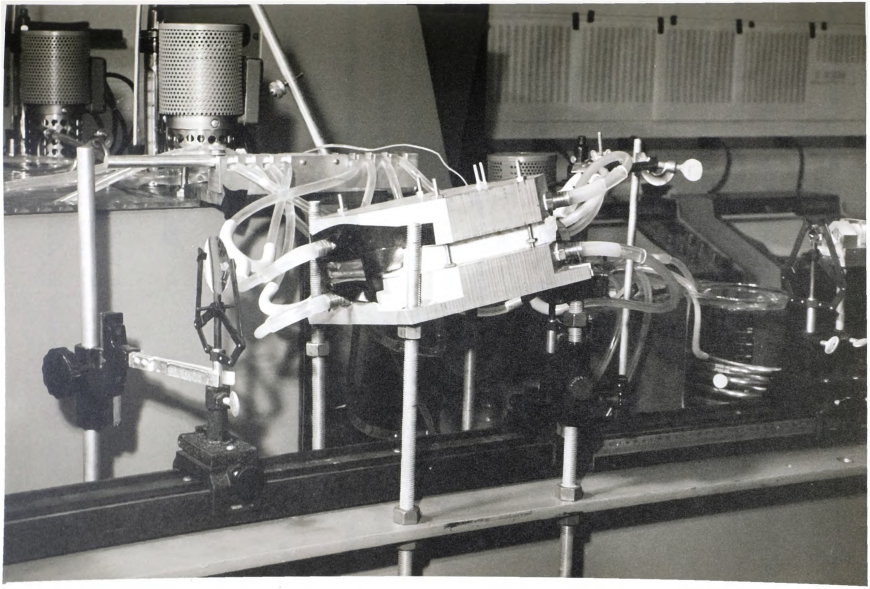

the air was pushed to the top by the entering liquid and was easily expelled.

Once filled, the cell was returned to its level position, and the glass walls were manually pushed sideways between the metal plates a distance of 1/8 in. Thus the filling holes were removed from the sample chamber, precluding both evaporation and diffusion through the holes, and at the same time removing the slightest perturbation on the temperature distribution due to the tubes passing through the reservoir. This feature is an important innovation in our cell.

Finally, strips of foam insulation were placed around the cell in the space between the reservoirs in order to prevent air currents across the metal plates and to avoid spurious heat transfer with the room air. Small flat glass plates were substituted for the foam along the optical path.

We have described the design, construction, and assembly of the cell, but we shall postpone a discussion of its operation until the next chapter. We consider next temperature control and measurement.

C. Temperature Control and Measurement

We chose circulating water baths for temperature control devices rather than electric heating coils in combination with cooling coils in order to avoid both spatial

variations in plate temperatures and the possibility of long term drifting.

The main disadvantage of our water baths, namely fluctuations due to the off-on heaters, has since been eliminated by the substitution of proportional heating elements which are always on but supply slightly more heat if the temperature drops and less if it increases.

Four baths were available for our experiments. The largest, a Lab-Line Tempmobile, was equipped with a compressor unit and served as a source of constant temperature cooling water for the other three baths. Tap water proved unsatisfactory for cooling even when its temperature was steady because only a trickle was needed, and fluctuations in pressure could change the effective cooling rate drastically.

The Lab-Line bath had a capacity of 90 liters and was equipped with a built-in heating element. The point of balance between the heating and cooling actions was adjusted by means of a Rota-Set mercury-contact thermoregulator connected to a relay switching mechanism which turned the compressor on and the heater off when the temperature fell below the preset level.

Additional modes of operation were also available. The compressor or the heater or both could be shut off manually while the circulating pump continued to operate. For example, with the water temperature well below room

temperature, the heater could be disconnected, and then, the cooling of the compressor would have to be balanced by an absorption of heat from the room. Because of the insulation, this would be a slow process and would result in a very long cycling time for the compressor and an accompanying slow drift of the water temperature. For a better balance and optimum temperature control, both the heater and the compressor were allowed to operate.

The bath's circulating pump delivered water through a 3/8 in. i.d. fitting at an uninhibited rate of 1300 ml/min. Near 25°C the temperature of the circulated water showed fluctuations of ±0.1°C coinciding with the off-on cycle of the compressor. A modification was made so that the used water was returned near the pump intake and the thermoregulator rather than to the opposite end of the bath, thus providing the needed increased mixing action. As a result, the fluctuations were reduced to ±0.01°C.

The two baths used to apply the temperature difference to the cell were nearly identical. Both were Tamson model T-45, with 45 liter capacities, and were obtained from Neslab Instruments, Durham, New Hampshire. One operated with 110 V ac and the other with 220 V ac. Both had coils of 1/4 in. stainless steel tubing for external cooling and both had quartz main heating elements. The quartz surrounded a piece of high resistance wire and served to dissipate the heat more slowly than the wire itself would,

hopefully providing a more constant source of heat than a conventional off-on heater.

Both baths had booster heaters for rapid warm up when desired. That in the 110 V bath was quartz, and the other was stainless steel. The difference is of no consequence since the booster heaters were never used during an experiment. Control of the heating cycle was governed by Jumo mercury-contact thermoregulators (0-50°C) and mercury relay switches in each of the baths. The circulating pumps caused excellent stirring of the baths while delivering a flow of water through a 1/4 in. i.d. outlet pipe at a rate of 3500 ml/min with a 10 ft head.

The manufacturer recommended that the cooling rate be adjusted so that the heater was on for about four seconds and off for about 16 seconds of each cycle. Such an adjustment, however, resulted in fluctuations in the temperature of the output water on the order of 0.01°C. We found that further reduction of the cooling rate, until a cycle of one second on and 30 seconds off was obtained, improved the fluctuations to about ±0.005°C. This adjustment was quite delicate since it meant only a slight trickle of cooling water was flowing through the bath and any further decrease could shut off the cooling completely, resulting in a breakdown in the cycle. If that happened, the bath temperature would slowly increase due to the heat developed by mechanical stirring, and the heater would never be turned on.

The fourth bath was a Tamson model T-9 with a 10 liter capacity, and it was maintained at the mean temperature. It was similar in most respects to the other Tamson baths. It had a quartz heater but no booster heater. The cooling coil was a length of 1/4 in. stainless steel tubing. This model had the same pump as the other two and consequently the same flow rate and head. Because of the smaller size, however, the temperature fluctuations of the unmodified bath were on the order of ±0.01°C.

We modified all four of the baths by making the outflow of each pass through a six foot length of 5/16 in. i.d. copper tubing formed in a 5 in. diameter coil. The coil was immersed in a 2000 ml beaker filled with water kept at the operating temperature of the bath. In the case of the T-9, the beaker was outside the bath (increasing the effective volume of the bath to 12 liters) and was stirred by means of a Sargent magnetic stirrer. The other three beakers and coils were positioned inside their respective baths and served as secondary semi-isolated thermostats.

The purpose of the copper coils and their associated volumes of agitated water was to act as heat exchangers and absorb any pulse of excess heat as it passed through the coil or to give heat to the circulating water whose temperature was slightly less than normal. In this way, fluctuations due to the off-on heating cycle were nearly damped out. The three Tamson baths operated routinely with

fluctuations of about ±0.003°C, and, with very careful balancing of the cooling rates, could be made to operate with fluctuations of less than 0.001°C. All of the temperatures mentioned above were monitored continuously with 40 gauge copper-constantan thermocouple junctions attached to the metal plates, and two Sargent model SR strip chart recorders specially modified by our electronics technician to display temperature changes as small as 0.002°C.

The water was suitable for use when it emerged from the copper coil. It was transported from there to the proper reservoir and back to the bath through 1/4 in. i.d. Tygon tubing. Joints between sections of the tubing were made with short lengths of 5/16 in. i.d. Tygon tubing. The material is soluble in methyl ethyl ketone, so when the ends of the tubing were dipped into the solvent for about one minute before slipping them together, a permanent bond was easily formed. Special Tygon Y-connectors, obtained from Scientific Glass Apparatus Co., were used in the same way. At the cell, the tubing was connected to 3/8 in. o.d. brass nipples screwed into tapped holes in the reservoirs. At no point along the line was the opening through which the water passed less than 1/4 in. in diameter.

Between the baths and the cell all of the tubing, including return lines, passed through a two position clamping valve (see Fig. 4.2) specially designed to allow instantaneous switching of the cell from the isothermal to

the nonisothermal configuration and vice versa. With both clamps closed, no water was admitted to the reservoirs. With only the left one open, a temperature difference was applied, and with only the right one open, the cell was isothermal at T_m. At no time could both clamps be open, or water would be transferred between the baths causing overflow. Bypasses had to be installed so that whenever a bath was isolated from the cell, its water could still circulate through the copper coil in order to maintain thermal equilibirium within the 2000 ml beaker.

The starting time of all experiments was taken to be that instant when the clamp for the T-9 was closed and the clamp for the other two baths was opened so that the temperature difference was applied to the cell.

Inside the reservoirs, the water flowed in the pattern shown in Fig. 4.1. There was a space of 3/32 in. between the baffles and the metal plates in order to eliminate the possibility of any dead space.

In order to promote a more uniform temperature distribution, the reservoirs extended beyond the area covered by the sample chamber. The temperature distribution across the bottom plate was checked at 20°C by means of a 40 gauge copper-constantan thermocouple junction held against the plate with a piece of styrofoam insulation and a 100 gram weight. The position of the thermocouple junction was measured, and it was allowed to remain undisturbed for two

minutes while the temperature at that point was measured by the strip chart recorder. Thirty seconds were usually required for thermal equilibrium, but the additional time was used to insure that no further change in temperature would occur.

The measurements were repeated at half-inch intervals across the whole plate. While the resulting 81 data points showed the presence of thermal gradients near the side walls of the reservoir, the temperature over the area occupied by the sample chamber remained constant to within 0.01°C with only randomly spaced variations.

Since we did not wish to conduct thermal diffusion experiments with thermocouple wire inside the cell disturbing the temperature distribution and possibly the diffusion flux, it was necessary to establish whether any systematic difference existed between the temperature of the metal plate inside the sample chamber and the measured plate temperature somewhere outside the cell. For this check, a thermocouple wire was passed through one of the filling tubes and attached to the upper plate by means of a very small piece of tape. The cell was then assembled and filled with a mixture of CCl_4 and C_6H_{12}. A second thermocouple junction was mounted outside of but close to the sample chamber on the upper metal plate. The junction was first placed in contact with the plate and then covered with a one inch square of aluminum foil to insure that the

measured temperature represented that of the plate and not some average influenced by the air temperature. The wire leads from the junction were kept in contact with the plate for a distance of about three inches in order to eliminate thermal gradients in the wire. The junction, foil, and wire were then covered with a piece of black electrician's tape.

When a temperature difference was applied to the liquid, and after a period of fifteen minutes passed, during which a thermal steady state was reached, the voltages of the two thermocouple junctions were recorded. Both reference junctions were in the same ice-water bath. According to a Leeds and Northrup K-3 potentiometer and a previously prepared temperature-emf calibration chart, both junctions indicated the same temperatures to within 0.002°C. Measurements were repeated for thirty minutes, during which only small random differences between the two temperatures were observed. Consequently we felt safe in using the temperature measured outside the cell as the plate temperature in the thermal diffusion experiments.

The above-mentioned thermocouple junction and a similar one on the lower plate were next used to investigate the time dependence of the plate temperatures at the beginning of an experiment. During the change of configuration, the temperature of each plate was monitored with a separate strip chart recorder, and as expected, an exponential shape was observed.

Experimental curves were fitted to functions of the type

$$T_h = T_m + \frac{\Delta T}{2}\left(1 - e^{-t/t_h}\right) = \phi_h(t) ,$$

$$T_c = T_m - \frac{\Delta T}{2}\left(1 - e^{-t/t_c}\right) = \phi_c(t) , \qquad (4.4)$$

where T_h and T_c are respectively the hot and cold plate temperatures, t is time measured from the instant of switching. The two constants t_c and t_h are the two relaxation times for heat conduction through the apparatus mentioned in Chapter II with the statement that they best determined experimentally.

The results of the curve fitting were:

$$t_c = 46 \text{ sec} ,$$

$$t_h = 46 \text{ sec} . \qquad (4.5)$$

Because the capacity of the T-9 bath is different from that of the others, the relaxation times were also measured for the initial part of the remixing experiment, which requires removal of an established temperature gradient. Here the functional form is:

$$T\left(\frac{a}{2},t\right) = T_m + \frac{\Delta T}{2} e^{-t/t_h'} \qquad (4.6)$$

$$T\left(-\frac{a}{2},t\right) = T_m - \frac{\Delta T}{2} e^{-t/t_c'} \qquad (4.7)$$

The relaxation times for the second case were found to be:

$$t_h' = 54 \text{ sec}$$

$$t_c' = 54 \text{ sec} . \qquad (4.8)$$

Measurement of the various temperatures required was accomplished with thermocouples made of 40 gauge matched copper and constantan wires. The wires, individually coated with Teflon, were wrapped together in an additional fabric insulation. A twelve inch length of the fine wire was soldered to about eight feet of more durable 20 gauge copper and constantan wires. The heavier wires were also of matched resistances, polymer coated and bound together by an outer clear plastic film. Both sets of wire were obtained from the Thermo-Electric Co., Inc., Saddle Brook, New Jersey.

Sixteen thermocouples were prepared. A small arc welder, obtained from the Chemical Rubber Company, was used to fuse the two metals into spherical junctions with 0.4 mm diameters. Because of the thinness of the wires, the energy of the arc was sufficient to destroy about an inch of the metal before forming the junction. For more satisfactory performance, the welder was plugged into a 15 A variable transformer, and the voltage was cut from 115 V to about 25V. With the lower energy arc, the junction was more easily formed.

The reference junctions were contained in an ice-water bath, with a four liter capacity, equipped to hold

up to twenty such junctions. Copper and constantan wires extended into 1/4 in. diameter glass tubes 6 in. in length containing 1-1/2 in. of mercury. The tubes were immersed in an ice-water slush. The entire apparatus was surrounded by a 1 in. layer of styrofoam insulation and encased in Fiberglas. The top was covered with a wooden lid, and a terminal panel was provided for convenience in changing thermocouples. After filling, the bath retained a constant temperature for up to four hours before it needed attention. Distilled water was used in the bath along with machine-made ice cubes initially 3/4 in. × 3/4 in. × 1/4 in. in size.

A sixteen junction Leeds and Northrup K-3 potentiometer was connected to an electronic null detector (Leeds and Northrup Model 9834) having nonlinear meter response and maximum sensitivity of ±0.2 microvolt per division. EMF's could be read to the nearest 0.1 microvolt, permitting calculation of the temperature to the nearest 0.002°C.

It should be noted that any shift in the temperature scale which might have developed due to a nonzero reference temperature or a decay of the standard cell in the potentiometer would be inconsequential, since only differences between measured temperatures had to be very accurately known.

Also available for measurements were two Sargent model SR potentiometric strip chart recorders. These showed full scale deflections of 200 microvolts, or 5 degrees Centigrade. Five different scales were available,

corresponding to the temperature ranges: 0-5°C, 15-20°C, 20-25°C, 25-30°C, and 30-35°C.

Again, any inaccuracies introduced by the expansion of the recorder scale were not important since the recorders were used only as indicators. Any critical measurements of temperature were obtained with the potentiometer. The recorders were entirely satisfactory; they showed fast response and a high degree of repeatibility, and registered temperature changes on the order of 0.002°C.

When the sixteen thermocouple junctions were compared against one another by placing them two at a time very close to each other in the same constant temperature bath at 25°C, they all registered the same voltage to within 0.1 microvolt or 0.002°C. Consequently it was not deemed necessary to perform separate calibrations for each of them. This extra step would have been impractical anyway since most of the junctions were broken and replaced at some time during the experiments and since each calibration would have required about three days.

The original calibration was carried out with a thermocouple which did not differ by more than 0.1 microvolt at 25°C from any of the others. A platinum resistance thermometer was used along with a constant current source (2.0 mA) and a resistance box. By using the galvanometer of the K-3 potentiometer, we could measure the resistances of the platinum wire at a series of temperatures. The known

temperature dependence of the resistivity of the platinum then allowed us to calculate the actual temperature.

The platinum thermohm and the thermocouple junction in question were placed in contact with each other and into the small open port of one of the T-45 baths. The emf of the thermocouple could be monitored on one of the recorders as well as with the potentiometer. After the recorder indicated that a steady temperature had been reached in the bath, the following measurements were taken five times at one minute intervals:

(1) resistance of the platinum wire at 2.0 milliamps,

(2) emf of the thermocouple junction.

If the measurements showed any large fluctuations or drifting, they were repeated until five consistent sets of values were obtained. Then the direction of the current was reversed, and the measurements were repeated.

The same measurements were repeated at one degree intervals from 16°C to 34°C. For each value of the resistance the temperature was calculated by means of Eq. (4.9).

$$T = \frac{R_T - T_0}{\alpha R_0} + \delta\left(\frac{T}{100} - 1\right)\frac{T}{100} + \beta\left(\frac{T}{100} - 1\right)\left(\frac{T}{100}\right)^3 , \quad (4.9)$$

where

T = temperature in degrees Centigrade

R_T = measured resistance, international ohms, at 2.0 mA

R_0 = 25.4884 int. ohms

$\alpha = 0.0039260_4$

$\beta = 0.110_6$; $T < 0°C$

$\beta = 0.0$; $T \geq 0°C$

$\delta = 1.491_9$.

The data of interest consisted of a list of temperatures calculated from the measured resistances and a list of corresponding thermoelectric potentials. A FORTRAN IV program, EMFVST, was written for use with MULTREG, a multinomial regression analysis program. The Control Data Corporation 3600 digital computer calculated the best smooth curve through the experimental points to be:

$$EMF = 2.33066 + 40.04151T + 1.300289 \times 10^{-5}T^4 \quad (4.10)$$

where EMF is in microvolts and T is in degrees Centigrade.

The standard errors of the coefficients of T and T^4 are respectively 5.52×10^{-2} and 8.13×10^{-7}. At 20°C and 30°C Eq. (4.10) gives EMF's of 0.8052 mV and 1.241 mV, respectively. The calibration table in the Handbook of Chemistry and Physics (44th edition) lists the corresponding numbers as 0.79 mV and 1.19 mV, respectively. In measuring differences in temperatures, however, we used the temperature coefficient of very nearly 0.4004 mV deg^{-1}, which compares well with the handbook value of 0.40 mV deg^{-1}.

Equation (4.10) was used in preparing an extensive table with which a measured voltage could be rapidly

converted to a temperature. EMF's for all of the temperatures between 14.00°C and 35.99°C were printed out at 0.01°C intervals, and interpolation to the nearest 0.002°C was easily accomplished. The computer calculated the 2200 numbers and printed them in tabular form. The table was hung on the laboratory wall for quick reference.

D. The Interferometer

Having decided to use optical rather than conductometric or sampling methods for analysis of concentration changes, we next had to choose from among the various types of suitable interferometers available. Pure thermal diffusion experiments require that an instrument be able to detect differences in mass fraction as small as one part in 10^5 over distances of a few millimeters. The wavefront shearing interferometer described by Bryngdahl (1963), unlike Rayleigh or Gouy instruments, had not yet been applied to diffusion studies. Bryngdahl's interferometer promised to be at least as sensitive as any of the others in use and had the added advantage of not being difficult to use. Also it offered a chance to make the first application of a new design. While our work was in progress, however, Bierlein (Gustafsson, 1965) published an account of some experiments conducted with a similar instrument, both confirming its advantages and relating the results of some studies on design optimization.

Before building the interferometer, we modified the plans by substituting for the conventional light source a helium-neon gas laser (λ = 6328Å). This produced an intense beam of parallel, monochromatic, polarized light, all features required by the instrument, but not present in a sodium or mercury lamp. The laser chosen was a Siemens model LG-64 having output power in the TEM_{00} uniphase mode of six milliwatts.

Since the light emerging from the laser was polarized in the vertical plane, the laser was rotated 45° about its long axis in order to provide the necessary orientation between the polarization plane and the refractive index gradient in the cell. The laser was mounted between four vertical 1/2 in. steel threaded rods which were attached to the 15 ft horizontal steel I-beam mentioned above. The threaded rods provided flexibility in positioning the laser. See Fig. (4.2).

The diameter of the beam emerging from the laser was 2.5 mm, much less than the cell height. A shutter was provided to keep light from the cell when not needed. A simple two lens system with focal lengths L1,f = 17 mm and L2,f = 203 mm produced a parallel beam 35 mm in diameter. See Fig. 4.3. After traversing the cell, the initially flat wavefront was distorted if a refractive index gradient was present. A second simple lens system (L3,f = 371 mm, L4,f = 22 mm) reduced the height of the beam from 7.41 mm

Figure 4.3.--Helium-neon laser and lenses L1 and L2.

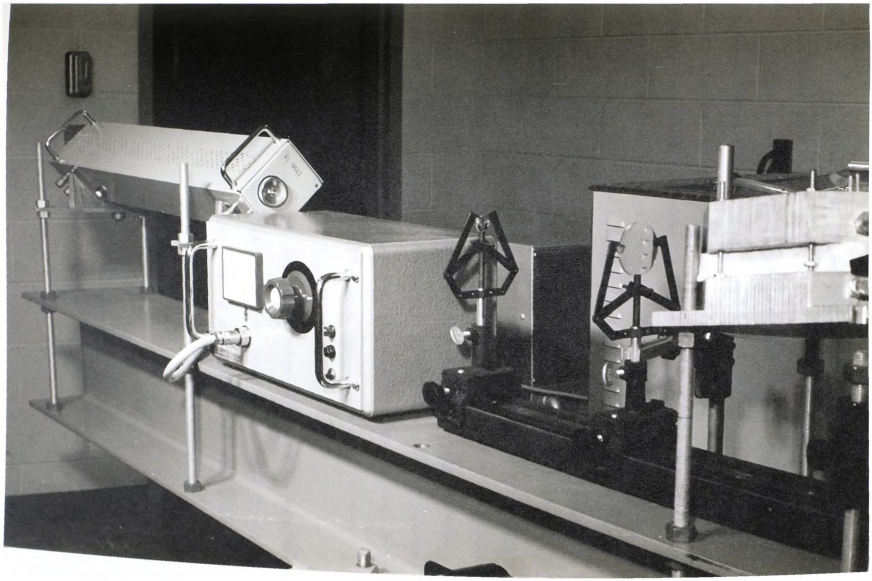

to 0.5 mm in order that it be compatible with the dimensions of the beam splitters.

The beam splitters (Bryngdahl, 1963), obtained from Valpey Optical Corporation, were modified Savart crystal quartz plates. These were cut at 45° from the axis and oriented so that the axes of the subplates were in the same plane but perpendicular to each other. An incident ray gave in the first plate an ordinary ray and an extraordinary ray. In order to get symmetrical light paths through the whole plate, the ordinary ray in the first subplate had to become the extraordinary ray in the second one and vice versa. A half-wave plate inserted between the two subplates so that its principal plane bisected the 90° angle between those of the subplates interchanged the polarization planes of the two rays. Thus there was a compensation of path differences, i.e., no path difference was introduced by the beam splitter in parallel light. See Fig. 4.4.

The net effect of the first beam splitter Q1 was the production of two identical beams of equal intensity having perpendicular polarization planes and separated vertically by a distance b_1. The separation of the two beams is given by:

$$b_1 = 2e \frac{\left(n_e^{2'} - n_0^2\right)}{\left(n_e^2 + n_0^2\right)} , \qquad (4.11)$$

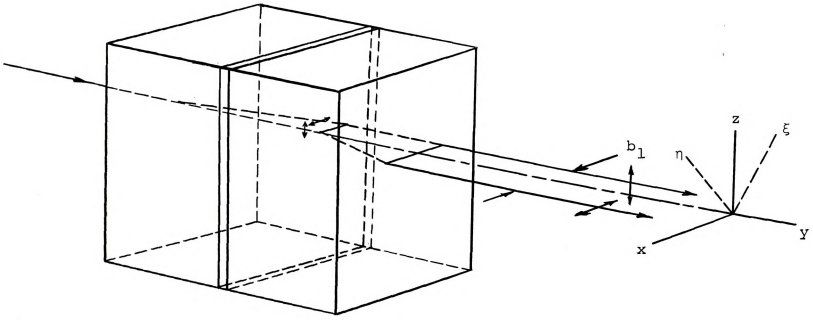

Figure 4.4--Path of light beam undergoing shearing in Q1.

where e is the thickness of each part of the double plate, and n_0 and n_e are the principal refractive indices of the quartz.

In convergent light, the beam splitter splits an entering wavefront into two wavefronts with polarization directions perpendicular to each other. In this case, the shear angle introduced results in an optical path difference Δ between the two emergent wavefronts which depends on the x-coordinate via the corresponding incident angle ψ and on the thickness of the crystal plate. For the plate used,

$$\Delta = b_1 \sin \psi \cos \gamma \qquad (4.12)$$

where ψ is the angle between the entering ray and the normal to surface and γ is its azimuthal angle.

The parallel light beam traverses the first beam splitter Q1 resulting in the formation of two identical beams displaced vertically from each other and having perpendicular polarization planes.

The second beam splitter was identical to the first but was turned through an angle of 90° in order to retain the proper orientation between polarization planes.

Between the two beam splitters Q1 and Q2 a simple double convex lens L5 having focal length 22 mm produced the convergent light for Q2. After the second beam splitter, the interference fringes were made visible in image plane 2

by means of a polarizer (a Nicol prism) oriented at right angles to the polarization plane of the original laser radiation. A final lens L6, consisting of an ordinary microscope objective with a magnification factor of 5, made possible adjustments in the beam size for convenient photographing. The interference fringes, representing the vertical refractive index gradient in the cell, appeared within a sharp double image of the cell. The use of Q1 and Q2 rather than ordinary Savart plates caused the fringes to be presented in Cartesian rather than hyperbolic coordinates (Bryngdahl, 1963). A photograph of the interferometer is shown in Fig. 4.5. A theoretical discussion of the paths followed by the light beams inside the quartz plates is given in Appendix G.

The working equation for the interferometer is

$$x = A(\Delta n/\Delta z) + B \ , \qquad (4.13)$$

where A is a magnification-related apparatus constant which is best determined by means of a separate calibration (discussed below), and B determines the family of fringes which is observed. B need not be known if we measure only the position of the same fringe at various times. The quantity $(\Delta n/\Delta z)$ is a finite difference expression for the refractive index gradient. Through it we can relate measurements of fringe position and shape to expressions for the gradients of temperature and composition.

Figure 4.5.--Interferometer components and Polaroid camera.

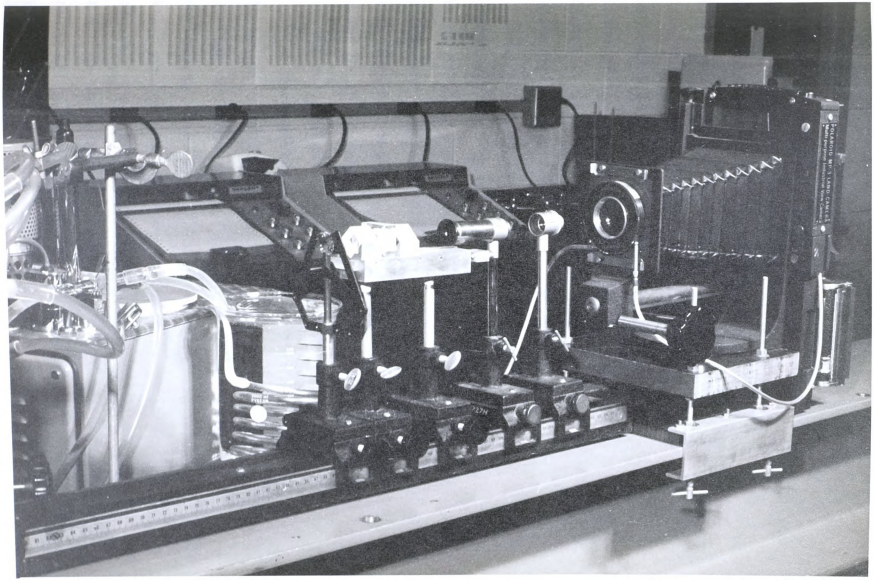

The image of the cell and the fringe pattern was projected through a Polaroid MP-3 camera and onto a ground glass plate. At any time the plate could be moved aside and replaced by a Polaroid roll film back, and a photograph could be taken on Polaroid type 413 infra-red sensitive film. Even though visible light was used, this film was required because of its greater sensitivity in the red range of the spectrum. The photographs, developed in the camera in 15 seconds, were 3-1/4 in. × 4-1/4 in. black and white positive prints.

A device to measure fringe positions on the photographs was made by mounting on a 4 in. × 6 in. × 1-1/2 in. block of aluminum a mechanical microscope stage with graduations and vernier scales which could be used in conjunction with a magnifying lens to determine the two dimensional shape of the fringes to 0.01 cm, or the equivalent of 0.13% of the cell height.

Each photograph cost about $0.50 and required five to ten minutes to analyze. To permit more practical accumulation of large amounts of data, an alternate measuring device was also used. This consisted of the same microscope stage mounted directly on the ground glass plate of the camera. The arrangement allowed the fringe position at $z = 0$ to be measured frequently and rapidly. A photograph could still be taken when more detailed information about the fringe shape was desired.

E. Working Equations

Let the vertical refractive index distribution in the cell be given by the expansion:

$$n(z,t) = \sum_{k=0}^{\infty} c_k(t) z^k \ , \tag{4.14}$$

where the coefficients c_k are functions of time:

$$\begin{aligned} c_0(t) &= n(0,t) \\ c_1(t) &= (\partial n/\partial z)_0 \\ c_2(t) &= \tfrac{1}{2}(\partial^2 n/\partial z^2)_0 \\ c_n(t) &= \tfrac{1}{n!}(\partial^n n/\partial z^n)_0 \ . \end{aligned} \tag{4.15}$$

The subscript zero means the derivative is evaluated at $z = 0$.

The finite difference expression for the fringe shape requires the quantity:

$$\Delta n(z,t) = n(z + \tfrac{as}{2},t) - n(z - \tfrac{as}{2},t) \tag{4.16}$$

It follows from Eqs. (4.13) and (4.16) that:

$$\begin{aligned} x = A\{&(c_1 + \tfrac{1}{4} c_3 a^2 s^2 + \tfrac{1}{16} c_5 a^4 s^4 + \ldots) \\ &+ (2c_2 + c_4 a^2 s^2 + \ldots) z \\ &+ (3c_3 + \tfrac{5}{2} c_5 a^2 s^2 + \ldots) z^2 + (4c_4 + \ldots) z^3 \\ &+ (5c_5 + \ldots) z^4 + \ldots \} + B \ . \end{aligned} \tag{4.17}$$

The quantity s is the amount of shear (0.19).

The experimentally measured fringe shapes are well represented by the polynomial:

$$x = \sum_{k=0}^{5} d_k(t)\eta^k \ , \tag{4.18}$$

where η is the dimensionless vertical cell coordinate observed on a photograph, and the d_k the coefficients giving the best least squares fit.

Because of the double image which is due to the shear s, the vertical coordinate z in the cell is related to the vertical coordinate η in the photograph by:

$$\eta = \frac{2z}{(1 - s)a} \tag{4.19}$$

where

$$-1 \leq \eta \leq 1 \ ,$$

and s is the shear, or amount of overlap of the two images.

The relationship between the coefficients d_k and c_k is discovered by using Eq. (4.19) and equating coefficients of like powers of z in Eqs. (4.14) and (4.18):

$$\begin{aligned}
d_0 &= A(c_1 + \tfrac{1}{4} c_3 a^2 s^2 + \tfrac{1}{16} c_5 a^4 s^4 + \ldots) + B \\
d_1 &= \tfrac{A}{2}(a - as)(2c_2 + c_4 a^2 s^2 + \ldots) \\
d_2 &= \tfrac{A}{4}(a - as)^2(3c_3 + \tfrac{5}{2} c_5 a^2 s^2 + \ldots) \\
d_3 &= \tfrac{A}{8}(a - sa)^3(4c_4 + \ldots) \\
d_4 &= \tfrac{A}{16}(a - as)^4(5c_5 + \ldots) \\
d_5 &= \tfrac{A}{32}(a - as)^5(6c_6 + \ldots)
\end{aligned} \tag{4.20}$$

The coefficient d_0 represents a uniform lateral shift of the whole fringe pattern. Since d_1 is the coefficient of the first power of η, it accounts for a skewness in the photographs which decays away as $(\partial^2 n/\partial z^2)_0$, or c_2, approaches zero, in exact agreement with Bierlein's observation.

Inversion of Equations (4.20) gives:

$$c_5 = \frac{16}{A}(a - as)^{-4}(\frac{1}{5} d_4 + \ldots)$$

$$c_4 = \frac{8}{A}(a - as)^{-3}(\frac{1}{4} d_3 + \ldots)$$

$$c_3 = \frac{4}{A}(a - as)^{-2}\left[\frac{1}{3} d_2 - \frac{1}{6} d_4 a^2 s^2 \left(\frac{a - as}{2}\right)^{-2} + \ldots\right]$$

$$c_2 = \frac{2}{A}(a - as)^{-1}\left[\frac{1}{2} d_1 - \frac{1}{8} d_3 a^2 s^2 \left(\frac{a - as}{2}\right)^{-2} + \ldots\right]$$

$$c_1 = \frac{2}{A}(a - as)^{-1}\left[d_0 - \frac{1}{2} d_2 a^2 s^2 \left(\frac{a - as}{2}\right)^{-2} + \ldots\right] . \quad (4.21)$$

Thus all of the coefficients in the expansion for $\partial n/\partial z$ which follows from Eq. (4.14) can be determined from measurements of d_k, (k = 0...5), A, s, and a.

The coefficients c_k are related to the transport parameters α_1, D, κ_i, and Q_1^* through the expression for the temperature and composition distributions and through relations such as:

$$c_1 = \left(\frac{\partial n}{\partial w_1}\right)_T \left(\frac{\partial w_1}{\partial z}\right)_0 + \left(\frac{\partial n}{\partial T}\right)_{w_1} \left(\frac{\partial T}{\partial z}\right)_0 \quad (4.22)$$

where $(\partial w_1/\partial z)_0$ is a function of α_1, etc.

In the next chapter calibration of the interferometer and the particular measurements involved are discussed, along with the other experimental details.

CHAPTER V

EXPERIMENTS

A. Weighing Procedure

Because we chose to work with carbon tetrachloride-cyclohexane mixtures in order to be able to compare our results with those of previous workers, we had to deal with the problem of evaporation. Such losses before and during an experiment can lead to miscalculations of the actual composition of the mixture. The following procedure was used in an attempt to avoid, or at least minimize, errors in the determination of the mass fractions of the components of the solution actually undergoing thermal diffusion in the cell.

Four 25 ml Pyrex pycnometers for volatile liquids were obtained from Scientific Glass Apparatus Company. The 80 gram capacity of our Mettler H-16 single pan analytical balance precluded the use of larger volumes of liquid. Each pycnometer consisted of a 25 ml bottle, a capillary stopper, and a cover which prevented evaporation from the open capillary tube. The three pieces fit together with ground glass joints, and each part was marked with the same number to prevent interchange between sets.

Only one of the pycnometers was used throughout the whole series of experiments. Before each use it was cleaned with a solution of potassium dichromate in 98% sulfuric acid, rinsed in distilled water, and dried in an oven at 105°C. When cool, it was placed in a water bath at 25.00°C for three minutes, removed, dried with Kimwipe tissues, and weighed on the previously zeroed H-16 balance. The volume of the pycnometer was determined from a series of measurements during which it was weighed while filled with either distilled water, carbon tetrachloride, or cyclohexane at 25.00°C. The water was obtained from the distilled water tap in the laboratory. The other two liquids were obtained from the J. T. Baker Chemical Company. The labels of the bottles used are reproduced in Tables 5a and 5b. All chemicals were used without further purification.

An excess amount of the particular liquid below 25°C was poured into a clean, dry 250 ml Erlenemeyer flask provided with ground glass stopper. The liquid was removed from the flask by means of a 100 ml capacity glass syringe fitted with a 12 in. length of Teflon tubing of 1/16 in. i.d. The Teflon tube was then replaced by a 1-1/2 in. size 18 stainless steel syringe needle, and the air in the syringe was removed. The liquid was then injected into the pycnometer bottle until the bottle was nearly full, at which time the capillary stopper was inserted, causing an overflow of the excess liquid and the exclusion of all air from the

Table 5a.--"Baker Analyzed" reagent lot analysis as given on bottle label for CCl_4.

1 pt. (473.2 ml) 1513

CARBON TETRACHLORIDE

CCl_4 F.W. 153.82

"Baker Analyzed" REAGENT

SPECTROPHOTOMETRIC

LOT NO. 34532

Color (APHA)	5
Density (g/ml) at 25°C	1.585
*Boiling Range 1-95 ml	0.1°C
95 ml-dryness	0.2°C
Residue after Evaporation	0.0004%
Acidity	Pass ACS Test
Free Chlorine (Cl)	Pass ACS Test
Sulfur Compounds (as S)	0.003%
Iodine Consuming Substances	Pass ACS Test
Substances Darkened by H_2SO_4	Pass ACS Test
Solubility for use in Dithizone Test	Pass ACS Test

*Recorded Boiling Point 76.7°C.

Table 5b.--"Baker Analyzed" reagent lot analysis as given on bottle label for C_6H_{12}.

1 pt. (473.2 ml) 9206

CYCLOHEXANE

$CH_2(CH_2)_4CH_2$ F.W. 84.16

'Baker Analyzed' Reagent

ACTUAL ANALYSIS OF LOT NO. 34840

Color (APHA)	2
Density (g/ml) at 25°C	0.773
*Boiling Range, 1-95 ml	0.1°C
95 ml-dryness	0.1°C
Residue after Evaporation	0.0008%
Substances Darkened by H_2SO_4	Passes Test
Water (H_2O)	0.014%

*Recorded Boiling Point 80.7°C.

container. The pycnometer was never touched directly. All handling was done with tissues or a wire holder consisting simply of a length of wire wrapped around the neck of the bottle.

By means of the wire holder, the partially assembled pycnometer was transferred to a wire basket in the T-9 water bath which was maintained at 25.00°C. The heating and resulting overflow of the sample liquid continued for about four minutes. When the liquid level was just even with the top of the capillary tube, the pycnometer cover was put tightly into place. The assembly was then removed from the water, dried carefully with a Kimwipe as before, and weighed on the H-16 balance. The air temperature, relative humidity, and barometric pressure were recorded at the time of the weighing for purposes of air buoyancy corrections. A Sargent hygrometer provided wet and dry bulb temperatures, and a Fortin-type mercurial barometer permitted determination of the atmospheric pressure. From the known densities of the liquids used, the 25° volume of the pycnometer could readily be calculated.

In a substitution weighing, the beam is brought into equilibrium with a set of weights[†] as the load and the scale reading are set to zero. Next an object is placed on the pan, and weights are removed to return the beam to equilibrium.

[†]Following custom, we call the standard masses "weights."

The balance indicates two numbers: (1) the nominal value of the weights removed; and (2) the indicated difference between the weight of the object and the weights removed.

The effect of gravity and air buoyancy on the weights must be taken into account, while other forces must be avoided or eliminated. Various forces such as electrostatic or magnetic forces, the "sail effect" from moving air, and air buoyancy on the beam or other parts of the moving system may act to change the balance indication. As long as these forces remain constant, their effect will go out in the difference between the two readings. Consequently only gravity and air buoyancy need be considered. The balance equation is:

$$(M_u - V_u\rho)g = (M_s - V_s\rho)g \qquad (5.1)$$

where

M_u = true mass of object

M_s = true mass of weights used

V_u = volume of object

V_s = volume of weights

ρ = air density

g = acceleration of gravity

Forces are eliminated by dividing by g, whence, upon rearrangement:

$$M_u = M_s + (V_u - V_s)\rho \ . \qquad (5.2)$$

Equation (5.2) requires knowledge of the true mass of the weights used, which differs from that of the nominal values observed. In the United States, Normal Conditions are defined to consist of air density of 1.2 mg/cm^3, temperature of 20°C, and standard weights having an ideal density of 8.4 g/cm^3 at 0°C and coefficient of cubical expansion of 5.4×10^{-5} deg^{-1} C. From this the ideal density at 20°C is 8.3909 g/cm^3.

Usually the air density differes somewhat from 1.2 gm/cm^3 as defined for normal conditions, and the density of the weights used differs from 8.3909 g/cm^3 at 20°C. According to L. B. Macurdy, Staff Metrologist of the Mettler Corporation, the weights in the Mettler Model H-16 balance are of one-piece stainless steel with a nominal density of 7.76 g/cm^3 to be assumed at 20°C. In order to obtain the true mass of the weights M_s, it is necessary to add the correction +11.63 micrograms per gram to the indicated value to take account of the fact that the density of the weights is not 8.4 g/cm^3. Also, since measured volumes are not usually available, Eq. (5.2) can be rearranged to give the true mass of the object in terms of densities:

$$M_u = M_s(1 - \rho/D_s)(1 + \rho/D_u + \rho^2/D_u^2 + \rho^3/D_u^3 + \ldots) , \tag{5.3}$$

where $M_s = M_{apparent} \times (1.00001163)$, D_s is the density of the weights, and D_u is the density of the object, both calculated at the ambient temperature. D_u is best

approximated by $D_u \approx M_s/V_u$. Most of our weighings were obtained at an ambient temperature of 24°C rather than 20°C. If the coefficient of cubical thermal expansion of the stainless steel is assumed to be:

$$-\beta = 51 \times 10^{-6} \text{ deg}^{-1} ,$$

then at 24°C:

$$D_u = 7.76(1 - 2.04 \times 10^{-4}) \text{g cm}^{-3} .$$

Since D_u was originally given with only three significant figures, the correction is certainly negligible.

In order to calculate the air density, measurements of the barometric pressure, the relative humidity, and the ambient temperature were required. The standard temperature for the density of the mercury in the barometer is 0°C. Since the mercury and the brass scales have different coefficients of thermal expansion, the pressure indications are affected by variations in the temperature. The manufacturer of the barometer, Precision Thermometer and Instrument Company, Philadelphia, supplied Temperature Correction Tables which combined the corrections for length of the scales and density of the mercury. We used Gravity Correction Tables to take account of the latitudinal variation of the gravitational constant. The combination of these corrections usually contributed about -2.9 mm Hg.

Tables supplied with the Sargent hygrometer were also used to calculate the relative humidity from the

measured values of the ambient temperature and the depression (in degrees Farenheit) of the wet bulb thermometer in the Sargent electric hygrometer. For most of our weighings, the air density was about 1.16 mg/cm^3.

To speed the recording of data and the calculation of weighing corrections, a simple form was typed on a Ditto master, and spirit copies were used for all of the weighings. A completed sample form is shown in Table 5c.

We used the data of Wood and Gray (1952) to obtain the densities of pure carbon tetrachloride and pure cyclohexane as well as the temperature and composition dependence of density. At 25°C:

$$\rho\left(CCl_4\right) = 1.58414 \text{ g/cm}^3$$

$$\rho\left(C_6H_{12}\right) = 0.77383 \text{ g/cm}^3 \ .$$

The volume of the pycnometer, based on the results of ten trials with water, CCl_4, and C_6H_{12}, was taken to be:

$$V = 25.7523 \pm 0.0025 \text{ cm}^3 \ .$$

Once the volume was known, the densities of mixtures of the two organic liquids could be determined by the same weighing technique. The density versus composition data of Wood and Gray at 25°C were expressed by the polynomial (from MULTREG, see Appendix H).

$$w_1^o = 1.99014 - 0.01505 \ - \frac{1.53114}{\rho} \ , \qquad (5.4)$$

where w_1^o is the mass fraction of CCl_4 in the mixture and ρ is the density of the liquid in g/cm^3. The dimensions of

Table 5c.--Sample weighing form.

Date 3-22-68 Time 10:00 a.m.

Run No. -- Pressure, mm Hg 745.4 → 742.5

Liquid CCl_4 T_{dry} 77°F; T_{wet} 54°F.

Liquid Temp., °C 25.00 Room Temp., 23.9°C; 75.0°F

Vol. Fraction 1.00 Rel. Humidity, 15%

Pycnometer No. 375 Time in Bath, Minutes 5

Liquid Density (Approx), g/cm^3 $D_u = 1.58414$

Air Density, g/cm^3 $\rho = 0.001158$

Weight of Bottle and Liquid, g.

65.99890

65.99886 65.99888

Weight of Empty Bottle, g.

25.22384

25.22384 25.22384

Apparent Mass of Liquid, g. $M_a = 40.77504$

True Mass of Weights Used, g. $M_s = M_a\ (1.00001163) - 40.77551$

True Mass of Liquid, g.

$$M_u = M_s(1 - \rho/7.76)(1 + \rho/D_u + \rho^2/D_u^2 + \ldots)$$

$$= 40.77551\ (.99985)(1.00073)$$

$$= 40.79920$$

Pycnometer Volume, cm^3. 25.7549 (calc.)

Liquid Density, g/cm^3. 1.58414 (lit.)

Mass Fraction, W_1 = 1.0000

he coefficients are appropriate to cancel those of ρ. The standard errors of the two coefficients in Eq. (5.4) are respectively 5.83×10^{-4} and 7.25×10^{-4}.

When the liquid being prepared was scheduled to undergo thermal diffusion in the cell, the following modifications were made in the above procedure. The two components were mixed in the 250 ml flask in the approximate proportions desired. For example, if the desired mole fraction was 0.6, then 40 ml of cyclohexane were added to 60 ml of carbon tetrachloride. No precaution against evaporation was taken at this point. The flask contained a 1-1/4 in. Teflon coated magnetic rod, which permitted excellent mixing of the two liquids when the flask containing them was placed on a magnetic stirrer.

When mixing was complete, the flask was chilled for a few seconds by placing it in contact with ice. This was done in order to insure that the temperature of the liquid entering the pycnometer was below 25°C. After the chilling, the flask and its contents were returned to the stirrer for about another minute to insure a uniform temperature and composition.

Then the stirrer was shut off, the stopper was removed, and about 80 ml of the liquid was drawn through the Teflon tube into the large syringe. The tube extended well below the surface of the liquid. The tube was replaced by a needle, and all air was removed from the syringe.

The first few milliliters of the liquid was discarded, and then the cell was filled as described in the following section. Immediately thereafter, a small quantity of the liquid was again discarded from the syringe (that portion which was in contact with air), and the pycnometer was carefully filled without disturbing the liquid surface or causing an unusual amount of evaporation. The pycnometer was overfilled so that the liquid close to the surface, whose composition may have changed by differential evaporation, was spilled out when the bottle was closed. The closing, thermal equilibration, and weighing of the filled pycnometer were the same as described above. The liquid in the pycnometer and the liquid in the cell were assumed to have the same composition.

B. Step-by-Step Procedures

All of the facets considered above, the cell, the temperature control system, the interferometer, and the weighing technique come together to fulfill their purposes in the actual execution of an experiment, which is most efficiently described by a series of steps.

1. Turn on all water baths to their desired preset temperatures at least 12 hours before the start of an experiment.
2. Switch on the potentiometer at least one hour before any measurements are to be made.

3. Dry the pycnometer parts in the oven at 105°C for at least two hours if not already dry. Handle only with tongs which have been cleaned in sulfuric acid, rinsed thoroughly in distilled water, and dried.
4. Check the water levels in all baths and in the beaker on the stirrer for T-9, and refill if necessary.
5. Refill the small (500 ml) beaker with fresh distilled water for rinsing the used pycnometer after cleaning.
6. Fill the thermocouple junction reference ice bath and allow to equilibrate.
7. Make certain the camera is loaded.
8. If pycnometer has been in oven for two hours remove, and let cool in air before assembling. Do not touch.
9. Clean the silver plated surfaces of the cell, removing any oxide coating with silver polish. Rinse thoroughly with a CCl_4 - C_6H_{12} mixture and dry without leaving streak marks.
10. Position thermocouple junctions, each between its plate and a piece of foil. Hold in place with electrician's tape, making sure that two or three inches of the lead wire is in contact with the metal plates.
11. Clean the glass cell walls with a CCl_4 - C_6H_{12} mixture and Kimwipe tissue to remove all old sealant and any marks.

12. Remove any air bubbles from bottom reservoir by holding it vertically so that the air exits through one of the ports at the highest point.
13. Level the bottom plate by using a bubble indicator and the four adjusting nuts on the large threaded rods supporting the cell.
14. Apply Dow FS Fluorosilicone Sealant to one surface of the glass cell wall assembly by means of a 10 ml glass syringe and needle.
15. Position the glass cell wall assembly on the inverted top reservoir assembly, coated side down, and with proper alignment of the filling tubes in one corner.
16. Apply silicone sealant to the upper side of the cell wall assembly with syringe.
17. Assemble the cell, fasten retaining nuts with light pressure only.
18. Turn on the laser and its timer. Align optics and focus interferometer on glass plate of camera.
19. Tilt the cell for filling and provide a Kimwipe to absorb spilled liquid.
20. Make sure the bath switch is in the isothermal configuration.
21. Clean the glassware for solution preparation and rinse with CCl_4 or C_6H_{12}.
22. Prepare 100 ml of the solution in a 250 ml Erlenmeyer flask with a ground glass stopper.

23. Mix the solution with a magnetic stirrer, but not vigorously enough to aerate.
24. Assemble the pycnometer, holding it with Kimwipe tissues.
25. Prepare the balance by cleaning, levelling, and zeroing it.
26. Record the room temperature, barometric pressure and wet and dry bulb temperatures on a weighing form.
27. Using a wire holder, place the empty pycnometer in the 25.00°C water bath for 1 or 2 minutes. Remove and dry it with two Kimwipes.
28. Weigh the pycnometer immediately and record weight on form.
29. Recheck the temperature of the 25°C bath with the potentiometer and temperature-emf chart. Reset if necessary.
30. Chill the flask containing the sample liquid in the ice bucket for 30 seconds. Remove and dry with paper towel.
31. Return flask to stirrer and mix gently for one minute.
32. With a 100 ml syringe and Teflon tube, withdraw about 80 ml of sample liquid from flask, keeping tube well below surface of liquid.

33. Exchange tube on syringe for 18 gauge stainless steel needle and expel all air from syringe.
34. Discard the 2 or 3 ml of solution which has been in contact with air.
35. Fill cell, using filling tube away from corner, until all air is removed from sample chamber and both filling tubes are full of liquid.
36. Discard the next 2-3 ml from syringe and fill pycnometer rapidly without making bubbles or disturbing the surface.
37. Insert the pycnometer's capillary top, but do not cover. Handle only with Kimwipes.
38. Using wire holder, place pycnometer into rack in 25° water bath.
39. While the pycnometer is in the bath, seal the cell by sliding the glass walls between the plates just enough to close off the filling tubes.
40. Tighten the nuts on the cell with a small wrench, being very careful to avoid breaking the glass.
41. Turn on the recorders to monitor the plate temperatures.
42. Observe the meniscus on top of the pycnometer, and place the cover on when the liquid is level with the capillary top.
43. Remove the pycnometer from the bath and dry with two Kimwipes as before.

44. Immediately weigh the full pycnometer, and record the weight on form.
45. Return the contents of the pycnometer and syringe to the flask for use as a rinsing solution for the next run. Do not touch the pycnometer.
46. Place pycnometer parts in acid cleaner ($K_2Cr_2O_7$ - H_2SO_4) for several hours, then into distilled water.
47. Disassemble syringe and cover with tissues.
48. Let the cell and contents equilibrate for about an hour. Insulate from room air.
49. Use laser to realign interferometer if necessary.
50. Set the experiment timer to 0.00 min.
51. Take t = 0.00 photo for line spacing and shear measurements.
52. Close the bypass valves in the two T-45 baths.
53. Apply the temperature difference and start timer simultaneously. Change scale on recorder if necessary.
54. Open the bypass valve on the T-9 bath.
55. Realign the optics at t = 4 or 5 min when the temperature gradient has been established.
56. When t = 8 or 10 min begin measuring the fringe position at z = 0 with the microscope stage apparatus. Use intervals of 1, 2, or 5 min until t = θ.

Between measurements use the shutter to prevent light from passing through the cell.

57. Check the plate temperatures regularly, and record the emf's on the charts. Refill the ice bath each hour.
58. Take photos occasionally for fringe shape and spacing and note the time on the back of each.
59. Continue taking measurements of fringe position at intervals of 10-15 min until t = 50 or 60.
60. Obtain several steady state measurements for t > 60. Recheck temperatures.
61. Reset timer to 0.00 min.
62. Close the bypass on the T-9 bath.
63. Remove temperature difference and restart timer simultaneously.
64. Open bypass valves on T-45's.
65. Check recorders; switch scales if necessary.
66. Realign optics at t = 5 min.
67. Repeat measurements of fringe position versus time. Take desired photos. Continue until t > 50.
68. When finished, shut everything off unless another run is planned.
69. Dismantle the cell. Press wire pins through the filling tube against the glass wall assembly in order to prevent leakage of the liquid from the bottom.

70. Empty the sample chamber with a syringe. Clean both metal plates and glass.
71. Record all data.
72. Coat and record photos.
73. Punch data cards.

. Discussion of Procedures

Some of the steps in the procedure enumerated above equire additional comment. It was found to be necessary o turn on the water baths well in advance of an experiment ven though they reached their nominal temperatures within n hour. The extra time was needed to allow the bath hous- ng and insulation materials to reach steady temperatures. ecause of the common source of cooling water, the three aths were indirectly interconnected and had to be balanced gainst each other very delicately whenever a new tempera- ure range was set. During a series of experiments slight hanges in the mean temperature and/or the temperature dif- erence between runs arose primarily because of daily hanges in the room temperature.

All of the carbon tetrachloride used was obtained rom the same lot, as was all of the cyclohexane. The hemicals, in their one pint amber sealed bottles, were tored in their closed shipping cases, which were kept in n exhaust hood. The liquids were exposed to light only uring the preparation for and execution of an experiment.

Each bottle was used an average of six times, and each bottle of CCl_4 was always used in conjunction with only one bottle of C_6H_{12}. The last 50 to 100 ml of the contents were never used.

It was convenient to prepare a total volume of 100 ml of solution, measured before mixing. The cell contained approximately 35 ml, and the pycnometer required slightly more than 25 ml. The excess was used for rinsing the apparatus. The advantage of our weighing technique is that the composition of the mixture is determined at nearly the same time that the cell is filled, rather than much earlier or much later.

Materials with which the chemicals came into contact were: glass, stainless steel, Teflon, silver, and fluorosilicone sealant. Horne (1962) showed that cyclohexane is oxidized in air to form small amounts of cyclohexylhydroperoxide:

$$C_6H_{12} + O_2 \rightarrow C_6H_{11}O_2H \ . \qquad (5.5)$$

Copper and brass catalyze the reaction and consequently were avoided. The effects of the materials in contact with the sample mixture were tested by placing only one of the liquids at a time into the cell and applying a temperature difference to the pure component. In none of the cases was any thermal diffusion detectable interferometrically. We then concluded that no measurable amounts of thermally diffusing impurities were present in the mixtures.

The effectiveness of the sealant was checked simply
watching for the appearance of air bubbles inside the
mple chamber indicating evaporation. Specifically for
is purpose the cell was left filled on occasion for as
ng as five days, and no loss of the volatile liquid was
served. Several times the application of the temperature
fference caused a net contraction of the liquid in the
ll resulting in a very small amount of air being drawn
to the cell. The size of the bubble was less than that
a drop of water, say 0.05 ml, and its effect, if any,
s neglected. In the later experiments however, at a mean
mperature of 35°C, the increased vapor pressure of the
quid resulted in the formation of many pinpoint bubbles
the surface of the top metal plate during filling.
ese were shaken loose before the run was started, but
ey remained in one corner of the cell. It is doubtful
at they had any measurable effect because they comprised
ch a small fraction of the total volume and because they
d not appear in the center of the cell where the measure-
nts were taken.

By sliding the glass walls slightly between the metal
ates before tightening the retaining nuts, a better seal
s obtained, and there could no longer be any diffusion
rough the filling tubes. In addition, the temperature
stribution across the upper plate was improved by removing
e perburbation of the filling tubes from the area of interest.

The cell was filled while in the isothermal configuration so that the beginning of the experiment could be well defined. About one minute was required to fill the cell. After that the mixture was allowed to equilibrate for up to 1 hour both to insure a uniform temperature distribution and to permit decay of the effects of any thermal diffusion which may have occurred when the liquid came in contact with the metal plates during filling. In all of our experiments, zero time was clearly taken to be that instant at which the valves controlling the temperature configuration of the cell were switched.

When the 30° and 35°C runs were begun, we observed that the steadiness of the interference fringes was very sensitive to the air currents passing the cell. This happened because the temperature difference between the 35°C liquid and the 23° or 24°C air on the outside was sufficient to cause a horizontal heat flux through the glass walls. Thus the temperature distribution of the liquid was upset, and a slight tendency for convection was observed. This was eliminated in subsequent experiments by enclosing the space outside the glass sample chamber but between the metal plates. Strips of styrofoam insulation were held in place by black plastic tape. In the optical path before and after the cell, standard 1 in. × 3 in. glass microscope slides were used to keep out air currents. With the foam in place, the air between the metal plates could attain the mean temperature

30°C or 35°C, resulting in no observable effects due to a izontal heat flux through the cell walls. The fringe tern remained very stable.

Because of the cell height used and the value of the fusion coefficient of the CCl_4 - C_6H_{12} mixtures, the re- ation time θ was very nearly one hour, but varied slightly to the temperature and composition dependence of the ual diffusion coefficient. Consequently at least six rs were required to reach a steady state. Remixing upied another six hours, so no more than one run could attempted in a day. Including preparation time, nearly teen hours of practically uninterrupted attention were uired to complete a full experiment.

Published Data for CCl_4 and C_6H_{12}

The tables in this section summarize the essential a avilable in the literature for carbon tetrachloride, lohexane, and their mixtures. Authors and sources are ed where appropriate. From the results of Wood and Gray 52), shown in Table 5d, we obtain the following expres- ns related to the density of CCl_4 - C_6H_{12} mixtures.

$$\frac{1}{\rho} = a + bT + cT^2 + dT^3 \ , \qquad (5.6)$$

re T is the temperature in degrees C, and

$$a = 1.06913 - 0.59379\ w_1 + 0.08972\ w_1^2 + 0.00027\ w_1^4 \ ,$$

le 5d.--Densities of CCl_4 - C_6H_{12} mixtures (Wood and Gray, 1952).

$1/\rho = a + bT + cT^2 + dT^3$; T in Degrees C.					
Cl_4	a	10^3b	10^6c	10^9d	Std. Dev. $10^5\Delta(1/\rho)$
000	1.25479	1.4362	2.529	5.37	2.6
289	1.11832	1.3106	1.568	9.62	1.0
512	1.01133	1.1940	1.205	10.15	1.5
514	1.01141	1.1803	1.471	8.31	0.9
720	0.92189	1.0855	1.171	8.57	1.2
978	0.84224	0.9768	1.381	5.81	0.8
506	0.75911	0.9080	0.687	8.74	0.7
482	0.71306	0.8456	0.777	7.68	0.5
475	0.71332	0.8479	0.790	7.12	0.9
716	0.66057	0.7946	0.528	7.92	0.9
000	0.61233	0.7294	0.722	5.52	1.4

$\rho^3 b = 1.25048 - 0.67403\ w_1 + 0.10391\ w_1^2 - 0.00034\ w_1^4$,

$\rho^6 c = 1.47942 - 1.11122\ w_1 + 0.12049\ w_1^2 + 0.00009\ w_1^5$,

$\rho^9 d = 7.71$.

e have also,

$$\partial\ \ell n\ \rho/\partial T)_{w_1} = ab + (2ac + b^2)T + 3(ad + bc)T^2 + (4bd + 2c^2)T^3 + (3cd + 2bc)T^4 + 3bdT^5 , \quad (5.7)$$

$$\partial\ \ell n\ \rho/\partial w_1)_T = \rho\left(\frac{da}{dw_1} + T\ \frac{db}{dw_1} + T^2\ \frac{dc}{dw_1} + T^3\ \frac{dd}{dw_1}\right) . \quad (5.8)$$

he relationship which we used to determine the mass fraction of CCl_4 in a mixture of known density at 25°C is:

$$(w_1)_{25°} = 1.99014 - 0.01505\rho - 1.53114\rho^{-1} . \quad (5.9)$$

his expression was obtained by fitting the data of Table d to a polynomial for w_1 in terms of ρ. The curve fitting outine MULTREG was used. See Appendix H.

Table 5e contains reported values of the refractive ndices of each of the pure components at various temperatures (in degrees Centigrade) and wavelengths (in Angstroms). sing MULTREG, we obtained the following expressions.

or CCl_4:

$$= 1.44299 - 5.754 \times 10^{-4}(T - 25) + 0.00499(\lambda \times 10^{-4})^{-2} . \quad (5.10)$$

he standard errors of the two coefficients are 8.3×10^{-6} nd 4.3×10^{-5}, respectively.

le 5e.--Pure component refractive indices. (Timmermans, 1950, 1959). (International Critical Tables, 1933)

CCl_4			C_6H_{12}		
°C	λ,Å	n	T,°C	λ,Å	n
3	6563	1.4599	10.85	6563	1.42910
0	6563	1.46005	13.5	6563	1.42777
0	6563	1.4576	15.0	6563	1.42670
0	6563	1.45461	16.1	6563	1.42626
3	5893	1.4656	20.0	6563	1.4242
0	5893	1.4631	20.0	6563	1.42405
0	5893	1.46305	25.0	6563	1.42134
0	5893	1.46325	44.6	6563	1.41056
0	5893	1.46005	10.85	5893	1.43119
0	5893	1.46044	14.8	5893	1.4292
0	5893	1.4602	15.0	5893	1.42886
0	5893	1.46023	20.0	5893	1.42623
0	5893	1.46026	20.0	5893	1.42615
0	5893	1.46036	20.0	5893	1.4262
0	5893	1.45704	20.0	5893	1.42637
0	5893	1.45732	20.0	5893	1.42630
0	5893	1.45759	20.0	5893	1.4263
0	5893	1.45732	25.0	5893	1.42358
0	5893	1.4576	25.0	5893	1.42354
0	5677	1.45833	25.0	5893	1.4233
5	5460	1.46086	30.0	5893	1.4210
3	4861	1.4726	25.0	5876	1.41825
0	4861	1.46970	25.0	5677	1.42440
0	4861	1.46400	23.5	5460	1.42643
0	4686	1.47405	10.85	4861	1.43668
3	4340	1.4835	13.5	4861	1.43531
0	4340	1.47530	15.0	4861	1.43430
0	4340	1.46954	16.1	4861	1.43381
			20.0	4861	1.54157
			25.0	4861	1.42878
			44.6	4861	1.41785
			15.0	4686	1.43762
			10.85	4340	1.44116
			13.5	4340	1.43972
			15.0	4340	1.43870
			16.1	4340	1.43820
			20.0	4340	1.43592
			25.0	4340	1.43310
			44.6	4340	1.42214

C_6H_{12}:

$$1.41215 - 5.337 \times 10^{-4}(T-25) + 0.00395(\lambda \times 10^{-4})^{-2} - 5.3 \times 10^{-6}(T-25)(\lambda \times 10^{-4})^2 \qquad (5.11)$$

standard errors are 6.6×10^{-6}, 1.8×10^{-5}, and $\times 10^{-6}$, respectively.

Table 5f contains refractive index measurements at C and 6563Å for mixtures of carbon tetrachloride and lohexane. From those reported values we obtain the fol- ing expression for the composition dependence of refrac- e index:

$$n_1w_1 + n_2w_2 - .02146w_1w_2[1 + 2.68048w_1^2 - 4.35141w_1^3 - 2.01856w_1^4] , \qquad (5.12)$$

re n_1 and n_2 are respectively, the refractive indices of e CCl_4 and pure C_6H_{12} at the temperature and wavelength ired.

The few measurements of thermal conductivity which available for the two compounds are shown below. The ues for water are also shown because water was used to ibrate the interferometer. We used the following ex- ssions for thermal conductivity:

water:

$$\kappa = 1.429 \times 10^{-3} + 3.5 \times 10^{-7}(T-20) \qquad (5.13)$$

ble 5f.--Composition dependence of refractive index in mixtures of CCl_4 and C_6H_{12} at 20°C and 6563Å. (Timmermans, 1959)

x_{CCl_4}	w_{CCl_4}	n
0.00	0.00	1.4242
0.10	0.17	1.4268
0.20	0.33	1.4297
0.30	0.45	1.4326
0.40	0.57	1.4359
0.50	0.66	1.4393
0.60	0.75	1.4425
0.70	0.82	1.4460
0.80	0.89	1.4497
0.90	0.95	1.4535
1.00	1.00	1.4576

or CCl_4:

$$\kappa = 2.47 \times 10^{-4} - 4.5 \times 10^{-7}(T-20) \qquad (5.14)$$

or C_6H_{12}:

$$\kappa = 3.2 \times 10^{-4} \qquad (5.15)$$

nits of κ are cal/(sec)(cm^2)(°C/cm). (From the Handbook f Chemistry and Physics, 44th ed.)

Table 5g contains measured values of the mutual diffusion coefficient D for mixtures of CCl_4 and C_6H_{12}. The esults of Kulkarni, Allen, and Lyons (1965) were chosen ver those of Hammond and Stokes (1955). Our values of $_1$ are not sensitive to the choice of D. We used the following expression for the "literature" diffusion coefficient:

$$D \times 10^5 = 1.481 - 0.201x_1 + 0.0258(T-25) , \qquad (5.16)$$

here x_1 is mole fraction CCl_4, and T is temperature in egrees C. Units of D are cm^2 sec^{-1}.

Table 5h summarizes previously reported values of he thermal diffusion factor α_1 at various temperatures nd compositions for mixtures of CCl_4 and C_6H_{12}.

The data of Horne are incorrect because no account as been taken for the temperature distribution in the eservoirs (Beyerlein, 1968). The results of Thomaes 1951) were probably vitiated by convection. The data of orchinsky have been obtained without correction for the forgotten effect," and the diffusion coefficients of ammond and Stokes (1955) contributed a small error.

able 5g.--Ordinary diffusion coefficient for CCl_4 - C_6H_{12} mixtures (Kulkarni et al., 1965).

x_1	$D \times 10^5$ cm^2 sec^{-1}	x_1	$D \times 10^5$ $cm^2 sec^{-1}$
	25°C		
.01655	1.481	0.697_5	1.328
$.0251_0$	1.481	0.795_8	1.311
$.0713_4$	1.476	0.933_3	1.295
$.173_9$	1.447	0.974_4	1.285
$.300_2$	1.417	0.985_3	1.287
$.398_8$	1.393	0.023_7	1.768
$.486_8$	1.374	0.475_0	1.633
$.605_3$	1.351	0.976_4	1.515

le 5h.--Thermal diffusion factor x_1; previous results for mixtures of CCl_4 - C_6H_{12}.

m Turner et al. (1967), T = 25°C			
l	$-\alpha_1$	x_1	$-\alpha_1$
15	2.16	.724	1.71
9	1.83	.730	1.72
9	1.78	.898	1.66
0	1.77	.904	1.70
6	1.78	.947	1.65
4	1.77	.9882	1.76
9	1.74	.530	(35.1°C) 1.60
m Beyerlein (1968), T = 25°C			
l	$-\alpha_1$	w_1	$-\alpha_1$
5	1.84	.65	1.75
5	1.85	.80	1.71
0	1.88	.95	1.77
m Thomaes (1951), T = 26.13°C			
l	$-\alpha_1$	w_1	$-\alpha_1$
5	2.10	$.50_5$	1.45
9	1.72	$.60_5$	1.38
0	1.80	.78	1.20
7_5	1.68	.87	1.17
3	1.62	.95	1.08
6	1.56		

le 5H Continued

m Tichacek et al. (1956), T = 40°C

w_1	$-\alpha_1$
$.31_3$	1.30
$.64_6$	1.27
$.87_9$	1.25

m Korchinsky (1965), T = 25°C

w_1	$-\alpha_1$
.50	1.82
.80	1.74

m Horne (1968), T = 25°C

1	$-\alpha_1$	w_1		$-\alpha_1$
0	1.86	.495	(28°C)	1.98
0	1.94	.649		1.88
9	1.92	.796		1.81
0	1.88	.946		1.92

. Calibration of Interferometer

The constant A in Eqs. (4.20) is the fringe displacement per unit refractive index gradient. It depends on the avelength of the light used, the path length through the ell, the amount of shear, the focal lengths of various enses and the distance between the last lens and the image lane where measurements are made. Because so many factors re involved, A is best determined experimentally. The ogical method is to measure the fringe displacement caused y a known refractive index gradient. The value of A thus alculated is valid only for the particular optical configuration used. If any of the lenses is moved, either A ust be remeasured, or some relationship between the values f A for the two arrangements must be known.

For our calibration we chose as a source of a known efractive index gradient a layer of water (in the cell) ontaining a known temperature gradient. The calibration xperiment consisted simply of filling the cell with distilled water, letting it equilibrate for about 15 minutes, nd then applying a vertical temperature difference with he warmer temperature on top. The motion of the fringe attern was observed on the ground glass plate of the amera. Measurements were made with the microscope stage described below) and from photographs. Six trials were ade with water. Sample calculations are presented here.

Temperature Difference: $\Delta T = 3.817$ deg C

Cell Height: $a = 0.741$ cm

Final Temperature Gradient at $z = 0$:

$$(dT/dz)_0 = \Delta T/a = 5.151 \text{ deg cm}^{-1}$$

Temperature Coefficient of Refractive Index at 25°C: $(dn/dT)_{25} = -9.80 \times 10^{-5} \text{ deg}^{-1}$

Final Refractive Index Gradient at $z = 0$:

$$(dn/dz)_0 = (dn/dT)_{25}(dT/dz)_0 = -5.05 \times 10^{-4} \text{ cm}^{-1}$$

Fringe Displacement at $z = 0$: 15.70 cm

$$d_0(\infty) = A(dn/dz)_0 = 15.70 \text{ cm}$$

$$A = -3.11 \times 10^4 \text{ cm}^2$$

The six experiments with water gave

$$A = -(3.11 \pm 0.03) \times 10^4 \text{ cm}^2.$$

Displacement of a lens for focusing changed not
y A but also the fringe spacing r. According to
ngdahl (1963), the apparatus constant A is related to
y

$$A = Lr/\lambda \ , \qquad (5.17)$$

re L is a function of cell length, lens focal lengths,
ar, and various distances. Since the wavelength, cell
gth, shear, and lens dimensions all remained the same
all of our experiments, any change in A due to lens
ement could be calculated from the change in fringe
cing. For our original calibration, the spacing was
4 cm. Thus, in more general form, we have

$$A = -(3.11 \pm 0.03)\ \frac{r}{1.74} \times 10^4\ \text{cm}^2\ . \qquad (5.18)$$

Methods of Calculation

Raw data from each experiment consisted of tempera-
e measurements and measurements of the interference fringe
pe and position. All of the information about the upper
lower plate temperatures was recorded on the strip
rts. The particular quantities available were the warm-
up parameters t_h and t_c, the steady temperature differ-
e, the initial, mean, and final temperatures, and
perature fluctuations.

The parameters t_h and t_c were the same for all of
pure thermal diffusion experiments. The initial tem-
ature was inconsequential as long as it did not differ
nificantly (more than 0.5 deg) from the mean temperature.
applied temperature difference ΔT and the mean tempera-
e T_m varied for different experiments and were carefully
orded. For the purpose of error analysis, a record was
o kept of temperature fluctuations. The continuously
rating strip chart recorders showed automatically any
perature drifting which would invalidate experimental
ults.

Information concerning the gradient of refractive
ex inside the cell was obtained in two forms: photo-
phs of interference fringes, and direct measurements of
nge displacements. The photographs had the advantage

providing a permanent record of both the shape and the
sition of the fringes at certain specified times.

The device with which the photographs were analyzed
nsisted of an aluminum block for a base, a clamp to hold
ch photograph in place, and a standard, adjustable,
aduated microscope stage which could be moved in two
rections. A precision magnifier, with a reticle contain-
g several scales, was mounted on a 1 x 3 inch glass slide
ld in place by a lever on the mechanical stage. A parti-
lar point on the photograph could be sighted through the
gnifier, and its coordinates could be read from the
rnier scales of the stage. The distance to a second
int was readily found by comparing its coordinates with
ose of the first. In such a way, the shape of the fringe
s characterized by a set of horizontal displacement x,
ch corresponding to a certain height η in the cell.
ually, 29 pairs of coordinates were recorded at intervals
0.1 cm vertically. The data were fit (by MULTREG) to the
lynomial

$$x(z,t) = \sum_{k=0}^{5} d_k(t)\eta^k \quad , \tag{5.19}$$

ere the dimensionless vertical coordinate η is related to
y

$$\eta = \frac{2z}{(1 - s)a} \quad , \tag{5.20}$$

here s is the amount of shear (0.19), measured from the hotograph, and

$$-1 \leq \eta \leq 1 \ . \qquad (5.21)$$

The coefficients $d_k(t)$, k = 1,...,5, were obtained y curve fitting. See Appendix H. The five terms of Eq. 5.19) fit the data to within measuring error.

At this point the data consisted of five coeffi- ients d_k, k = 1,...,5, for each value of time at which a hotograph was taken. Equations (4.15) and (4.21) provide he necessary relationships for calculating the various erivatives of the refractive index from the measured alues of the d's. In Table 5i are representative measure- ents of fringe shape taken directly from photograph No. 155 or run B5. Figure 5.1 shows a plot of the same data to- ether with the smooth curve expressed by Eq. (5.19), where he five calculated coefficients and their respective stan- ard errors are

k	d_k	Std. Error
1	0.492	0.028
2	4.47	0.030
3	0.732	0.053
4	0.566	0.016
5	2.68	0.022

leasurements of the fringe shape yield a great deal of in- formation. With them one can calculate simultaneously he temperature and composition dependences of the thermal iffusion factor and the thermal conductivity. With

able 5i.--Measurements of fringe shape. Run B5, t = 70.00 min, photo No. 155.

η	x,cm	η	x,cm
.686	1.825	-0.049	0.009
.637	1.576	-0.098	0.064
.588	1.350	-0.147	0.140
.539	1.150	-0.196	0.250
.490	0.932	-0.245	0.372
.441	0.732	-0.294	0.502
.392	0.565	-0.343	0.730
.343	0.432	-0.392	0.922
.294	0.311	-0.441	1.097
.245	0.210	-0.490	1.350
.196	0.112	-0.539	1.584
.147	0.052	-0.588	1.900
.098	0.014	-0.637	2.280
.049	0.002	-0.686	2.815
.000	0.000		

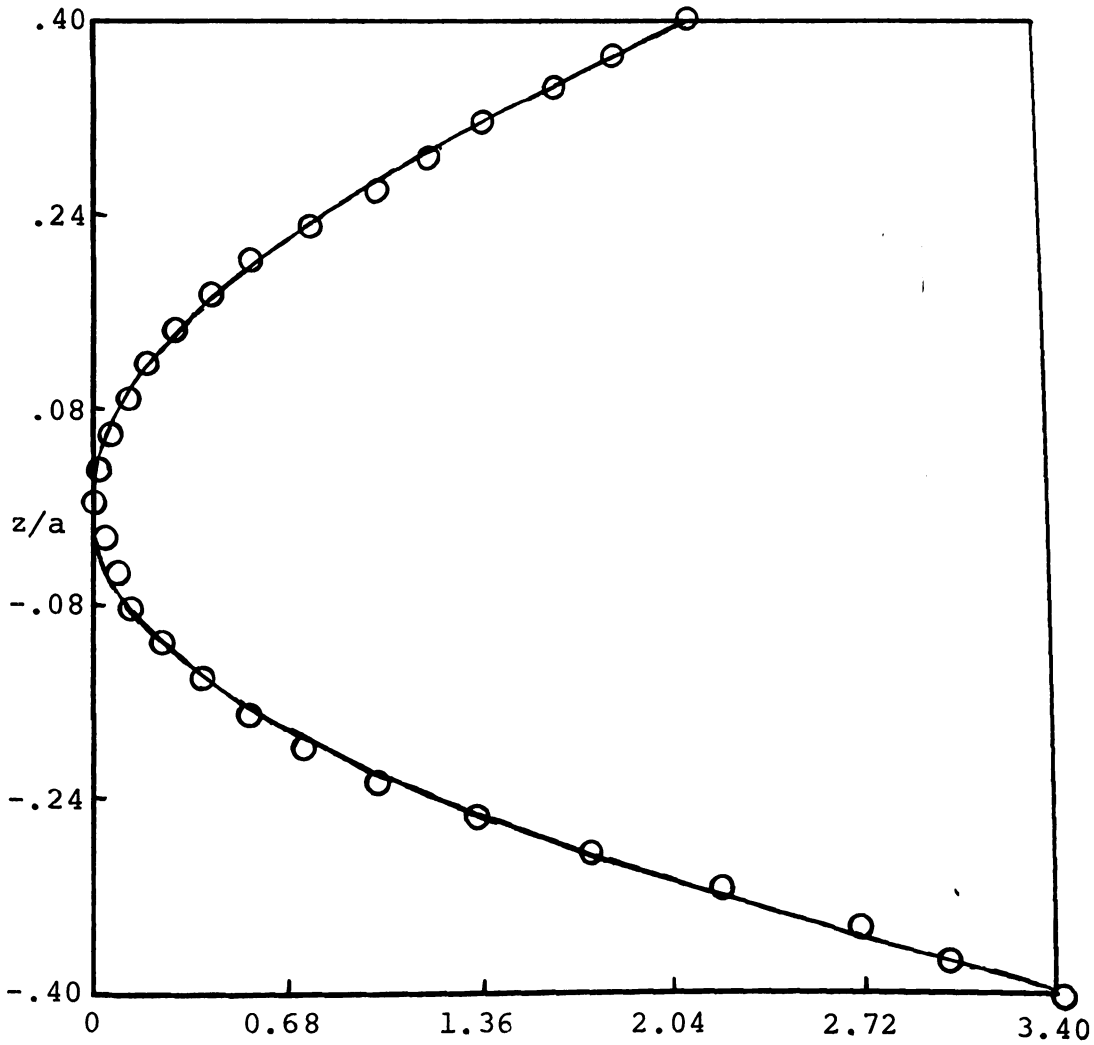

Figure 5.1--Plot of measured fringe shape (circles) showing agreement with fifth-order polynomial (solid line).

sufficient sensitivity, such measurements could also permit calculation of the heat of transport. One requires accurate refractive index data, however, in order to extract information from the fringe shape. As we show below, the refractive index data in the literature are too poor to be used with any reliability in measurements of this type.

Since we were interested only in measuring α_1 and D, we were able to use the second type of measurement, that of fringe displacement at z = 0. These measurements were obtained by means of the same microscope stage mounted directly on the ground glass plate of the camera. Operated vertically, the stage held a 1 x 3 inch glass slide which was marked in black ink with a cross to be used as a reference point. Nearly an inch of clear plexiglass separated the glass slide from the viewing plate on which the fringe image appeared. Parallax errors were eliminated by requiring simultaneous alignment of the fringe image, the cross mark, and the reflection of the cross mark in the glass plate.

At prescribed or convenient intervals of time, varying in length from 30 seconds to 20 minutes or more, as indicated by the timer which was started at t = 0, measurements of the fringe position at z = 0 were taken and recorded along with the time. The fringes in this method were characterized by a set of numbers $d_0(t)$. With this method, many more data points could be measured efficiently, and once they were recorded, no further treatment was

equired. The d_0's were converted to measurements of the efractive index gradient by means of Eq. (4.20). Typical ringe displacement data are given in Table 5j. Figure 5.2 hows a plot of the demixing data from Table 5j and a curve f the form

$$d_0 = X_1' \exp(-X_2 t) + X_3' \tag{5.22}$$

btained by means of a least squares treatment.

The coefficient d_0, which depends mainly on $(\partial n/\partial z)_0$, assumes a much wider range of values than does ny of the higher order coefficients d_1, d_2..., and is a etter source of accurate measurements. Moreover, d_0 is ess sensitive than the other coefficients to transient efractive index changes due to fluctuations in the metal late temperatures.

From Eq. (4.20) we have

$$d_0 = A\left[c_1 + \frac{1}{4} c_3 a^2 s^2 + \frac{1}{16} c_5 a^4 s^4 + \ldots\right] + B . \tag{5.23}$$

By virtue of the solutions $T(z,t)$ and $w_1(z,t)$, discussed in Chapter III, and the chain rule for differentiation, we have expressions for c_k, $k = 1,2,\ldots$, in terms of the experimental transport parameters α_1, D, and κ_i. In particular, we have

$$c_1 = (\partial n/\partial T)_{w_1} (\partial T/\partial z)_0 + (\partial n/\partial w_1)_T (\partial w_1/\partial z)_0$$

Table 5j.--Fringe position $d_0(t)$ for run F6.

t, min.	c_0,† cm	t	d_0	t	d_0
Demixing:		130	9.41	20	7.49
10	4.76	140	9.46	25	7.10
15	4.95	150	9.74	30	6.84
20	5.38	160	9.58	35	6.50
25	5.71	170	9.80	40	6.22
30	5.97	180	9.82	45	5.85
35	6.22	190	9.85	50	5.59
40	6.54	200	9.90	55	5.32
45	6.75	212	9.93	60	5.15
50	7.13	222	9.95	72	4.72
55	7.30	250	9.96	85	4.48
60	7.63	252	9.97	98	4.12
65	7.90	266	9.96	112	3.88
71	8.16	280	9.99	128	3.66
75	8.39	300	10.07	155	3.31
80	8.45	314	10.07	170	3.23
90	8.66	364	10.07	192	3.14
100	8.78	Remixing:		212	3.06
110	9.11	10	8.18	230	3.04
120	9.31	15	7.87	256	3.00
				273	2.96

†The reference point is arbitrary.

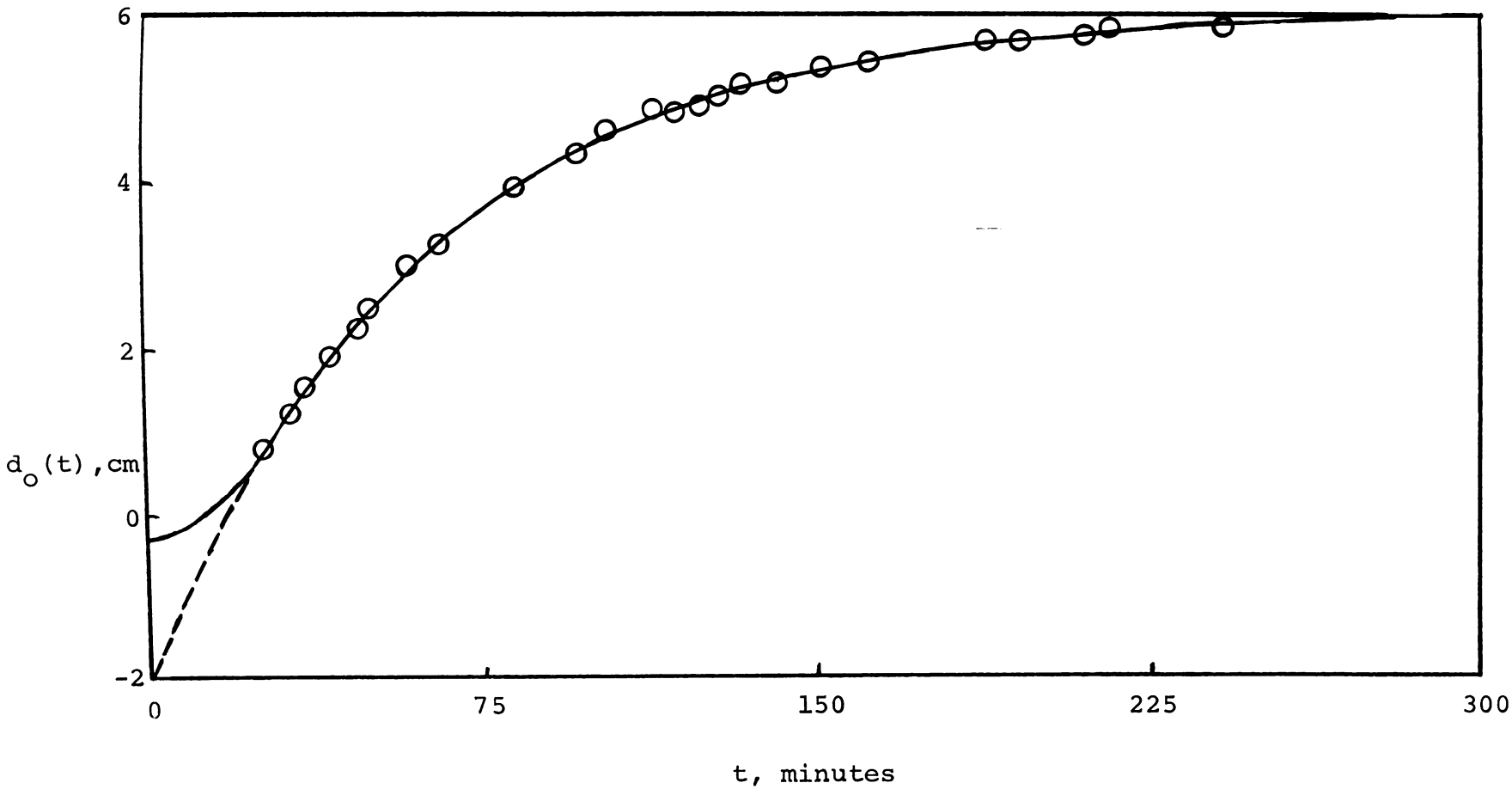

Figure 5.2--Plot of fringe displacement at z = 0 as a function of time (circles) and least squares curve. Dotted line shows improper extrapolation.

$$
\begin{aligned}
{}_3 = {} & (\partial n/\partial T)_{w_1}(\partial^3 T/\partial z^3)_0 + (\partial n/\partial w_1)_T(\partial^3 w_1/\partial z^3)_0 \\
& + 3(\partial^2 n/\partial T^2)_{w_1}(\partial T/\partial z)_0(\partial^2 T/\partial z^2)_0 \\
& + 3(\partial^2 n/\partial w_1^2)_T(\partial w_1/\partial z)_0(\partial^2 w_1/\partial z^2)_0 \\
& + (\partial^3 n/\partial T^3)_{w_1}(\partial T/\partial z)_0^3 \\
& + (\partial^3 n/\partial w_1^3)_T(\partial w_1/\partial z)_0^3 \, . \qquad (5.24)
\end{aligned}
$$

The N experimentally measured fringe displacements (t_i), i = 1,..., N, coincide with the function in Eq. .23) when proper values are chosen for α_1, κ_i, D, and B. practice we confined our measurements to values of time rge enough so that the temperature distribution was not anging. Then, by expressing all of our measurements as fferences, e.g., $d_0(t_2) - d_0(t_1)$, both B and the terms volving temperature disappear. Terms involving products derivatives are certainly negligible, since the maximum lue of $|(\partial w_1/\partial z)_0|$ is about 5×10^{-3} cm^{-1}. When the lution $w_1 = w_1^* + G$ from Chapter III is inserted where eded, we obtain the final working equation

$$d_0(t) - g_1(t) = X_1 \exp(-X_2 t) + X_3 \, , \qquad (5.25)$$

ere $d_0(t)$ represents the measured values of the fringe splacement at z = 0 relative to some reference point (t_r); $g_1(t)$ is a correction term given by Eq. (3.68); d the x_j, j = 1,2,3, are given by

$$X_1 = \frac{\alpha_1}{T_m} \Delta T w_1^0 w_2^0 \frac{2}{\pi^3} S_0' \ , \qquad (5.26)$$

is the derivative of the first term of S (Eq. 3.8) with spect to z, evaluated at z = 0, and multiplied by $e^{-t/\theta}$.

$$X_2 = \theta^{-1} = \pi^2 D/a^2 \ , \qquad (5.27)$$

d

$$X_3 = d_0(t_r) - g_1(t_r) - X_1 \exp(-X_2 t_r) \ . \qquad (5.28)$$

Our method of analysis consisted of fitting the inge position data to a function like Eq. (5.25) and timizing the coefficients X_1, X_2, and X_3 according to least squares criterion. (See PROGRAM ALPHA in Appendix) The thermal diffusion factor α_1 was calculated from e numerical value of X_1 by means of Eq. (5.26), and the dinary diffusion coefficient D was calculated from X_2 d Eq. (5.27).

Besides giving values for both α_1 and D, our curve tting method has the advantage of smoothing the data and mbining all of the measurements from an experiment to tain a single set of results and an estimate of the andard deviation.

Another approach could have been used if it were t desired to determine D, or if only a few data pairs vering a short period of time were available. If we had ed a literature value for D, the time dependence of $d_0(t)$

uld have been fixed (since $\theta = a^2/D\pi^2$). In that case, a ngle difference $d_0(t_2) - d_0(t_1)$ would have sufficed to de- rmine α_1.

The time dependence of $d_0(t)$ is shown in Figure 2. The tailing off for $t < \theta/4$ reflects the fact that e infinite Fourier series solution for $w_1^*(z,t)$ does not nverge rapidly for $t < \theta/3$. If only the leading term of e series is retained, one gets the function shown by the tted line. The figure shows clearly that if one wishes include in his measurements data for $t < \theta/3$, enough rms of the Fourier series must be retained to insure nvergence to within some specified tolerance. The dis- vantage in this case is that the simple form of Eq. .25) is not obtained.

If, on the other hand, only the first term of the urier series is retained, one must be certain to use ly data corresponding to $t < \theta/3$.

Table 5k shows a sample laboratory notebook record a pure thermal diffusion experiment.

ble 5k.--Sample laboratory notebook record of a pure thermal diffusion experiment.

te:	4-23-68		
n:	F6, CCl_4 - C_6H_{12}, x_1^o = .250, w_1^o = .406		
T_h	37.008 ± 0.004°C		
T_c	33.032 ± 0.004°C		
T	3.976 ± 0.008°C		
T_m	35.020 ± 0.004°C		
T_f	34.950 ± 0.004°C		
A	$-3.11 \cdot 10^4$ cm^2	a	0.741 cm
θ	64 min		
D	$1.4 \cdot 10^{-5}$ cm^2 sec^{-1}	s	0.19

arting Time: 12:57 pm ; 7:03 pm.

otos: 290

arts: 105

marks: After about two hours of continuous operation, the ser generated enough heat to cause the frame to expand ightly, causing the mirror alignment to change and resulting in a gradual diminishing in the light beam intensity. e trouble was corrected by making an adjustment in the tension on the retaining rings holding the mirrors in place.

CHAPTER VI

EXPERIMENTAL RESULTS

. Tabulation of Data

Table 6a summarizes the results of our experiments. ach run is identified by a code consisting of a letter, a umber, and another letter. The first letter (A through H) enotes the bottles from which the chemicals were obtained. lthough the same lot number in every case was used for ach of the liquids, a record was kept of the particular ottle used, and the CCl_4 from any one bottle was mixed nly with the C_6H_{12} from the corresponding bottle. Some of he early sets of runs (A through D) either were trials r showed poor temperature control.

The second figure in the code is a number (1 through) which denotes the number of the run in the series. sually, each chemical bottle was used about six times in reparing new mixtures. The last letter in the code is ither D or R, corresponding to demixing or remixing, hichever is appropriate for that tun. Not every number ppears with both a D and an R. The final two experiments, or example, which were conducted with temperature

ble 6a.--Summary of experiments.

n	Date 1968	Num	T_m	w_1^o	x_1^o	ΔT	$Dx10^5$	$-\alpha_1$
R	5-13	29	293.42	.40731	.25867	4.147	1.304	1.856
R	5-14	24	293.04	.67369	.51178	4.160	1.228	1.784
D	5-15	28	293.00	.86107	.75886	4.152	1.230	1.741
R	5-15	20	293.06	.86107	.75886	4.152	1.234	1.714
R	3-21	33	298.22	.18045	.10055	4.066	1.463	1.777
D	3-7	44	298.14	.27577	.16201	4.040	1.451	1.840
R	3-7	40	298.22	.27577	.16201	4.040	1.511	1.812
D	3-8	46	298.14	.27577	.16201	4.064	1.503	1.785
R	3-8	43	298.22	.27577	.16201	4.064	1.420	1.777
D	3-6	30	298.20	.34326	.20972	4.178	1.492	1.810
R	3-6	37	298.27	.34326	.20972	4.178	1.415	1.778
D	3-5	42	298.26	.39899	.25209	4.194	1.481	1.778
R	3-5	40	298.26	.39899	.25209	4.194	1.494	1.763
R	5-10	31	298.16	.40731	.25867	4.077	1.438	1.841
D	2-5	36	298.16	.41454	.26444	4.058	-	1.754
D	3-1	31	298.08	.46666	.30760	3.970	-	1.793
R	3-1	42	298.24	.46666	.30760	3.970	1.437	1.752
D	2-26	44	298.16	.57738	.40957	4.100	1.402	1.761
R	1-30	50	298.21	.58439	.41655	4.170	1.316	1.739
D	2-23	37	298.19	.63477	.46878	4.108	1.422	1.757
R	2-23	36	298.24	.63477	.46878	4.108	1.385	1.732
D	5-8	36	298.22	.67269	.51065	4.114	1.424	1.759
R	5-8	30	298.17	.67269	.51065	4.114	1.375	1.721
D	2-9	64	298.22	.67465	.51287	4.160	1.331	1.734
D	3-11	42	298.14	.71725	.56293	4.088	1.388	1.720
R	3.11	41	298.20	.71725	.56293	4.088	1.374	1.706
D	2-13	66	298.20	.75781	.61371	4.146	1.326	1.702
R	2-13	22	298.19	.75781	.61371	4.146	1.396	1.698
D	3-12	39	298.14	.79224	.65942	4.076	1.377	1.705
R	3-12	46	298.20	.79224	.65942	4.076	1.301	1.702
D	3-13	44	298.15	.85922	.75603	4.063	1.340	1.699
R	3-13	42	298.18	.85922	.75603	4.063	1.371	1.722
D	5-9	38	298.22	.86074	.75835	4.098	1.361	1.683
R	5-9	28	298.16	.86074	.75835	4.098	1.368	1.653
R	5-16	32	298.16	.86107	.75886	7.922	1.309	1.691
R	5-17	29	298.20	.86107	.75886	12.092	1.322	1.728
D	3-18	44	298.16	.89337	.80967	4.082	1.332	1.682
R	3-18	31	298.19	.89337	.80967	4.082	1.316	1.678
D	3-19	29	298.15	.91520	.84568	4.047	1.307	1.643
R	3-19	30	298.16	.91520	.84568	4.047	-	1.698
D	5-6	30	303.15	.40669	.25818	3.812	1.536	1.757
R	5-6	33	303.17	.40669	.25818	3.812	-	1.753
D	4-30	29	303.10	.67307	.51108	4.015	1.440	1.669

able 6a Continued

an	Date	Num	T_m	w_1^o	x_1^o	ΔT	$Dx10^{-5}$	$-\alpha_1$
1R	4-30	23	303.15	.67307	.51108	4.015	1.563	1.668
2D	5-2	26	303.07	.86049	.75797	3.912	1.451	1.633
2R	5-2	29	303.16	.86049	.75797	3.912	1.520	1.622
5D	4-23	33	308.21	.40775	.25902	4.036	1.673	1.713
5R	4-23	28	308.11	.40775	.25902	4.036	1.657	1.702
5R	4-22	37	308.11	.40818	.25936	3.950	1.715	1.682
2R	4-12	18	308.16	.67382	.51193	3.538	1.674	1.627
4D	4-18	26	308.29	.67403	.51216	3.700	1.671	1.623
4D	4-18	28	308.11	.67403	.51216	3.700	1.613	1.665
3D	4-15	33	308.52	.86135	.75928	3.514	1.609	1.589
3R	4-15	30	308.16	.86135	.75928	3.514	1.619	1.569

differences of 8°C and 12°C, were not studied during demixing because the large temperature gradients produced refractive index gradients great enough to deflect the light beam out of the optical components of the interferometer. For those experiments, the demixing was allowed to continue unobserved until $t = 6\theta$. Then the temperature difference was removed, and the isothermal remixing was monitored in the usual way. The number of measurements of fringe position for each run is recorded in the column labelled Num.

B. Error Analysis

Systematic Errors

In this section several possible sources of systematic error are discussed. (1) Uncertainties in w_1^o. Our technique for determining the initial composition w_1^o is based on the assumption that the liquid in the filled cell has the same composition as that in the filled pyconmeter. We tried to achieve that condition by filling both vessels from the same syringe with the smallest time lapse possible. Of course, evaporation occurred during the filling, but we do not attribute a significant error to that for the following reasons. First, differential evaporation of the two components, acting to change w_1^o, should occur in both containers. Second, such evaporation takes place only at the surface of the liquid, and by overfilling we discarded in both cases that portion of the liquid which was exposed to air during

lling. Other systematic errors due to balance inaccuracies re effectively cancelled out since we always measured mass fferences. Probably the most significant source of sys- matic error in the determination of w_1^o was the possible esence of impurities in the pure reagents. Both CCl_4 and H_{12} were used without further purification. If, however, ch had nearly the same amount of impurities by weight, eir net effect very nearly cancelled in the calculation the mass fraction. We consider the possible effect of purities on thermal diffusion below. An error of 0.01°C the temperature of the bath in which the pycnometer was aced would lead to a systematic error in w_1^o of less than $\times 10^{-5}$. We estimate that the effect of any systematic ror here is less than 0.01% of w_1^o and thus contributes ss than 0.01% to α_1.

(2) Uncertainty in T. The only significant systematic rors in T arose when the plate temperatures drifted due loss of bath control. Consequently, because those errors re obvious and large, we discarded the results of those periments.

(3) Uncertainties in cell geometry. Because of ne nature of our cell, the spacing between the plates did ot change with ΔT as it does in thermogravitational columns, or example. The cell height depends only on the thickness the glass wall assembly and on the amount of sealant

tween the glass and the metal. Throughout our experiments
followed the same procedure for cleaning and replacing
e glass, for applying the sealant, and for tightening
e bolts holding the cell together. We found no change in
e height of the cell during the course of our experiments.
is highly unlikely that any vibrations transferred to the
ll through its 3000 lb. support were significant.

(4) Impurities. We discussed above the influence
w_1^o of impurities present in the reagents. Those initial
purities may also thermally diffuse. We tested for such
effect by placing one of the liquids, either carbon
trachloride or cyclohexane, into the cell and applying
temperature difference. The steady temperature gradient
s established within five minutes. During the next six
urs, no further change in the position of the interference
inges was observed except that attributable to temperature
uctuations. Since the interferometer was capable of de-
cting composition gradients of the order of 1×10^{-5} cm^{-1},
estimate that any impurities present (including cyclo-
xylhydroperoxide and phosgene) contributed less than 0.1%
the steady state composition gradient and hence less
an 0.1% to α_1.

A second type, accumulated impurities, may be formed
the mixture in the cell. Reactions between the components
the solution, reactions with the metal plates, and re-
tions with or dissolution of the sealant would cause an

lation of impurities, even after t = 60. We found,
r, that all of our experiments reached a true steady
(to within the sensitivity of the interferometer),
ting that if accumulated impurities were present they
ot detectable.

(5) Convection. Previous pure thermal diffusion
ments have often been questionable on the grounds
convective remixing caused incorrect results. We
e that our isothermal remixing experiments were
tely free from convection, first, because no tempera-
difference existed, and there was no possibility for
tion to be induced by density inversions due to
ontal components of the temperature gradient. Second,
the uninsulated cell at T_m = 35.00°C the fringe pat-
was highly unstable and moved erratically. Since the
plate temperatures remained constant to within 0.005°C
25°C), we attributed the phenomenon to convection
panying the horizontal heat transfer from the liquid
cooler room air. This claim was substantiated when
sulated the cell with styrofoam. The same experimental
ions produced stable (non-fluctuating) fringes, be-
the air surrounding the cell was allowed to reach the
emperature distribution as the liquid in the cell,
ating the horizontal heat flux.

Bartelt (1968) is investigating the degree of in-
de required to produce convection due to heat loss

in through the vertical walls. In the meantime, our ferometric observations of convection (or the lack of nd the essential agreement of our results for demixing emixing techniques lead us to conclude that the demix- xperiments were also not affected by convection.

(6) Uncertainty in the calibration of the inter- eter. We chose water for the calibration because the rature dependence of its refractive index is known r than that of either carbon tetrachloride or cyclo- e. Also, the thermal conductivity of water is better cterized, and thus the temperature gradient in water own more accurately. Hence the refractive index gra-, and consequently the apparatus constant, could be fied with the greatest accuracy. The limiting factor e accuracy of the apparatus constant is the fringe ion, which is discussed under random errors. There was stematic change in the apparatus constant, since the ength, cell length, and lens focal lengths all remained nged.

(7) Uncertainty in $(\partial n/\partial w_1)_T$. The composition de- nce of refractive index is the only quantity from the rature which enters directly into the calculation of hermal diffusion factor. Equation (5.12) was obtained gh curve fitting, and the random error resulting from er of the data is discussed below. Any systematic or bias is small and disappears at $w_1 = 0$ and $w_1 = 1$,

ıere Eq. (5.12) reproduces the refractive indices of the ıre components. For w_1 less than 0.4, n changes slowly .th increasing w_1, and an uncertainty in w_1 of 0.1% con- ıibutes less than 0.005% to n. For w_1 greater than 0.8, increases more rapidly with increasing w_1, but any sys- ematic errors must remain small in order for n to approach ıe correct limiting value. We estimate that any such un- ertainties contribute less than 0.05% to α_1.

(8) Uncertainty in time. An electric timer which ıdicated digitally minutes and hundredths of minutes was sed. The combination of its inherent inaccuracy and the ıcertainty in starting it and reading it was less than .01 min. Since we recorded fringe position as a function f time, we compare the ratio of those relative uncertain- ies and observe that the effect of the time uncertainty ı α_1 is about 1% of the effect of the uncertainty in the ringe measurement, which itself contributes less than 1%) α_1.

(9) Uncertainty in $g_1(t)$. The term $g_1(t)$ makes its argest contribution for very small ($t < \theta/3$) values of ime and becomes less significant as the steady state is pproached. Systematic errors in $g_1(t)$ are due almost en- irely to uncertainties in the initial values chosen for ıe temperature and composition derivatives of the experi- ental transport parameters, of which we were confident) better than 5% initially. Those values were improved

n iterating the calculations so that they contributed at t a 2% uncertainty in $g_1(t)$, which itself influences the culated value of α_1 by about 0.1%. Consequently, we esti- e that systematic uncertainties in $g_1(t)$ contribute less n 0.01% to α_1.

(10) Uncertainty in fringe position. Any systematic ors involved in the measurement of fringe position due parallax disappeared in taking differences.

(11) Neglect of ϕ_1, $\partial p/\partial z$, and $j_{iz}\, \partial(\overline{H}_1 - \overline{H}_2)/\partial z$. entropy source term ϕ_1 due to bulk flow is, for a pure rmal diffusion experiment, zero except for about two utes during the warming up period. Sedimentation due the pressure gradient contributes about 0.1% to the position gradient due to thermal diffusion and conse- ntly less than 0.1% to α_1. The term $j_{iz}\, \partial(\overline{H}_1 - \overline{H}_2)/\partial z$ approximately

$$\rho D \frac{\partial T}{\partial z} (\overline{c}_{p1} - \overline{c}_{p2}) \frac{\partial T}{\partial z} ,$$

about 2×10^{-4} at most for very small values of time, decreases to zero at the steady state. All other sible sources of systematic error are related to the ic assumptions we made and justified in Chapter II. the values of time which we used to calculate α_1 they tainly contribute less than 0.1%. We now show that the tematic errors discussed above are much smaller than ıdom errors which occur.

Random Errors

The formula which allows us to calculate a thermal diffusion factor, Eq. (5.26), depends ultimately on such direct measurements as the fringe position, refractive index, thermocouple emf, and mass of the liquid in a pycnometer. We investigate now the propagation of the uncertainties in each of those direct measurements resulting in some uncertainty in the calculated value of the thermal diffusion factor.

Consider a general derived property U which is related to the directly measured properties X_1, X_2,...,X_m by the functional relation

$$U = U(X_1, X_2, \ldots X_m) \ , \tag{6.1}$$

which is continuous and differentiable over the region of interest. The uncertainty ε_U in U is obtained from the formula (Parratt, 1961)

$$\varepsilon_U^2 = \left(\frac{\partial U}{\partial X_1}\right)^2 \varepsilon_{X_1}^2 + \left(\frac{\partial U}{\partial X_2}\right)^2 \varepsilon_{X_2}^2 + \ldots$$

$$= \sum_{i=1}^{m} \left(\frac{\partial U}{\partial X_i}\right)^2 \varepsilon_{X_i}^2 \ , \tag{6.2}$$

where ε_{X_i} is the estimated uncertainty in X_i.

In principle, Eq. (6.2) can be applied only to statistical uncertainties of the same kind. That is, all ε's must be standard deviations, or all must be probable errors, or all must be 90% confidence limits, etc.

Furthermore, Eq. (6.2) is valid only if each ε is independent. Our uncertainties are not all independent. For example, an uncertainty in w_1^o is due in part to temperature uncertainties. We said in the preceding section, however, that such linkages are extremely weak, and we now assume that we can use Eq. (6.2). We express all of our uncertainties, or estimates thereof, as standard deviations.

Because of the small size of the correction term $g_1(t)$ in our theory, uncertainty in $g_1(t)$ has virtually no effect on the uncertainty in α_1, which is given by the following expression derived from Eqs. (5.26) and (6.2):

$$\frac{\varepsilon_{\alpha_1}^2}{\alpha_1^2} = \left(\frac{\varepsilon_{X_1}}{X_1}\right)^2 + \left(\frac{\varepsilon_{T_m}}{T_m}\right)^2 + \left(\frac{\varepsilon_A}{A}\right)^2 + \left(\frac{\varepsilon_{\partial n/\partial w_1}}{\partial n/\partial w_1}\right)^2 + \left(\frac{\varepsilon_{\Delta T}}{\Delta T}\right)^2 + \left(\frac{\varepsilon_{w_1^o w_2^o}}{w_1^o w_2^o}\right)^2 + \left(\frac{\varepsilon_{S_0'}}{S_0'}\right)^2 . \qquad (6.3)$$

In order to obtain an estimate of the expected uncertainty in α_1, we estimate the uncertainties in Eq. (6.3) in the following way.

(1) Uncertainty in X_1. The quantity X_1 is essentially a measurement of fringe displacement. Neglecting experimental scatter, which we consider later, we find that the uncertainty in X_1 is due completely to the uncertainty in measuring the fringe position. The magnitude of X_1 is about 5 cm, and repeated measurements of the same stationary fringe show a standard deviation of about 0.005 cm. Thus,

we have

$$\left(\frac{\varepsilon_{X_1}}{X_1}\right)^2 = 1 \times 10^{-6} \quad . \tag{6.4}$$

(2) Uncertainty in T_m. Random errors in T_m are due mainly to random fluctuations in the temperatures of the water baths, and only insignificantly to variations in the thermocouples, the reference ice bath, or the potentiometer. We estimate the standard deviation of measurements of T_m in a single experiment to be 0.0056°C, so that

$$\left(\frac{\varepsilon_{T_m}}{T_m}\right)^2 = 2 \times 10^{-10} \quad . \tag{6.5}$$

(3) Uncertainty in the apparatus constant. The uncertainty in A is itself a function of two other uncertainties, that of the measured value for r = 1.74 cm, and that of the value of r for the experiment at hand. We estimate the standard deviation of A in the original determination to be 0.01×10^4 cm^2, and that of the fringe spacing r to be 0.01 cm. There results

$$\left(\frac{\varepsilon_A}{A}\right)^2 = 5 \times 10^{-6} \quad . \tag{6.6}$$

(4) Uncertainty in $(\partial n/\partial w_1)_T$. This uncertainty depends on the value of w_1^o. The standard deviation obtained in the fitting of the data of Table 5f to a polynominal in w_1^o is 4.6×10^{-5}. The values of $(\partial n/\partial w_1)_T$ for

$T = 25°C$ and $\lambda = 6328\text{Å}$ and the uncertainties at the three compositions are

w_1^o	$\left(\frac{\partial n}{\partial w_1}\right)_T$	$\left(\frac{\varepsilon_{\partial n/\partial w_1}}{\partial n/\partial w_1}\right)^2$	
0.25	0.0186	2.80×10^{-6}	(6.7)
0.50	0.0284	3.10×10^{-6}	(6.8)
0.75	0.0438	5.20×10^{-6}	(6.8a)

(5) Uncertainty in ΔT. The remarks of paragraph (2) apply here. We estimate the standard deviation of the plate temperatures to be 0.004°C. Hence the standard deviation of ΔT is 0.0056°C, and

$$\left(\frac{\varepsilon_{\Delta T}}{\Delta T}\right)^2 = 2 \times 10^{-6} \ . \tag{6.9}$$

(6) Uncertainty in $w_1^o w_2^o$. This term is also composition dependent. There are three possible sources of random error in the determination of w_1^o: the polynomial in ρ, the calculated mass of liquid in the pycnometer, and the calculated volume of the pycnometer. Estimating the uncertainty in the mass at $w_1^o = 0.5$ to be 0.00025 g, and calculating the uncertainty in the volume to be 0.02 cm^3, we obtain as upper limits

w_1^o	$\left(\frac{\varepsilon_{w_1^o w_2^o}}{w_1^o w_2^o}\right)^2$	
0.25	1.5×10^{-6}	
0.50	1.3×10^{-6}	(6.10)
0.75	1.5×10^{-6}	

(7) Uncertainty in S_o'. The quantity S_o' is an analytical function $-\pi^2/2a$, and its uncertainty is related only to that of the cell height. From Chapter IV, $\varepsilon_a = .0005$ cm, hence

$$\left(\frac{\varepsilon_{S_o'}}{S_o'}\right)^2 = 1 \times 10^{-8} . \tag{6.11}$$

With the above estimates, Eq. (6.3) gives

$$\left(\frac{\varepsilon_{\alpha_1}}{\alpha_1}\right)^2 = 15 \times 10^{-6} , \tag{6.12}$$

or an estimated standard deviation of

$$\varepsilon_{\alpha_1} = 4 \times 10^{-3} |\alpha_1| . \tag{6.13}$$

Thus, the a priori estimated standard deviation is 0.4% of $|\alpha_1|$.

The expression from which the uncertainty in the ordinary diffusion coefficient is obtained is

$$\left(\frac{\varepsilon_D}{D}\right)^2 = \left(\frac{\varepsilon_\theta}{\theta}\right)^2 + w\left(\frac{\varepsilon_a}{a}\right)^2 . \tag{6.14}$$

We estimate that our measurements should give θ to within 2% or better, so

$$\left(\frac{\varepsilon_\theta}{\theta}\right)^2 = 4 \times 10^{-4} , \tag{6.15}$$

and

$$\left(\frac{\varepsilon_a}{a}\right)^2 = 7 \times 10^{-7} \ . \qquad (6.16)$$

Thus,

$$\left(\frac{\varepsilon_D}{D}\right)^2 = 4 \times 10^{-4} \ . \qquad (6.17)$$

We can expect deviations in measured values of D of about $\pm 0.03 \times 10^{-5}$ cm^2 sec^{-1}.

The numbers listed in the preceding paragraphs are estimates. They merely suggest anticipated values for the uncertainties in the thermal diffusion factor and the ordinary diffusion coefficient. The actual experimental standard deviations, which are measures of the scatter, must be calculated from the data. At several different compositions we had enough replicate experiments to calculate standard deviations for α_1 and D. The results of those measurements are shown in Table 6b.

Table 6b.--Experimental Uncertainties.

x_1	$\varepsilon_{\alpha_1}/\alpha_1$		ε_D/D	
	Observed	Estimated	Observed	Estimated
0.162	0.0066	0.0039	0.014	0.010
0.511	0.0046	0.0041	0.012	0.010
0.759	0.0153	0.0045	0.010	0.010

C. Results

In Figure (6.1)-(6.3)(Section D) are plotted the results of our calculations of the thermal diffusion factor for CCl_4 - C_6H_{12} at various temperatures and compositions. For the results at 25° we used MULTREG and allowed for the possibility of a fourth order polynomial in x_1. The data from Table 6a at 25° produced the smallest standard error when a straight line was fit to them. The composition dependence of α_1 at 25° is given by

$$-\alpha_1 = 1.82_7 - 0.181x_1 \qquad (6.18)$$

with a calculated standard error in α_1 of 0.022.

We obtained the temperature dependence of α_1 by finding the least squares straight line through the data at four temperatures. The same calculation was made for three compositions:

$$x_1 = 0.259 : -\alpha_1 = 1.79_8 - 0.0098(T - 25) , \qquad (6.19)$$

$$x_1 = 0.512 : -\alpha_1 = 1.73_3 - 0.0100(T - 25) , \qquad (6.20)$$

$$x_1 = 0.759 : -\alpha_1 = 1.68_2 - 0.0102(T - 25) . \qquad (6.21)$$

The temperature and composition results can be expressed by the single function

$$-\alpha_1 = 1.74_1 = 0.181(x_1 - 0.5) - 0.0100(T - 25) + 0.0008(x_1 - 0.5)(T - 25) , \qquad (6.22)$$

where the calculated standard error of α_1 is 0.019, and the coupling term (x_1T) contributes only about 0.1% to α_1.

Similar calculations for the ordinary diffusion coefficient were carried out for the composition dependence and for the temperature dependence. The results in this case are, for 25°, (units of $cm^2\ sec^{-1}$):

$$10^5 D = 1.48_2 - 0.187 x_1 \ , \qquad (6.23)$$

with an uncertainty of 0.03×10^{-5} in D. Measurements of D at four temperatures for each of three compositions yielded the least squares lines:

$$x_1 = 0.259 : 10^5 D = 1.43_8 + 0.0250(T - 25) \ , \qquad (6.24)$$

$$x_1 = 0.512 : 10^5 D = 1.39_0 + 0.0256(T - 25) \ , \qquad (6.25)$$

$$x_1 = 0.759 : 10^5 D = 1.35_0 + 0.0261(T - 25) \ . \qquad (6.26)$$

The combined temperature and composition formula is

$$10^5 D = 1.38_8 - 0.187(x_1 - 0.5) + 0.00256(T - 25) + 0.0024(x_1 - 0.5)(T - 25) \ , \qquad (6.27)$$

with a calculated standard error in D of 0.03. The results and their significance are discussed in more detail in the next section.

D. Discussion

The results of our calculations of the thermal diffusion factor for the carbon tetrachloride-cyclohexane system at 25°C are presented in Figure 6.1. Figure 6.2 is a comparison with previously reported values. There is no

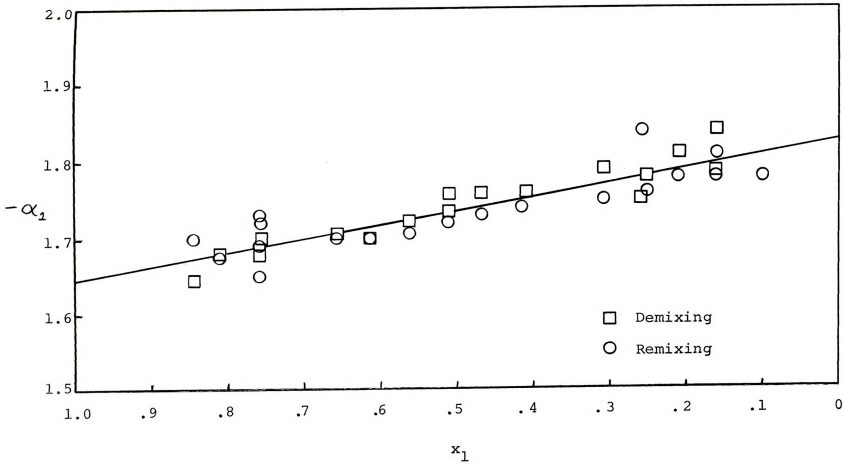

Figure 6.1--Experimental thermal diffusion factor for CCl_4 - C_6H_{12} as a function of mole fraction CCl_4 at 25° C.

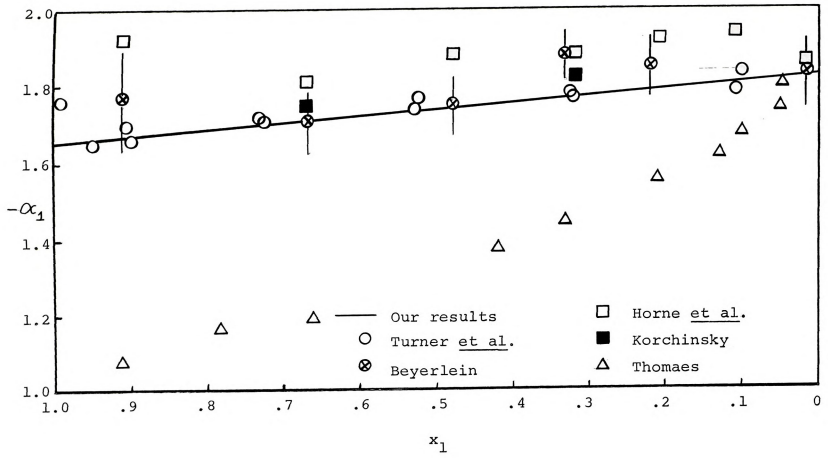

Figure 6.2--Experimental thermal diffusion factor for CCl_4 - C_6H_{12} as a function of mole fraction CCl_4 at 25° C; comparison with previous results.

significant difference between our results and those of Turner, Butler, and Story, who used a flow cell method. The agreement between the two sets and the internal consistency within each set clearly indicate that the composition dependence of the thermal diffusion factor for CCl_4 - C_6H_{12} at 25°C is a linear function of the mole fraction.

The thermogravitational results of Beyerlein and Bearman show large scatter, but three of their points coincide with our results, and two differ from ours by less than their reported uncertainties. Their value for $x_1 = 0.32$ is definitely incorrect, however. The comparison demonstrates that although a rigorous phenomenological theory (Horne and Bearman, 1968) was used, the results are not reliable. There is obviously some large random error producing the observed scatter, which is not attributable to either uncertainty in w_1^o or the effects of impurities. The source of the experimental difficulty must be discovered before the thermogravitational technique can be trusted.

The only other results for the CCl_4 - C_6H_{12} system obtained by means of pure thermal diffusion are those of Thomaes, which have always been questionable, which for twenty years cast a shadow over pure thermal diffusion in general, and which are now discredited. The claim that Thomaes' results were invalidated by convection is probably true.

Horne and Bearman and Korchinsky independently reported values for the thermal diffusion factor of this system obtained from thermogravitational studies. In both cases the slope of the α_1 vs x_1 line is close to ours, but their absolute values of α_1 are higher. Such a systematic difference could, as we pointed out earlier, result from the fact that Horne and Bearman did not account for the possible effects of temperature gradients in their reservoirs, and Korchinsky did not include the forgotten effect, which amounts to about 1% of α_1.

Our experimental standard errors of calculated thermal diffusion factors were, for most experiments, less than 1% of α_1. At 25°C our results can be expressed by the function

$$-\alpha_1 = 1.82_7 - 0.181x_1 \ , \qquad (6.28)$$

with a standard error of 0.0159.

Ours has been the first systematic study of the temperature dependence of the thermal diffusion factor for CCl_4 - C_6H_{12}. Figure 6.3 shows that the absolute value of α_1 decreases with increasing temperature. The function which characterizes our data for the range 20-35°C is

$$-\alpha_1 = 1.74_1 - 0.181(x_1 - 0.5) - 0.0100(T - 25) + 0.0008(x_1 - 0.5)(T - 25) \qquad (6.29)$$

which has a calculated standard error of 0.019. The single point for $x_1 = .5$ reported by Turner, Butler, and Story at

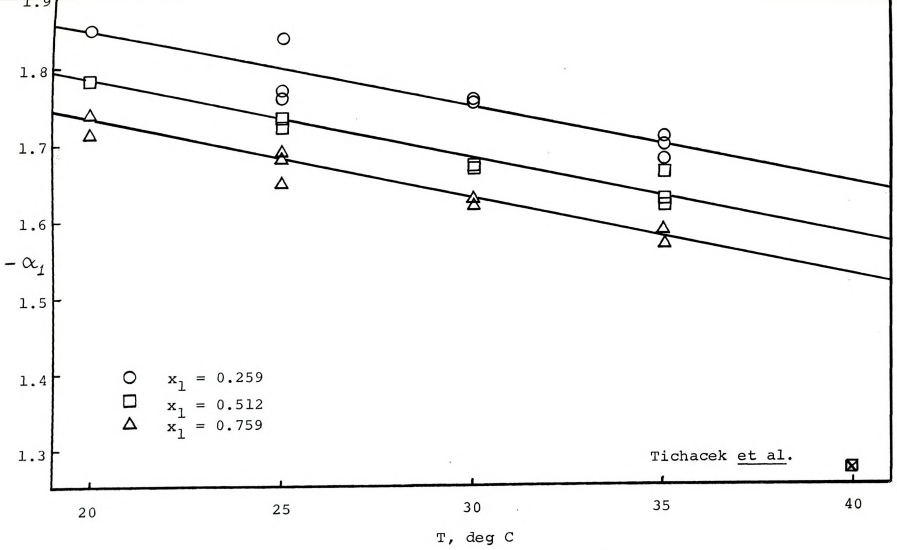

Figure 6.3--Experimental thermal diffusion factor as a function of temperature at three compositions for CCl_4 - C_6H_{12}.

35.1°C agrees within less than 2% with our value there. The (stirred diaphragm method) results of Tichacek, Kmak, and Drickamer at 40°C, however, are 20% lower (in absolute value) than the numbers we obtain by extrapolating our lines to 40°.

Beyerlein and Bearman (1968) have just shown that for thermogravitational experiments the thermal diffusion factor shows a significant dependence on the magnitude of the applied temperature gradients in the upper and lower reservoirs. A pure thermal diffusion cell has no such reservoirs containing the sample liquid, but it is conceivable that the apparatus material or construction might in some way effect the shape of the temperature distribution in the liquid. In fact Longsworth (1957) observed that for his apparatus the temperature distribution depended on the type of seal present between the glass cell walls and the metal plates.

In order to determine whether our calculated thermal diffusion factors would be influenced by the size of the temperature gradient, we conducted a set of experiments in which all conditions were identical except ΔT.

Our results (Figure 6.4) are certainly not comprehensive in this area, but they do indicate that there is very likely no significant dependence of the calculated value of α_1 on ΔT. Of course, for extremely small gradients (less than 1 deg cm^{-1}) very little thermal diffusion takes

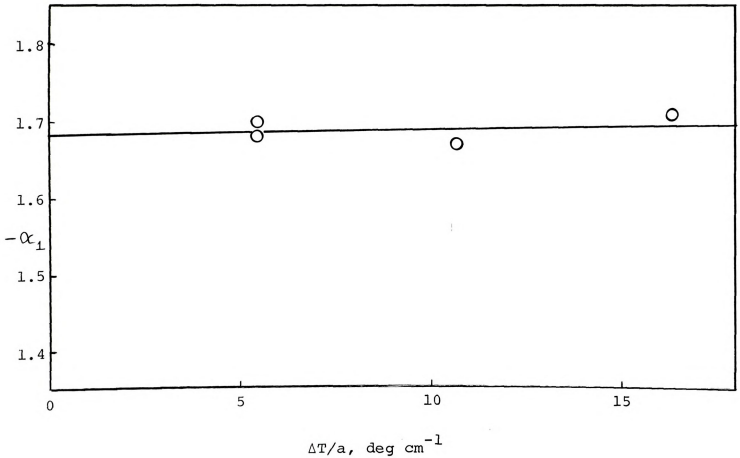

Figure 6.4--Experimental thermal diffusion factor for CCl_4 - C_6H_{12} as a function of applied temperature gradient; $x_1^o = 0.5$, $T_m = 25°$ C.

place, and α_1 is difficult to measure. For large gradients the terms involving the temperature and composition dependences of α_1 and D become more important. For very large gradients the linear phenomenological relations fail.

Two quite different tests showed that convection was absent except for the unimportant (for our method) first minute or two of an experiment. In the demixing experiment poor temperature control or poor insulation of the cell can result in horizontal components of the temperature gradient which cause density inversions and convection. Convection, when it occurs, causes remixing of the solution in addition to that due to ordinary diffusion. During a remixing experiment, however, no temperature gradient exists, and perturbing convection is much less likely to occur. Our results for both thermal diffusion factor (Figure 6.1) and ordinary diffusion coefficient (Figure 6.5) are identical for demixing and remixing:

At 25°,

$$\text{Demixing:} \quad -\alpha_1 = 1.84_4 - 0.212\, x_1 , \quad (6.30)$$

$$\text{Remixing:} \quad -\alpha_1 = 1.84_0 - 0.201\, x_1 , \quad (6.31)$$

$$\text{Demixing:} \quad 10^5 D, \text{ cm}^2 \text{ sec}^{-1} = 1.49_3 - 0.203\, x_1 , \quad (6.32)$$

$$\text{Remixing:} \quad 10^5 D, \text{ cm}^2 \text{ sec}^{-1} = 1.48_8 - 0.208\, x_1 , \quad (6.33)$$

Since there is no convection during remixing, and since the demixing results are the same as the remixing results, we conclude that there is no convection during demixing.

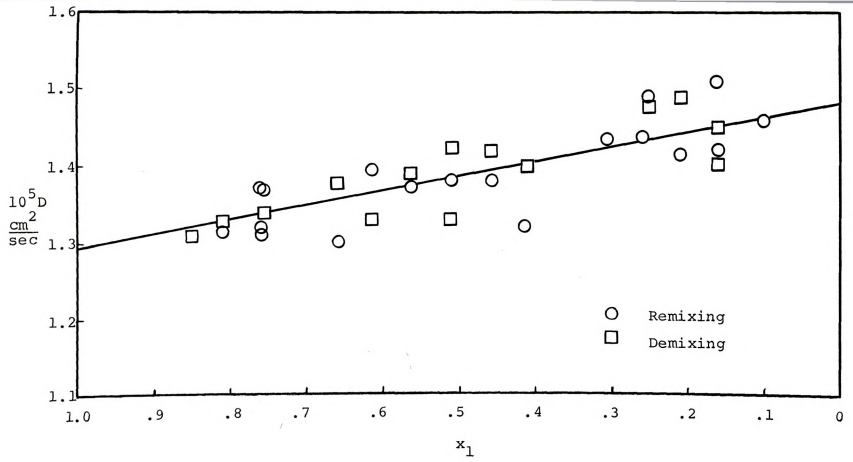

Figure 6.5--Experimental mutual diffusion coefficient for CCl_4 - C_6H_{12} as a function of mole fraction CCl_4 at 25° C.

Our experience with cell insulation substantiates this conclusion. Tests with an uninsulated cell at 35°C showed heat loss from the warm liquid to the cooler room air. The horizontal component of the temperature gradient caused density inversions and resulted in convection which was visible interferometrically as very unsteady fringe patterns. When the cell was insulated so that the air immediately surrounding the glass sample chamber could reach thermal equilibrium with the glass and the liquid, the horizontal heat flux was eliminated and the fringe pattern was steady.

Our calculated values of the ordinary diffusion coefficient show more scatter than do the results for the thermal diffusion factor. The apparent reason for this is that fluctuations in the metal plate temperatures can change the apparent time-dependence of the diffusion process (change the calculated θ and hence D) without changing the final value of α_1. The effect of the temperature fluctuations is also reflected in standard error of α_1. At 25° we obtain the following expression for the composition dependence of D:

$$10^5 D = 1.38_8 - 0.187(x_1 - 0.5) \ , \qquad (6.34)$$

where the standard error in D is 0.035, and where D has units of $cm^2\ sec^{-1}$. Present diffusion coefficient results are plotted, along with results of others, in Figure 6.6. Our results for D compare quite well with those of

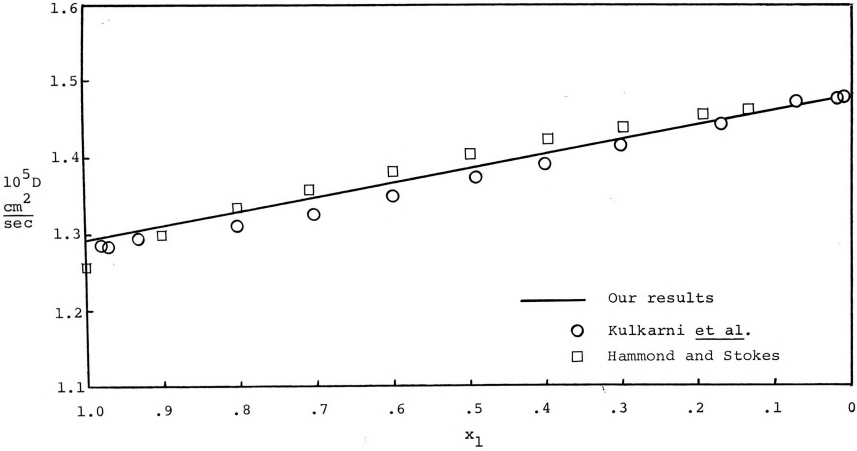

Figure 6.6--Experimental mutual diffusion coefficient for CCl_4 - C_6H_{12} as a function of mole fraction at 25° C; comparison with previous results.

Kulkarni, Allen, and Lyons and substantiate their conclusion that the stirred diaphragm results of Hammond and Stokes are invalid. (Figure 6.5)

Previously, very little information about the temperature dependence of D has been available. Our result (see Figure 6.7),

$$10^5 D = 1.388 - 0.187(x_1 - 0.5) + 0.0256(T - 25) + 0.0024(x_1 - 0.5)(T - 25) , \quad (6.35)$$

gives at $x_1 = 0.5$,

$$10^5 \partial D/\partial T = 0.0256 , \quad (6.36)$$

which is essentially the same as the 0.0258 of Kulkarni et al.

Dicave and Emery have claimed that the ordinary diffusion coefficient measured when a temperature gradient is present (when thermal diffusion is occurring) necessarily differs from that measured in an isothermal remixing experiment. According to the phenomenological theories of the various types of thermal diffusion the diffusion coefficient D should not change from one type of experiment to another. Our results indicate that no systematic difference exists between the ordinary diffusion coefficients measured in our two types of experiments.

We suggest that perhaps Dicave and Emery's experiments were perturbed by one or more of the following effects: (1) The phenomenological theory of their stirred

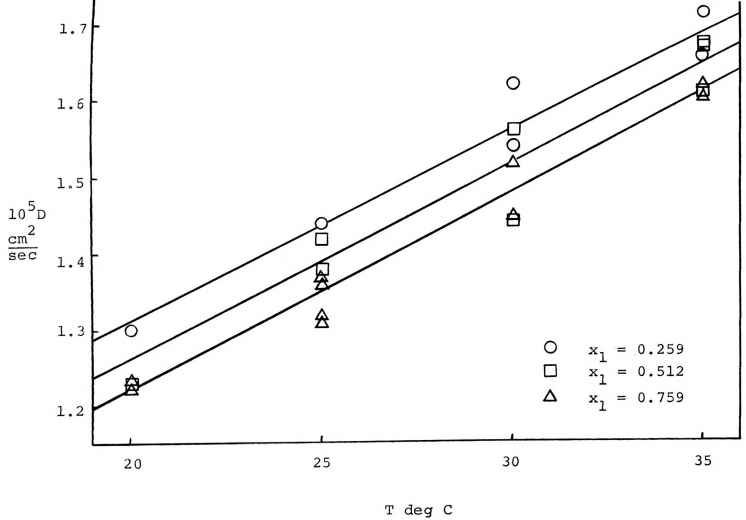

Figure 6.7--Experimental mutual diffusion coefficient for CCl_4 - C_6H_{12} as a function of temperature at three compositions.

diaphragm does not adequately account for the remixing due to the constant stirring; (2) The horizontal temperature gradient across the porous glass plate results in local fluid density inversions and unaccounted-for convection in the glass disc; (3) The stirring of the fluid near the disc causes a mixing flow through a portion of the disc near the surface, changing the effective thickness of the disc and, consequently, changing the value of D calculated from a given measurement of the relaxation time θ; (4) The temperature gradients they used were large enough to make the (ignored) temperature derivatives of transport parameters significant. We conclude that there is no difference between the isothermal and nonisothermal ordinary diffusion coefficients (provided they are referred to the appropriate temperatures).

It is interesting to note that the entire class of stirred diaphragm techniques is suspect since our results indicate that such methods lead to incorrect answers in three different cases: (1) The thermal diffusion factors of Tichacek, Kmak, and Drickamer at 40°C appear to be 20% too low in magnitude. (2) The ordinary diffusion coefficients of Hammond and Stokes are only a few percent too high, but have a parabolic, rather than linear, composition dependence. (3) We have shown that there is no difference between the isothermal ordinary diffusion coefficient and the nonisothermal one, and we therefore reject the contrary conjecture of Dicave and Emery, which

was based on stirred diaphragm thermal diffusion and diffusion experiments.

E. Temperature Dependence of Refractive Index

While testing for the possible effects of thermal diffusion of impurities in the "pure" carbon tetrachloride and the "pure" cyclohexane, we discovered some new information about the temperature dependence of the refractive index in each case. The theory of the interferometer predicts (Eq. (4.20)) that a uniform nonzero refractive index gradient should produce interference fringes indentical to those for a zero gradient but shifted horizontally by some fixed distance. What we in fact observed for both CCl_4 and C_6H_{12}, when a temperature difference was imposed vertically, and a steady temperature distribution developed, were curved interference fringes of a generally parabolic shape much like that in Figure 5.1.

Analysis of the refractive index data from the literature for the two pure compounds showed that only a linear dependence on temperature was statistically significant. Use of those data and the working equations for the interferometer required that the temperature distribution inside the liquid be sigmoidal in shape in order to explain the shape of the interference fringes.

Such a temperature distribution would, in turn, require either anomalous variations in the thermal conductivity

of the liquid or some inexplicable apparatus effect. Believing that the thermal conductivity is a well-behaved function of the temperature, and that our apparatus caused no strange effects (since the same temperature difference, applied to water, gave the expected straight fringes), we turned our attention to the validity of the reported values of the temperature dependence of the refractive index for CCl_4 and C_6H_{12}.

Since only second order thermal conductivity temperature dependence affects the value of $(dT/dz)_0$, and since the effect is less than 0.1°, we have, at the center of the cell, $(dT/dz)_0 = \Delta T/a$. The coefficients c_j defined by

$$c_j = \frac{1}{j!} \left(d^j n/dz^j\right)_0 , \tag{6.37}$$

then become

$$c_j = \left(\frac{\Delta T}{a}\right)^j \left(\partial^j n/\partial T^j\right)_0 . \tag{6.38}$$

Thus, to evaluate the temperature derivatives of refractive index, we need only the c_j of Eq. (4.20). For $j > 1$, these are directly related to the d_{j-1} which describes the fringe shape, and therefore second and higher temperature derivatives are obtainable from fringe shape analysis. c_1 and therefore first derivatives are proportional to d_0, but d_0 contains an arbitrary reference point and is therefore unobtainable from a single experiment. However, by performing experiments at two different values of ΔT and

determining the shift in d_0, we may calculate $(\partial n/\partial T)_0$ according to

$$c_1(2) - c_1(1) = \frac{1}{A}[d_0(2) - d_0(1)]$$

$$= \frac{1}{A}(\partial n/\partial T)_0 \left[\left|\frac{\Delta T}{a}\right|_2 - \left|\frac{\Delta T}{a}\right|_1\right] . \qquad (6.39)$$

In the CCl_4 experiments, the temperature gradients were $(\Delta T/a)_1 = 4.534$ deg cm^{-1}, $(\Delta T/a)_2 = 5.108$ deg cm^{-1}, the measured shift in d_0 was $[d_0(a) - d_0(1)] = 9.84$ cm, the measured value of the fringe spacing was 1.61 cm, and the mean temperature was 25°C. By Eqs. (4.20) and (6.39),

$$CCl_4,\ 25°,\ 6328Å:\ \frac{\partial n}{\partial T} = -5.96 \times 10^{-4} \text{ deg}^{-1} . \qquad (6.40)$$

The fringe shape for $(\Delta T/a) = 4.534$ deg cm^{-1} was fit by MULTREG, with the result

$$x = 1.454z'^{2} - 0.341z'^{3} + .0488z'^{5} , \qquad (6.41)$$

where z' is the vertical distance (in cm) on the photograph. By Eqs. (6.38) and (4.20),

$$CCl_4,\ 25°,\ 6328Å:\ (\partial^2 n/\partial T^2) = 0 \qquad (6.42)$$

$$(\partial^3 n/\partial T^3) = -1.00 \times 10^{-6} \text{ deg}^{-3} . \qquad (6.43)$$

Higher order coefficients are also calculable from the numbers in Eq. (6.41).

In the C_6H_{12} experiments, the temperature gradients were $(\Delta T/a)_1 = 5.177$ deg cm^{-1}, $(\Delta T/a)_2 = 4.563$ deg cm^{-1},

the measured shift in d_0 was $[d_0(2) - d_0(1)] = 9.63$ cm, the measured value of the fringe spacing was 1.62 cm, and the mean temperature was 25°. The corresponding results are,

C_6H_{12}, 25°, 6328Å: $\frac{\partial n}{\partial T} = -5.44 \times 10^{-4}$ deg^{-1} . (6.44)

The fringe shape for $\Delta T/a = 4.564$ deg cm^{-1} was

$$x = 0.763z'^2 + 0.0563z'^3 + 0.0307z'^4 . \quad (6.45)$$

As above, these lead to

C_6H_{12}, 25°, 6328Å: $(\partial^2 n/\partial T^2) = 0$ (6.46)

$$(\partial^3 n/\partial T^3) = -0.516 \times 10^{-6} \text{ deg}^{-3} . \quad (6.47)$$

We conclude from these measurements that the sensitivity of the wavefront shearing interferometer has permitted us to measure the temperature dependence of refractive index more precisely than it has previously been measured. Classical techniques have required measurements of the absolute refractive index at various temperatures. Analysis of the rather scarce literature data yields for 25° and 6328Å, $(\partial n/\partial T)_{CCl_4} = -5.75 \times 10^{-4}$ deg^{-1}, and $(\partial n/\partial T)_{C_6H_{12}} = -5.47 \times 10^{-4}$ deg^{-1}. These agree well with our results, and it is likely that our results are to be preferred, since we determine this coefficient directly. Derivatives of higher than first order have previously been undetected because they are much smaller than the experimental errors involved. With our method we sacrifice knowledge of the

absolute refractive index, but gain significant information about variations in the third and higher decimal places.

Our results require more verification before we can make a definite statement about the temperature dependence of refractive index. We are confident that our numbers for the first three derivatives are accurate to better than 1%, but higher derivatives are probably less accurate. We can conclude that the curved interferometric fringe shape observed for the pure components can be explained by the temperature dependence of refractive index, and that the laser wavefront shearing interferometer can be extremely valuable in studies of refractive index. Clearly, detailed temperature dependence will be most useful in testing microscopic theories of refractive index.

CHAPTER VII

CONCLUSION

A. Summary

In the preceding chapters we have set forth, for the first time, a phenomenological theory of pure thermal diffusion which is not restricted by traditional mathematical simplifications. Our use of the series expansion technique has allowed us to take full account of the temperature and composition dependences of the transport parameters involved.

Our solution for the composition of the fluid in a pure thermal diffusion cell as a function of position and time contains explicitly the effects of transient vertical convection and a varying temperature gradient during the warming up period. By allowing for time-dependent temperature gradients in our differential equations, we have been able to match the theoretical boundary conditions to the ones which are observed experimentally. Consequently, there is no doubt about when an experiment begins. We have consistently chosen the zero of time to be just that instant when the temperatures of the metal plates begin to change.

We have eliminated an additional source of error by allowing for a variable thermal conductivity. It has not been necessary to assume that the temperature gradient in the fluid has a constant, uniform value.

That all of our measurements of fringe displacement were made at the center of the cell was not accidental. We chose to avoid the ambiguities introduced by previous workers (Gustafsson, 1965) in measuring differences between refractive index gradients at two positions in the cell where the temperature gradients may not be the same.

We are convinced of the absence of convection. Both the interferometric observation of induced convection and the agreement of demixing and remixing results support this claim.

The laser wavefront shearing interferometer provides much more information than has heretofore been available from a single experiment. Its sensitivity and ease of operation make it far superior to other types of interferometers which have been used in the past.

We have also introduced computer technology to the study of thermal diffusion. Automatic analysis of fringe displacements makes feasible the use of more data. An automated data gathering device, when coupled with a computer, can remove the necessity for tedious manual measurements and permit routine analysis of thermal diffusion experiments.

Our theoretical and experimental investigations have combined to eliminate the doubts and questions prompted by the conflicting reports of previous thermal diffusion experiments. We have shown that when properly executed and when adequately described, pure thermal diffusion can be a reliable experimental technique.

With respect to numerical results, we conclude the following:

(1) The thermal diffusion factor of CCl_4 - C_6H_{12} at 25°C is given by

$$-\alpha_1 = 1.83 - 0.18x_1 ,$$

with standard error no greater than 1.2%. This result is in close agreement with the flow cell result of Turner et al. (1967). It appears also to be in agreement with the thermogravitational results of Beyerlein, whose scatter is rather large. The "pure" results of Thomaes are now clearly incorrect. The thermogravitational results of Horne and Bearman and of Korchinsky and Emery appear to have the same composition dependence as ours, but are a few percent higher in absolute value. With the close agreement of our results and those of Turner, Butler and Story, the thermal diffusion factor and its composition dependence at 25°C are now firmly established.

(2) The temperature dependence of α_1 is given by

$$\left(\frac{\partial \alpha_1}{\partial T}\right)_{x_1} = 0.011 \text{ deg}^{-1} .$$

(3) Diffusion coefficients for this system are given with standard error of less than 3%, by

$$D \times 10^5 = 1.482 + 0.0256(T - 25) - 0.187\, x_1 ,$$

which agrees well with the results of Kulkarni, Allen, and Lyons. The stirred diaphragm results of Hammond and Stokes appear to be incorrect. Further, we have refuted the claim of Dicave and Emery that diffusion coefficients in thermal diffusion experiments are different from those in isothermal experiments.

(4) The temperature dependence of the refractive index of CCl_4 at 6328Å is given by (CCl_4, 6328Å):

$$n = n^{25°} - 5.96 \times 10^{-4}(T - 25) - 1.00 \times 10^{-6}(T - 25)^3 ,$$

while that for C_6H_{12} is given by (C_6H_{12}; 6328Å):

$$n = n^{25°} - 5.44 \times 10^{-4}(T - 25) - 0.516 \times 10^{-6}(T - 25)^3 .$$

The standard error in each of the above coefficients is less than 2%.

B. Suggestions for Further Work

It has not been our purpose to collect thermal diffusion data for a large number of systems. Rather, we have shown that pure thermal diffusion can be a useful experimental tool, and that both our phenomenological theory and our analytical method can be used in routine studies.

Further improvement can be made, however, especially in the area of temperature control, the element which most

limits the precision of the method. We have considered redesigning the cell, eliminating the circulating water, and substituting sealed chambers which make use of the constant temperatures of phase changes. The reservoirs then would be hollow metal blocks lined on the inside with a porous fiber material. The upper portion of the top reservoir would be heated electrically just enough to vaporize a portion of the liquid in the pores of the fiber. Heat would be transferred by the gas downward to the bottom of the upper reservoir where the gas would condense at a constant temperature determined by the particular substance chosen and the pressure inside the chamber. The newly formed liquid would move by capillary action up the side walls of the chamber and back to its original position. By means of such an arrangement, the required constant temperature would be maintained at the top metal plate in contact with the fluid in the thermal diffusion cell.

The heat which was put into the system electrically would flow downward through the sample fluid and become available at the metal plate forming the upper boundary of the lower chamber. There the heat would be used to vaporize a different liquid at another constant temperature. The gas produced would carry the heat downward to the bottom of the lower chamber where the gas would condense on porous fibers cooled electrically by means of the Peltier effect.

Heat transfer by convecting gases has been studied (Eastman, 1968). The efficiency of such heat transfer is much greater than that of pure heat conduction. In tests described in the above-mentioned article, the effective heat transfer coefficients were one to three orders of magnitude larger for the "heat pipes" than for a copper bar of similar dimensions. If this method can be adapted to pure thermal diffusion experiments, it should provide highly stable and uniform plate temperatures. Alternatively, further refinements in the more conventional method may be attempted.

A second place for improvement is the method of collecting data. The main advantage of pure thermal diffusion is that it permits one to make a very large number of measurements without disturbing the system. We usually used 20 to 40 measurements of fringe displacement in our calculations of fringe displacement in our calculations. We were limited mainly by the time and labor involved in making each measurement. If some automated measuring device were available, more information could be obtained from each experiment. The simplest arrangement would consist of photoelectric sensors which could continuously monitor the fringe position and eliminate the need for intermittent manual measurements.

A more sophisticated improvement would make use of stop motion photography to obtain hundreds, or even

thousands, of records of the interference fringes. A necessary adjunct would be an optical scanning device to determine the shape and position of each fringe and store that information in the memory of a computer, where it would be accessible for programmed analysis.

The use of the entire fringe shape would have the advantage of providing second and higher derivatives of the refractive index. Consequently, a single experiment could be used to determine not only the thermal diffusion factor and the ordinary diffusion coefficient, but also the thermal conductivity and the temperature and composition derivatives of all three quantities.

We mentioned in Chapter VI that the apparent thickness of the interference fringes could be decreased by using a more intense light source. If the interferometer then proved to be sufficiently sensitive, one could, in principle at least, measure the heat of transport by determining the thermal conductivity of the initial, uniform mixture and that of the mixture at the steady state of demixing. This could be done by watching interferometrically the time dependence of temperature changes when a temperature difference is applied to or removed from the test liquid. The relaxation time for heat conduction is a function of the thermal conductivity. The difference between the two thermal conductivities is $\rho D Q_1^* w_1 w_2 \alpha_1$, which is numerically about 1% of κ.

Finally, in further work with thermal diffusion, the possible applicability of new techniques such as radioisotope tracing and nuclear spin-echo methods should not be overlooked.

BIBLIOGRAPHY

Abrahamowitz, M., and I. A. Stegun, Handbook of Mathematical Functions, National Bureau of Standards, Applied Mathematics Series, 55, U. S. Government Printing Office, Washington, D. C., 1964.

Agar, J. N., Trans. Faraday Soc. 56, 776 (1960).

_____, and J. C. R. Turner, J. Phys. Chem. 64, 1000 (1960).

Bartelt, J. L., Michigan State University, personal communication, 1967.

_____, Ph.D. Thesis, Michigan State University, East Lansing, Michigan, 1968.

Bartels, R. C. F., and R. V. Churchill, Bull. Amer. Math. Soc. 48, 276 (1942).

Bates, O. K., Ind. Eng. Chem. 25, 421 (1931).

_____, Ind. Eng. Chem. 28., 494 (1936).

Bearman, R. J., J. Chem. Phys. 30, 835 (1959).

_____, and F. H. Horne, J. Chem. Phys. 42, 2015 (1965).

Bellman, R., Perturbation Techniques in Mathematics, Physics and Engineering, New York, N. Y.: Holt, Rinehart, and Winston, Inc., 1964.

Beyerlein, A. L., Ph.D. Thesis, University of Kansas, University Microfilms, Ann Arbor, Michigan, 1966.

_____, and R. J. Bearman, to be published.

Bierlein, J. A., J. Chem. Phys. 23, 10 (1955).

Birkett, J. D., Ph.D. Thesis, Yale University, New Haven, Conn., 1962.

Bischoff, K. B., and D. M. Himmelblau, Ind. Eng. Chem. 60, (1), 66 (1968).

Born, M., and E. Wolf, Principles of Optics, New York, N.Y.: Pergamon Press, 1964.

Bryngdahl, O., J. Opt. Soc. Amer. 53, 571 (1963).

_____, and S. Ljunggren, J. Phys. Chem. 64, 1264 (1960).

Butler, B. D., and J. C. R. Turner, Trans. Faraday Soc. 62, 3114 (1966).

_____, and J. C. R. Turner, Trans. Faraday Soc. 62, 3121 (1966).

Carslaw, H. W. and J. C. Jaeger, Conduction of Heat in Solids, 2nd. ed., London: Oxford University Press, 1959.

Churchill, R. V., Fourier Series and Boundary Value Problems, New York, N.Y.: McGraw-Hill, 1963.

Coleman, B. D., and W. Noll, Arch. Rational Mech. Anal. 13, 167 (1963).

Courant, R., and D. Hilbert, Methods of Mathematical Physics, New York, N.Y.: Interscience, 1953.

de Groot, S. R., Physica 9, 699 (1942).

_____, l'Effet Soret, Amsterdam: North-Holland Publishing Co., 1945.

_____, Thermodynamics of Irreversible Processes, Amsterdam: North-Holland Publishing Co., 1951.

_____, W. Hoogenstraaten, and C. J. Gorter, Physica 9, 923 (1942).

_____, and P. Mazur, Non-Equilibrium Thermodynamics, Amsterdam: North-Holland, 1962.

Dicave, S., and A. H. Emery Jr., Ind. Eng. Chem., Fundam. 7, 95 (1968).

Dike, P. H., "Thermoelectric Thermometry," Philadelphia, Pa.: Leeds and Northrup Company, 1954.

Dufour, L., Ann. Physik. 148, 302 (1873).

Eastman, G. Y., Scientific American 218 (5), 38 (1968).

Eisenhart, C., Science 160, 1201 (1968).

Fitts, D. D., Nonequilibrium Thermodynamics, New York, N.Y.: McGraw-Hill, 1962.

Francon, M., Optical Interferometry, New York, N. Y.: Academic Press, 1966.

Fulks, W., Advanced Calculus, New York, N. Y.: John Wiley & Sons, 1964.

Grove, G. R., "Thermal Diffusion: A Bibliography," AEC Report MLM - 1088, 1959.

Gustafsson, S. E., J. C. Becsey, and J. A. Bierlein, J. Phys. Chem. 69, 1016 (1965).

Hammond, B. R., and R. H. Stokes , Trans. Faraday Soc. 51, 1641 (1955).

Hodgman, C. D., Handbook of Chemistry and Physics, 44th. ed., Cleveland, Ohio: Chemical Rubber Publishing Company, 1962.

Horne, F. H., Ph.D. Thesis, University of Kansas, University Microfilms, Ann Arbor, Michigan, 1962.

_____, J. Chem. Phys. 45, 3069 (1966).

_____, J. Chem. Phys. 49, 0000 (1968).

_____, and R. J. Bearman, J. Chem. Phys. 37, 2842 (1962).

_____, and R. J. Bearman, J. Chem. Phys. 46, 4128 (1967).

Irving, J., and N. Mullineux, Mathematics in Physics and Engineering, New York, N. Y.: Academic Press, 1959.

Jeener, J., and G. Thomaes, J. Chem. Phys. 22, 566 (1954).

Johnson, D. E., and J. R. Johnson, Mathematical Methods in Engineering and Physics, New York, N. Y.: Ronald Press, 1965.

Kirkwood, J., and B. Crawford, J. Phys. Chem. 56, 1048 (1952).

Korchinsky, W. J., Ph.D. Thesis, Purdue University, University Microfilms, Ann Arbor, Michigan, 1965.

Kulkarni, M. V., G. F. Allen, and P. A. Lyons, J. Phys. Chem. 69, 2491 (1965).

Longsworth, L. G., J. Phys. Chem. 61, 1557 (1957).

Ludwig, C., Akad. Wiss. Wien, Math. naturw. Kl. 20, 539 (1856).

Macurdy, L. B., Preprint No. 14.8-5-65, Instrument Society of America, 20th. Annnual Conference, Los Angeles, California, 1965.

Margulies, S., Rev. Sci. Instrum. 39, 478 (1968).

Martin, W. T., and E. Reissner, Elementary Differential Equations, Reading, Massachusetts: Addison-Wesley, 1961.

McCracken, D. D., A Guide to Fortran IV Programming, New York, N. Y.: John Wiley & Sons, 1965.

Müller, I., Arch. Rational Mech. Anal. 28, 1 (1968).

Mulliken, R. S., J. Am. Chem. Soc. 44, 1033 (1922).

Murphy, G. M., Ordinary Differential Equations and Their Solutions, Princeton, New Jersey: Van Nostrand, 1960.

Parratt, L. G., Probability and Experimental Errors in Science, New York, N. Y.: John Wiley & Sons, 1961.

Powell, M. J. D., The Computer Journal 7, 155 (1965).

Ralston, A., and H. S. Wilf, Mathematical Methods for Digital Computers, New York, N. Y.: John Wiley & Sons, 1960.

Rastogi, R. P., and G. L. Madan, J. Chem. Phys. 43, 4179 (1965).

Soret, C., Arch. Sci. (Geneva) 2, 48 (1879).

Tanner, C. C., Trans. Faraday Soc. 23, 75 (1927).

_____, Trans. Faraday Soc. 49, 611 (1953).

Thomaes, G., Physica 17, 885 (1951).

Tichacek, L. J., W. S. Kmak, and H. G. Drickamer, J. Phys. Chem. 60, 820 (1956).

Timmermans, J., Physico-Chemical Constants of Pure Organic Compounds, New York, N. Y.: Elsevier, 1950; Physico-Chemical Constants of Binary Systems, Vol. 1, New York, N. Y.: Interscience Publishers, 1959.

Truesdell, C., and R. A. Toupin, Handb. Phys., Vol. III/1, edited by S. Flügge, Springer, Berlin, 1960.

Turner, J. C. R., B. D. Butler, and M. J. Story, Trans. Faraday Soc. 63, 1906 (1967).

Tyrrell, H. J. V., Diffusion and Heat Flow in Liquids, London: Butterworths, 1961.

Washburn, E. W., ed., International Critical Tables of Numerical Data, National Research Council, New York, N. Y.: McGraw-Hill Book Company, 1933.

Wentworth, W. E., J. Chem. Educ. 42, 96 (1965).

Wood, S. E., and J. A. Gray, III, J. Am. Chem. Soc. 74, 3729 (1952).

APPENDICES

APPENDIX A

A RELATION BETWEEN PHENOMENOLOGICAL COEFFICIENTS†

Postulate: There exists a scalar, invariant, positive, bilinear function (the entropy production) defined by

$$\alpha = \sum_{\alpha=0}^{\nu} \underset{\sim}{J}_\alpha \cdot \underset{\sim}{X}_\alpha \geq 0 \ , \tag{A.1}$$

where the $\underset{\sim}{X}_\alpha$ form a linearly independent set of vectors. The vectors $\underset{\sim}{J}_\alpha$ are specified uniquely by the scalars $\Omega_{\alpha\beta}$ defined by

$$\underset{\sim}{J}_\alpha = \sum_{\beta=0}^{\nu} \Omega_{\alpha\beta} \underset{\sim}{X}_\beta \ , \ \alpha = 0,1,\ldots,\nu \ . \tag{A.2}$$

We seek a proof of the theorem

"If $\sum_{\alpha=1}^{\nu} \Omega_{\alpha\beta} = 0$, then

$$\sum_{\beta=1}^{\nu} \Omega_{\alpha\beta} = 0 \ , \ \alpha = 0,1,\ldots,\nu \ ." \tag{A.3}$$

Lemma I: The quadratic form $q(\underset{\sim}{Y})$,

$$q = \underset{\sim}{Y}^T A \underset{\sim}{Y} = \overbrace{Y_1 Y_2}^{} \begin{pmatrix} a_{11} & a_{12} \\ a_{12} & a_{22} \end{pmatrix} \begin{pmatrix} Y_1 \\ Y_2 \end{pmatrix} , \tag{A.4}$$

†This proof is due to Bartelt (1968).

is positive (i.e., $q \geq 0$) for any Y if and only if both

$$a_{11} \geq 0 \tag{A.5}$$

and

$$a_{11}a_{22} - a_{12}^2 \geq 0 \ . \tag{A.6}$$

Proof:

$$q = a_{11}Y_1^2 + 2a_{12}Y_1Y_2 + a_{22}Y_2^2$$

$$q = a_{11}\left(Y_1 + \frac{a_{12}}{a_{11}} Y_2\right)^2 + \left(a_{22} - \frac{a_{12}^2}{a_{11}}\right) Y_2^2 \ . \tag{A.7}$$

Thus, if for any Y_1 and Y_2, $a_{11} \geq 0$ and $a_{11} - a_{12}^2 \geq 0$, then $q \geq 0$. On the other hand, if $q \geq 0$ for any $\underset{\sim}{Y}$, and if $Y_2 = 0$, then

$$a_{11} \geq 0 \ . \tag{A.8}$$

Furthermore, if $Y_1 + \frac{a_{12}}{a_{11}} Y_2 = 0$, then

$$a_{11}a_{22} - a_{12}^2 \geq 0 \ . \tag{A.9}$$

Definitions:

$$B_\delta \equiv \sum_{\alpha=1}^{\nu} \Omega_{\alpha\delta} \ , \tag{A.10}$$

$$C_\delta \equiv \sum_{\beta=1}^{\nu} \Omega_{\delta\beta} \ ; \ \delta = 0,1,\ldots,\nu \ . \tag{A.11}$$

Lemma II:

$$\Omega_{\delta\delta} \sum_{\varepsilon=1}^{\nu} B_\varepsilon \geq \frac{1}{4}\left(B_\delta + C_\delta\right)^2, \ \delta = 0,1,\ldots,\nu \ . \tag{A.12}$$

Proof: For each $\delta = 0,1,\ldots,\nu$, choose

$$\underset{\sim}{X}_0 = \underset{\sim}{0} \ ,$$

$$\underset{\sim}{X}_\alpha = \underset{\sim}{X}_\gamma \ , \quad \alpha = 1,2,\ldots,\nu$$
$$\gamma \neq \delta$$
$$\alpha \neq \delta \ . \tag{A.13}$$

Then

$$\sigma = \sum_{\alpha=0}^{\nu} \sum_{\beta=0}^{\nu} \Omega_{\alpha\beta} \underset{\sim}{X}_\alpha \cdot \underset{\sim}{X}_\beta \ ,$$

$$\sigma = \sum_{\alpha=1}^{\nu} \sum_{\beta=1}^{\nu} \Omega_{\alpha\beta} \underset{\sim}{X}_\alpha \cdot \underset{\sim}{X}_\beta \ ,$$

$$\sigma = \sum_{\substack{\beta=1 \\ \beta\neq\delta}}^{\nu} \sum_{\substack{\beta=1 \\ \beta\neq\delta}}^{\nu} \Omega_{\alpha\beta} \underset{\sim}{X}_\gamma \cdot \underset{\sim}{X}_\gamma + \sum_{\substack{\alpha=1 \\ \alpha\neq\delta}}^{\nu} \Omega_{\alpha\delta} \underset{\sim}{X}_\gamma \cdot \underset{\sim}{X}_\delta$$

$$+ \sum_{\substack{\beta=1 \\ \beta\neq\delta}}^{\nu} \Omega_{\delta\beta} \underset{\sim}{X}_\delta \cdot \underset{\sim}{X}_\gamma + \Omega_{\delta\delta} \underset{\sim}{X}_\delta \cdot \underset{\sim}{X}_\delta \ ,$$

$$\sigma = \left\{ \sum_{\varepsilon=1}^{\nu} B_\varepsilon - B_\delta - C_\delta + \Omega_{\delta\delta} \right\} (X_\gamma)^2$$

$$+ \{ B_\delta + C_\delta - 2\Omega_{\delta\delta} \} \underset{\sim}{X}_\gamma \cdot \underset{\sim}{X}_\delta + \Omega_{\delta\delta} (X_\delta)^2 \ ,$$

$$\sigma = \underbrace{\underset{\sim}{X}_\delta \ X_\delta} \begin{pmatrix} \Omega_{\delta\delta} & \frac{1}{2}(B_\delta + C_\delta) - \Omega_{\delta\delta} \\ \frac{1}{2}(B_\delta + C_\delta) - \Omega_{\delta\delta} & \sum_{\varepsilon=1}^{\nu} B_\varepsilon + \Omega_{\delta\delta} - B_\delta - C_\delta \end{pmatrix} \begin{pmatrix} X_\delta \\ X_\gamma \end{pmatrix} . \tag{A.14}$$

From Eq. (A.1) and Lemma I we have

$$\Omega_{\delta\delta} \geq 0 \ , \tag{A.15}$$

nd

$$\Omega_{\delta\delta}\left\{\sum_{\varepsilon=1}^{\nu} B_\varepsilon - B_\delta - C_\delta + \Omega_{\delta\delta}\right\} - \left\{\frac{1}{2}(B_\delta + C_\delta) - \Omega_{\delta\delta}\right\}^2 \geq 0 \ . \tag{A.16}$$

n other words,

$$\Omega_{\delta\delta} \sum_{\varepsilon=1}^{\nu} B_\varepsilon \geq \frac{1}{4}(B_\delta + C_\delta)^2 \ , \ \delta = 0,1,\ldots,\nu \ . \tag{A.17}$$

heorem:

$$\text{If } \sum_{\alpha=1}^{\nu} \Omega_{\alpha\delta} = 0 \ , \ \delta = 0,1,\ldots,\nu \ ,$$

hen

$$\sum_{\beta=1}^{\nu} \Omega_{\delta\beta} = 0 \ , \ \delta = 0,1,\ldots,\nu \ .$$

roof: According to our postulate,

$$B_\delta = 0 \ , \ \delta = 0,1,\ldots,\nu \ .$$

hus

$$\sum_{\varepsilon=1}^{\nu} B_\varepsilon = 0 \ , \tag{A.18}$$

and by Lemma II

$$-C_\delta^2 \geq 0 \ , \tag{A.19}$$

or

$$C_\delta = \sum_{\beta=1}^{\nu} \Omega_{\delta\beta} = 0 \ , \ \delta = 0,1,\ldots,\nu \ . \tag{A.20}$$

APPENDIX B

SIMPLIFIED COMPOSITION DISTRIBUTION

The following derivation is essentially that of
:rlein (1954) and de Groot (1945). The introduction of
:s fractions instead of mole fractions, however, is ours.

Consider the continuity equation (3.6)

$$\frac{\partial w_1^*}{\partial t} = D \left\{ \frac{\partial^2 w_1^*}{\partial z^2} - \frac{\alpha_1 \Delta T}{T_m a} (1 - 2w_1^o) \frac{\partial w_1^*}{\partial z} + \frac{\partial \ell n \rho}{\partial z} \frac{\partial w_1^*}{\partial z} \right.$$

$$\left. - \frac{\alpha_1 \Delta T}{T_m a} [w_1^o (1 - w_1^o) + (1 - 2w_1^o)(w_1^* - w_1^o)] \frac{\partial \ell n \rho}{\partial z} \right\} , \tag{B.1}$$

ere $0 > z > a$,

d $t > 0$.

define the quantity R by

$$\frac{\partial \ell n \rho}{\partial z} = R \frac{\Delta T}{a} , \tag{B.2}$$

ere R is assumed to be constant. The other symbols are
scussed in Chapters II and III.

For convenience we define the following dimension-
ss quantities:

$$\xi = z/a$$

$$r = Dt/z^2$$

$$A = R\Delta T$$

$$p = -\alpha_1 \Delta T/T_m \ . \qquad \text{(B.3)}$$

uation (B.1) becomes

$$\frac{\partial w_1^*}{\partial r} = \frac{\partial^2 w_1^*}{\partial \xi^2} + [A + p(1 - 2w_1^o)] \frac{\partial w_1^*}{\partial \xi} + Apw_1^*(1 - 2w_1^o) + Apw_1^{o\,2} \ .$$

xiliary conditions are (B.4)

$$\lim_{r \to 0} w_1^* = w_1^o \ , \ 0 > \xi > 1 \ , \qquad \text{(B.5)}$$

$$\lim_{\substack{\xi \to 0 \\ \xi \to 1}} \left[\frac{\partial w_1^*}{\partial \xi} + p(1 - 2w_1^o) w_1^* + pw_1^{o\,2} \right] = 0 \ , \ r > 0 \ . \qquad \text{(B.6)}$$

The solution of these equations in a Fourier series facilitated by rewriting them as functions of a new riable:

$$\phi = \left[w_1^* + \frac{w_1^{o\,2}}{(1 - 2w_1^o)} \right] \exp \left\{ \frac{1}{2} [A + p(1 - 2w_1^o)] \xi \right\} . \qquad \text{(B.7)}$$

e equation to be solved becomes

$$\frac{\partial \phi}{\partial r} = \frac{\partial^2 \phi}{\partial \xi^2} - \left[\frac{1}{4} Q^2 - Ap(1 - 2w_1^o) \right] \phi \ , \qquad \text{(B.8)}$$

ere

$$Q = A + p(1 - 2w_1^o) \ .$$

‹iliary conditions are

$$\lim_{r\to 0} \phi = e^{\frac{1}{2}Q\xi} \quad , \; 0 < \xi < 1 \; , \tag{B.9}$$

$$\lim_{\substack{\xi\to 0 \\ \xi\to 1}} \left(\frac{\partial\phi}{\partial\xi} - \phi[\frac{1}{2} Q - (1 - 2w_1^o)p] \right) = 0 \; . \tag{B.10}$$

Equation (B.8) can be solved by the separation of les technique. When the initial and boundary condi- are imposed, the solution is seen to be

$$w_1^* = w_1^\theta - 2\pi p w_1^o (1 - w_1^o) S' \; , \tag{B.11}$$

w_1^θ is the steady state term given either by

$$w_1^\theta = \frac{1}{2} w_1^o \left[\frac{p(1 + N) \exp(-pN\xi)}{1 - \exp(-pN)} + \frac{N - 1}{N} \right] \; , \tag{B.12}$$

$$N \equiv 1 - 2w_1^o \neq 0 \; ,$$

$$w_1^\theta = \frac{1}{2}[1 + \frac{1}{2} p(\frac{1}{2} - \xi)], \text{ when } N = 0 \tag{B.13}$$

nction S' is given by

$$S' = \sum_{k=1}^{\infty} \frac{kV_k W_k \exp[-(B^2 + k^2\pi^2)r - p\xi]}{(B^2 + k^2\pi^2)(P^2 + k^2\pi^2)} \; . \tag{B.14}$$

antities appearing in the summation are

$$B = \frac{1}{2}(A - pN)$$

$$P = \frac{1}{2}(A + pN)$$

$$V_k = 1 - (1 - 1)^k \exp P \qquad (B.15)$$

$$W_k = B \sin k\pi\xi + k\pi \cos k\pi\xi$$

Since the complete solution is so cumbersome, it seful to derive from it some convenient expressions h, due to the magnitudes of the parameters involved, still accurate. If we consider the usual ranges of parameters which determine B and P (viz., $-0.002 <$ $0, 3 > -\alpha_1 > 0, 20 > \Delta T > 0, 1 > N > -1$), it is r that B and P will typically lie between the limits 1. Thus the squares of these constants are negligible ared with $k^2\pi^2$. Also, since $0.2 > p > 0$, we may, with igible error, represent w_1^θ by

$$w_1^\theta = w_1^o \left[1 + p\,(1 - w_1^o)\,(\tfrac{1}{2} - \xi)\right] . \qquad (B.16)$$

sual, we use the formula for the relaxation time

$$\theta = \frac{a^2}{\pi^2 D} . \qquad (B.17)$$

Our final expression for the solution is

$$w_1^* = w_1^o + \frac{\alpha_1}{T_m}\,\Delta T w_1^o\,(1 - w_1^o)\left(\frac{z}{a} + \frac{2}{\pi^3}\,s\right) , \qquad (B.18)$$

where

$$s = \sum_{k=1}^{\infty} k^{-3} v_k w_k \exp(-k^2 t/2 - pz/a - p/2) ,$$

$$v_k = 1 - (-1)^k \exp P,$$

$$w_k = B \sin\left[k\pi\left(\frac{z}{a} + \frac{1}{2}\right)\right] + k\pi \cos\left[k\pi\left(\frac{z}{a} + \frac{1}{2}\right)\right] ,$$

and where we have transformed variables so that Eq. (B.18) is valid for

$$-a/2 < z < a/2$$

$$t > 0 .$$

APPENDIX C

CONTRIBUTION OF CONVECTION TO THE TEMPERATURE DISTRIBUTION

The temperature inside the fluid in a pure thermal diffusion apparatus is described by Eq. (3.18):

$$\rho \bar{c}_p \frac{\partial T}{\partial t} = -\frac{\partial q_z}{\partial z} - \rho \bar{c}_p u_z \frac{\partial T}{\partial z} , \qquad (C.1)$$

$$-\frac{a}{2} < z < \frac{a}{2} , \quad t > 0 ,$$

where

$$-q_z = \kappa_i \frac{\partial T}{\partial z} + \rho D Q_1^* \frac{\partial w_1}{\partial z} , \qquad (C.2)$$

and the auxiliary conditions are

$$\begin{aligned} T(z,0) &= T_m \\ T\left(-\frac{a}{2},t\right) &= \phi_c(t) \\ T\left(\frac{a}{2},t\right) &= \phi_h(t) . \end{aligned} \qquad (C.3)$$

We identify by T^* the contribution to the temperature due to pure heat conduction, so that the equation

$$\frac{\partial T^*}{\partial t} = \frac{\kappa_i}{\rho \bar{c}_p} \frac{\partial^2 T^*}{\partial z^2} \qquad (C.4)$$

is equivalent to the equation describing heat conduction in a solid with constant thermal conductivity. To obtain an approximation to the complete local temperature, we add a contribution due to convective heat transport when a temperature gradient exists and when the center of mass velocity is nonzero. If the temperature gradient is zero, convective flow will produce no net transfer of heat through any fixed volume element. When a nonzero temperature gradient does exist, the convective contribution to the local temperature is proportional to the magnitude of the velocity. Accordingly, we write

$$T(z,t) = T^*(z,t) + b\, u_z(z,t)\, \frac{\partial T^*}{\partial z}(z,t), \qquad (C.5)$$

where b is a proportionality constant which must be chosen to make Eq. (C.5) satisfy Eq. (C.1). When Eq. (C.5) is inserted into Eq. (C.1) and Eq. (C.4) is subtracted, there remains

$$\begin{aligned} b\,\frac{\partial T^*}{\partial z}\,\frac{\partial u_z}{\partial t} + b\,u_z\,\frac{\partial}{\partial t}\left(\frac{\partial T^*}{\partial z}\right) &= \frac{\kappa_i}{\rho c_p}\left\{\frac{\partial^2 T^*}{\partial z^2}\right. \\ + b\,\frac{\partial T^*}{\partial z}\,\frac{\partial^2 u_z}{\partial z^2} + b\,\frac{\partial u_z}{\partial z}\,\frac{\partial^2 T^*}{\partial z^2} &+ b\,u_z\,\frac{\partial^3 T^*}{\partial z^3} \\ \left. + b\,\frac{\partial^2 T^*}{\partial z^2}\,\frac{\partial u_z}{\partial z}\right\} &- u_z\,\frac{\partial T^*}{\partial z} - u_z\, b\,\frac{\partial T^*}{\partial z}\,\frac{\partial u_z}{\partial z} \\ - b\,u_z^2\,\frac{\partial^2 T^*}{\partial z^2}\,. & \end{aligned} \qquad (C.6)$$

the quantities in Eq. (C.6) are evaluated at z = 0
t = t_0 (i.e., when $u_z = u_{00}$) we can make use of the
tional relations

$$\left(\frac{\partial u_z}{\partial t}\right)_{0,t_0} = 0 \ ,$$

$$\left(\frac{\partial u_z}{\partial z}\right)_{0,t_0} = 0 \ , \qquad \text{(C.7)}$$

$$\left(\frac{\partial^2 u_z}{\partial z^2}\right)_{0,t_0} = \frac{24\ u_{00}}{a^2} \ ,$$

btain

$$- \frac{\partial}{\partial t}\left[\left(\&n\ \frac{\partial T^*}{\partial z}\right) - \frac{24\ \kappa_i}{a^2 \rho \bar{c}_p} - \frac{(\partial^3 T^*/\partial z^3)}{(\partial T^*/\partial z)} + u_{00}\ \frac{(\partial^2 T^*/\partial z^2)}{(\partial T^*/\partial z)}\right]^{-1}_{\substack{z=0 \\ t=t_0}} ,$$

n is very nearly

$$b = \frac{a^2 \rho \bar{c}_p}{24\ \kappa_i} \ . \qquad \text{(C.8)}$$

APPENDIX D

TEMPERATURE DISTRIBUTION DUE TO HEAT CONDUCTION DURING THE WARMING UP PERIOD

The conductive part T* of the temperature of a
d in a pure thermal diffusion cell during the warming
eriod, when variations in the thermal conductivity
unimportant, satisfies Eq. (3.20):

$$\frac{\partial T^*}{\partial t} = \frac{\kappa_i}{\rho \bar{c}_p} \frac{\partial^2 T^*}{\partial z^2} \quad , \qquad (D.1)$$

$$0 < z < a \,^{\dagger} ,$$

$$t > 0 ,$$

auxiliary conditions

$$T^* = \phi_c (t) \quad , \text{ when } z = 0$$

$$T^* = \phi_h (t) \quad , \text{ when } z = a \qquad (D.2)$$

$$T^* = T_m \quad , \text{ when } t = 0 .$$

ie $K = \kappa_i/(\rho \bar{c}_p)$. (D.3)

---

†Note the limits on the variable z. A transforma-
to $(-a/2 < z < a/2)$ is made at the end of this section.

Let $T^* = r_1 + r_2$, (D.4)

ere

$$\frac{\partial r_i}{\partial t} = K \frac{\partial^2 r_1}{\partial z^2} \quad , \quad 0 < z < a \quad , \quad t > 0 \quad , \tag{D.5}$$

$$r_1 = 0 \quad , \quad \text{when } z = 0 \quad ,$$
$$r_1 = 0 \quad , \quad \text{when } z = a \quad , \tag{D.6}$$
$$r_1 = T_m \quad , \quad \text{when } t = 0 \quad ,$$

d

$$\frac{\partial r_2}{\partial t} = K \frac{\partial^2 r_2}{\partial z^2} \quad , \quad 0 < z < a \quad , \quad t > 0 \quad , \tag{D.7}$$

$$r_2 = \phi_c (t) \quad , \text{ when } z = 0 \quad ,$$
$$r_2 = \phi_h (t) \quad , \text{ when } z = a \quad , \tag{D.8}$$
$$r_2 = 0 \quad , \text{ when } t = 0 \quad .$$

The solution for r_1 is well known to be (see, for ample, Carslaw and Jaeger (1959), p. 96)

$$r_1 = \frac{4T_m}{\pi} \sum_{n=0}^{\infty} \frac{1}{(2n+1)} \sin\left[\frac{(2n+1)\pi z}{a}\right] \exp\left[-\frac{K}{a^2}(2n+1)^2 \pi^2 t\right]. \tag{D.9}$$

To obtain r_2, we use Duhamel's integral formula rtels and Churchill, 1942) which expresses the solution boundary tempeatures ϕ_c (t) and ϕ_h (t) in terms of the ution to the same problem with constant boundary

temperatures T_c and T_h. The formula, as stated in Carslaw and Jaeger, p. 30, (1959) is: "If $v = F(x,y,z,\lambda,t)$ represents the temperature at (x,y,z) at the time t in a solid in which the initial temperature is zero, while its surface temperature is $\phi(x,y,z,\lambda)$, then the solution of the problem in which the initial temperature is zero, and the surface temperature is $\phi(x,y,z,t)$ is given by

$$v = \int_0^t \frac{\partial}{\partial t} F\ (x,y,z,\lambda,t - \lambda)\ d\lambda." \qquad (D.10)$$

In this case the temperature at time t, when the temperature through the fluid at $t = \lambda$ is zero, and the plates are kept at $\phi_1(\lambda)$ and $\phi_2(\lambda)$ from $t = \lambda$ to $t = t$, is given by

$$r_2 = \phi_1(\lambda)\left\{1-\frac{z}{a}-\frac{2}{\pi}\sum_{n=1}^{\infty}\frac{1}{n}\sin\frac{n\pi z}{a}\exp\left[-Kn^2\pi^2(t-\lambda)/a^2\right]\right\} \qquad (D.11)$$

$$+\ \phi_2(\lambda)\left\{\frac{z}{a}+\frac{2}{\pi}\sum_{n=1}^{\infty}\frac{1}{n}\cos(n\pi)\sin\frac{n\pi z}{a}\exp\left[-Kn^2\frac{2}{\pi}(t-\lambda)/a^2\right]\right\}.$$

Hence, when the plate temperatures are $\phi_c(t)$ and $\phi_h(t)$, we obtain

$$r_2 = \int_0^t [\phi_c(\lambda)\frac{\partial}{\partial t}F_1(z,t-\lambda) + \phi_h(\lambda)\frac{\partial}{\partial t}F_2(z,t-\lambda)]d\lambda, \qquad (D.12)$$

where

$$F_1(z,t-\lambda) = 1 - \frac{z}{a} - \frac{2}{\pi}\sum_{n=1}^{\infty}\frac{1}{n}\sin\frac{n\pi z}{a}\exp[-Kn^2\pi^2(t-\lambda)/a^2] \qquad (D.13)$$

d where

$$(z,t-\lambda) = \frac{z}{a} + \frac{2}{\pi} \sum_{n=1}^{\infty} \frac{1}{n} \cos(n\pi) \sin\left(\frac{n\pi z}{a}\right) \exp$$

$$[-Kn^2\pi^2(t-\lambda)/a^2] \quad . \tag{D.14}$$

ıus,

$$r_2 = \frac{2k\pi}{a^2} \sum_{n=1}^{\infty} n \exp\left[-Kn^2\pi^2 t/a^2\right] \sin\left(\frac{n\pi z}{a}\right) I \ , \tag{D.15}$$

ıere

$$I = \int_0^t \exp\left[Kn^2\pi^2\lambda/a^2\right] \left[\phi_c(\lambda) - (-1)^n \phi_h(\lambda)\right] d\lambda \ . \tag{D.16}$$

The final solution for T* is the sum of Eqs. (D.9) nd (D.15). This solution, however, was obtained for < z < a. In order to express the equivalent solution or -a/2 < z < a/2, we replace z in the above equations by z + a/2) so that now -a/2 < z < a/2. The result is

$$T^* = r_1 + r_2 \ , \tag{D.17}$$

$$_1 = \frac{4T_m}{\pi} \sum_{n=0}^{\infty} \frac{1}{(2n+1)} \sin\left[(2n+1)\pi\left(\frac{z}{a} + \frac{1}{2}\right)\right] \exp$$

$$[-K(2n+1)^2\pi^2 t/a^2] \ , \tag{D.18}$$

$$_2 = \frac{2k\pi}{a^2} \sum_{n=1}^{\infty} n \sin\left[n\pi\left(\frac{z}{a} + \frac{1}{2}\right)\right] I \exp\left[-Kn^2\pi^2 t/a^2\right] , \tag{D.19}$$

$$I = \int_0^t \exp\left[kn^2\pi^2\lambda/a^2\right] \left[\phi_c(\lambda) - (-1)^n \phi_h(\lambda)\right] d\lambda \ . \tag{D.20}$$

APPENDIX E

PERTURBATION SOLUTION FOR THE STEADY TEMPERATURE DISTRIBUTION

At the thermal steady state, defined by the vanishing f $(\partial T/\partial t)$, the temperature must satisfy the second order ifferential equation (3.25):

$$\frac{d}{dz}\left[\kappa\ (z)\ \frac{dT}{dz}\right] = 0\ ,\ \frac{a}{2} < z < \frac{a}{2}\ , \qquad (E.1)$$

nd the boundary conditions:

$$\begin{aligned} T\ (a/2) &= T_m + \Delta T/2\ , \\ T\ (-a/2) &= T_m - \Delta T/2\ . \end{aligned} \qquad (E.2)$$

The purpose of the present treatment is to take ccount of the temperature and composition dependences of hermal conductivity. We use the following perturbation xpansion:

$$\kappa = \kappa_0\ (1 + \varepsilon k_1 z + \varepsilon^2 k_2 z^2 + \ldots + \varepsilon^n k_n z^n + \ldots)\ , \qquad (E.3)$$

hich defines the quantities k_n. κ_0 is the value of κ t the center of the cell, and ε is an ordering parameter hich does not vary. We next substitute Eq. (E.3) into q. (E.1) along with the formal solution

$$T = T_0 + \varepsilon T_1 + \varepsilon^2 T_2 + \ldots , \qquad (E.4)$$

in which the subscripts denote the order of the solution. The zeroth order solution is obtained by neglecting all terms containing ε. Integration yields directly

$$T_0 = \frac{c_0}{\kappa_0} z + c_0' \quad . \qquad (E.5)$$

The integration constants c_0 and c_0' can be found by imposing the boundary conditions

$$\begin{aligned} T_0\ (a/2) &= T_m + \frac{\Delta T}{2} = T_h \quad , \\ T_0\ (-a/2) &= T_m - \frac{\Delta T}{2} = T_c \quad . \end{aligned} \qquad (E.6)$$

It follows that

$$c_0 = \kappa_0\ \Delta T/a \ , \qquad (E.7)$$

$$c_0' = T_m \quad . \qquad (E.8)$$

Thus, the zeroth order solution is, as expected,

$$T_0 = T_m + \frac{\Delta T}{a} z \quad . \qquad (E.9)$$

We repeat the procedure, this time retaining only terms with powers of ε less than two. The equation which immediately appears is

$$T_1 + k_1 \frac{\Delta T}{a} \frac{z^2}{2} = \frac{c_1}{\kappa_0} z + c_1' \ . \qquad (E.10)$$

According to Eqs. (E.2), (E.4), and (E.6), the boundary conditions are

$$T_1 \ (a/2) = 0 \ , \qquad T_1 \ (-a/2) = 0 \ . \tag{E.11}$$

Thus,

$$c_1 = 0 \ , \tag{E.12}$$

$$c_1' = k_1 \frac{\Delta T}{a} \frac{a^2}{8} \ , \tag{E.13}$$

and the first order solution is

$$T_1 = k_1 \frac{\Delta T}{a} \left(\frac{a^2}{8} - \frac{z^2}{2}\right). \tag{E.14}$$

The quantity k_1 is given by

$$k_1 = \left(\frac{\partial \ell n \ \kappa}{\partial T}\right)_{w_1} \left(\frac{dT}{dz}\right)_0 + \left(\frac{\partial \ell n \ \kappa}{\partial w_1}\right)_T \left(\frac{dw_1}{dz}\right)_0 \ , \tag{E.15}$$

where the zeroth-order solutions for $(dT/dz)_0$ and $(dw_1/dz)_0$ must be used.

Higher order solutions for the steady tempeature distribution are obtained by successive iterations of the above procedure. The complete solution through terms of order ε^2 is

$$T = T_m + \frac{\Delta T}{a}\left[z + \varepsilon k_1\left(\frac{a^2}{8} - \frac{z^2}{2}\right) + \varepsilon^2\left(k_2 - k_1^2\right)\left(\frac{a^2 z}{12} - \frac{z^3}{3}\right)\right] + O\left(\varepsilon^3\right) \tag{E.16}$$

erms of order ε^3 and greater involve third and higher erivatives of thermal conductivity and products of erivatives which are extremely small. At the thermal teady state the correction f(z) to the temperature gra- ient is

$$f(z) = \frac{dT}{dz} - \frac{\Delta T}{a} = \frac{\Delta T}{a}\left[-\varepsilon k_1 z + \varepsilon^2\left(k_2 - k_1^2\right)\left(\frac{a^2}{12} - z^2\right)\right] + O\left(\varepsilon^3\right) \tag{E.17}$$

t is obviously advantageous to make all measurements at = 0, since deviations of the temperature distribution here are of second and higher order.

APPENDIX F

PERTURBATION SOLUTION FOR THE STEADY STATE COMPOSITION DISTRIBUTION

At the staedy state of a pure thermal diffusion experiment the diffusion flux j_{1z} vanishes, and we have from Eq. (3.34)

$$\frac{dw_1}{dz} = \frac{\alpha_1 w_1 w_2}{T} \frac{dT}{dz} \tag{F.1}$$

To take account of the variation with temperature and composition of the quantity $(\alpha_1 w_1 w_2/T)$ we introduce the expansion

$$\frac{\alpha_1 w_1 w_2}{T} \equiv \mathcal{S} = \sum_{n=0}^{\infty} \varepsilon^n s_n z^n \quad , \tag{F.2}$$

where ε is an ordering parameter, and where

$$s_n = \frac{1}{n!} \left(d^n \mathcal{S}/dz^n\right)_0 \tag{F.3}$$

By the chain rule for differentiation we have, for example,

$$s_1 = \left(\frac{\partial \mathcal{S}}{\partial T}\right)_{w_1} \frac{dT}{dz}_0 + \left(\frac{\partial \mathcal{S}}{\partial w_1}\right)_T \left(\frac{dw_1}{dz}\right)_0 \quad , \tag{F.4}$$

where the zeroth-order solutions for $(dT/dz)_0$ and $(dw_1/dz)_0$ must be used. The temperature gradient is given by Eq. (E.17):

$$\frac{dT}{dz} = \frac{\Delta T}{a} \left[1 - \varepsilon k_1 z + \varepsilon^2 (k_2 - k_1^2) \left(\frac{a^2}{12} - z^2\right)\right] + O(\varepsilon^3). \qquad \text{(E.17)}$$

Due to the nature of the perturbation approach, the formal solution is

$$w_1 = w_{1,0} + \varepsilon\, w_{1,1} + \varepsilon^2\, w_{1,2} + \ldots , \qquad \text{(F.5)}$$

where the second subscripts denote the order of the solution.

A sufficient boundary condition for Eq. (F.1) is

$$\int_{-\frac{a}{2}}^{\frac{a}{2}} w_1 \, dz = a\, w_1^o \qquad , \qquad \text{(F.6)}$$

which merely expresses the fact that the average composition does not change from w_1^o during an experiment.

As in Appendix E we first neglect all terms containing ε explicitly. We obtain

$$w_{1,0} = s_0 \frac{\Delta T}{a} z + c_0 \, . \qquad \text{(F.7)}$$

The value of the integration constant follows from Eq. (F.6) and

$$\int_{-\frac{a}{2}}^{\frac{a}{2}} w_{1,0} \, dz = a\, w_1^o \, . \qquad \text{(F.8)}$$

The zeroth order solution is

$$w_{1,0} = w_1^o + \varepsilon_0 \frac{\Delta T}{a} z \ , \qquad \text{(F.9)}$$

where

$$\varepsilon_0 = \frac{(\alpha_1)_0 \ w_1^o \ (1-w_1)^0}{T_m} \ . \qquad \text{(F.10)}$$

Repeated application of the same procedure through successively higher orders of ε gives

$$w_1 = w_1^o + \frac{\Delta T}{a} \left\{ \left[\varepsilon_0 \ z + \varepsilon (\varepsilon_1 - k_1 \varepsilon_0) \left(\frac{z^2}{2} - \frac{a^2}{24} \right) \right] \right.$$
$$\left. + \varepsilon^2 \left[\varepsilon_0 (k_2 - k_1^2) \left(\frac{a^2 z}{12} - \frac{z^3}{3} - \frac{a^3}{48} \right) - (\varepsilon_1 k_1 + \varepsilon_2) \frac{z^3}{3} \right] \right\}$$
$$+ O(\varepsilon^3) \qquad \text{(F.11)}$$

Higher order terms involve third and higher derivatives of κ and S and products of first and second derivatives which are extremely small.

APPENDIX G

THEORY OF THE WAVEFRONT
SHEARING INTERFEROMETER

The wavefront shearing interferometer of Bryngdahl (1963) provides a comparison of the wavefront with a sheared image of itself. The method utilizes birefrigence interferences. We can describe the vertical component of the light wave entering the cell by a transversal electric field strength amplitude vector referred to the basic system of vectors $\underset{\sim}{\xi}$ and $\underset{\sim}{\eta}$ and to the object plane by

$$\underset{\sim}{U} = (\underset{\sim}{\xi} + \underset{\sim}{\eta})\ (A/\sqrt{2})\ e^{iky} , \qquad (G.1)$$

where $k = 2\pi/\lambda$, λ is wavelength, and A is the scalar amplitude. If we denote the refractive index of the substance in the cell by $n(x,y,z)$ and the thickness of the cell by h, then the optical path through the cell will be

$$W\ (x,z) = \int_0^h n\ (x,y,z)\ dy . \qquad (G.2)$$

The amplitude vector of the light leaving the cell, referred to the object plane, will therefore be

$$\underset{\sim}{U} = (\underset{\sim}{\xi} + \underset{\sim}{\eta})(A/\sqrt{2})\ \exp\ \{ik[W\ (x,z) + y_0]\} , \qquad (G.3)$$

where y_0 is an arbitrary reference plane.

Next, the light passes through a lens system, the purpose of which is to effect a scale reduction in order to keep down the dimensions of the beam splitters. Denoting the reduction factor by r, we have to introduce a new function

$$w(rx,rz) = W(x,z) \ , \qquad (G.4)$$

and we can then write the amplitude vector of the wave entering the first beam splitter Q_1 in the following way, as referred to the first image plane:

$$\underset{\sim}{U} = (\underset{\sim}{x} + \underset{\sim}{z}) \left(\frac{A}{r\sqrt{2}} \right) \exp \{ik[w(x,z) + y_1]\} \ , \qquad (G.5)$$

since the laser light is polarized in the $\underset{\sim}{\xi}$ direction. New constants $y_1, y_2, y_3, \ldots$ are introduced after each transformation.

In passing Q_1, the component of $\underset{\sim}{U}$ in the $\underset{\sim}{x}$ direction is displaced downward by an amount $\frac{1}{2} b_1$ and becomes polarized in the $\underset{\sim}{z}$ direction, while the component of $\underset{\sim}{U}$ in the $\underset{\sim}{z}$ direction is displaced upward by the same amount and polarized in the $\underset{\sim}{x}$ direction. See Fig. (4.5). After Q_1 we have, therefore, the following amplitude vector, also referred to the first image plane,

$$\begin{aligned} \underset{\sim}{U} = {} & \underset{\sim}{x}(A/r\sqrt{2}) \exp \{ik[w(x,z + b_1/2) + y_2 + \chi/2]\} \\ & + \underset{\sim}{y}(A/r\sqrt{2}) \exp \{ik[w(x,z - b_1/2) + y_2 - \chi/2]\} \end{aligned} \qquad (G.6)$$

Referred to the second image plane, the light leaving Q_1 is described by the vector

$$\underset{\sim}{U} = \underset{\sim}{x}(A/rm\sqrt{2}) \exp\{ik[V(x,z + \frac{mb_1}{2}) + y_3 + \chi/2]\} + \underset{\sim}{y}(A/rm\sqrt{2}) \exp\{ik[V(x,z - \frac{b_1 m}{2}) + y_3 - \chi/2]\}. \quad (G.7)$$

We have introduced the quantity χ, the path difference between the two sheared wavefronts, related to a possible tilting angle of the beam splitter. When we refer to the second image plane, we must introduct the magnification factor m and the new function

$$V(mx,mz) = w(x,z) . \quad (G.8)$$

On passing the second beam splitter Q_2, there is introduced first a lateral displacement and second an optical path displacement Δ according to

$$\Delta = b_1 \frac{z}{d} \cos \psi , \quad (G.9)$$

where d is the distance between the focal plane of the lens L5 and the second image plane, and ψ is the angle between the crystal surface normal and the entering ray.

The expression for the wave emerging from Q_2, referred to the second image plane is

$$\underset{\sim}{U} = \underset{\sim}{x}(A/rm\sqrt{2}) \exp\{ik[V(x - \frac{b_1}{2}, z - \frac{mb_1}{2})$$

$$+ \Delta/2 + y_4 - \chi'/2]\} + \underset{\sim}{y}(A/rm\sqrt{2}) \cdot$$

$$\cdot \exp\{ik[V(x + \frac{b_1}{2}, z + \frac{mb_1}{2})$$

$$\Delta/2 + y_4 + \chi'/2] \qquad (G.10)$$

After the beam passes the polarizer, the amplitude is

$$U = \underset{\sim}{U} \cdot (\underset{\sim}{x} + \underset{\sim}{z})/\sqrt{2}$$

$$U = (A/2rm) \exp\{ik[V(x - b_1/2, z - mb_1/2)$$

$$+ \Delta/2 + y_5 - \chi'/2]$$

$$+ (A/2rm) \exp\{ik[V(x + b_1/2, z + mb_1/2)$$

$$- \Delta/2 + y_5 + \chi'/2]\} . \qquad (G.11)$$

Hence, the image intensity becomes

$$I = |U|^2 = \frac{1}{2}(\frac{A}{rm})^2 (1 + \cos\phi) \qquad (G.12)$$

where

$$\phi = k[V(x + b_1/2, z + mb_1/2) - V(x - b_1/2, z - mb_1/2)$$

$$- \Delta + \chi'] .$$

Destructive interference is obtained for $\phi = 2n\pi$ ($n = 0,1,\ldots$) with crossed polarizers. The expression

for Δ can be written

$$\Delta = b_1 \frac{x}{d} [1 - O(\psi^2)] , \qquad (G.13)$$

and the equations of the curves of constant intensity (constant ϕ) can be written

$$x = dV'_x (x + \theta_3 b_1/2, z + \theta_4 mb_1/2) + mdV'_z (x + \theta_3 b_1/2, z + \theta_4 mb_1/2) - \frac{h}{b_1} [\frac{\phi}{k} - \chi'] + x O(\psi^2) , \qquad (G.14)$$

where $-1 < \theta_3 < 1$,

and $-1 < \theta_4 < 1$.

If the substance in the cell has a one-dimensional refractive index gradient (n constant in the x and y directions), then Eq. (G.14) becomes

$$x = mdV'(z) + \theta_4 (m^2 db_1/2) V''(z + \theta_4\theta_6 mb_1/2) - \frac{d}{b_1} [(\frac{\phi}{k}) - \chi'] + O(\psi^2) , \qquad (G.15)$$

where $-1 < \theta_4 < 1$

$0 < \theta_6 < 1$.

Now,

$$V(z) = w(\frac{z}{m}) = W(\frac{z}{mr}) ,$$

whence

$$V'(z) = \frac{1}{mr} W'\left(\frac{z}{mr}\right) \quad , \tag{G.16}$$

and

$$V''(z) = \left(\frac{1}{m^2 r^2}\right) W''\left(\frac{z}{mr}\right) .$$

Thus, the final equation is

$$x = \frac{d}{r} W'\left(\frac{z}{mr}\right) + \theta_4 \frac{db_1}{2r^2} W'' \left(\frac{z}{mr} + \theta_4\theta_6 \frac{b_1}{2r}\right)$$

$$- \frac{d}{b_1} \left(\frac{\phi}{k} - \chi'\right) + x\, O(\psi^2) \quad , \tag{G.17}$$

where $\quad -1 < \theta_4 < 1 ; \quad 0 < \theta_6 < 1 .$

According to Eq. (G.2),

$$W(z) \int_0^h n(z)\, dy = hn(z) \quad , \tag{G.18}$$

for a one-dimensional variation in the refractive index. Thus, we obtain the equations

$$x = A \left(\frac{\Delta n}{\Delta z}\right) + B \quad , \tag{G.19}$$

where now

$$A = hd/b_1 \quad ,$$

$$\Delta z' = b_1/r \quad ,$$

and

$$B = -\frac{d}{b_1}\,[\phi/k) - \chi'] \ .$$

The quantity $z' = \frac{z}{mr}$ is the height coordinate in the object plane, while z refers to the second image plane.

It is seen that an increase in ϕ of 2π , which means passing from one interference fringe to the next, changes x by the same amount as a change in $\Delta n/\Delta z'$ amounting to λ/h.

As appears from the above derivation, precise adjustment of the crystal plates is not critical. This makes the method very easy to adjust and insensitive to mechanical vibrations.

It is apparent that there are two sources of systematic error. One is the term

$$\theta_4\ db_1 h\ n''\ (z' + \theta_4\theta_6\ b_1/2r)/(2r^2) \ ,$$

in Eq. (G.17), which is the difference between the difference quotient $\Delta n/\Delta z'$ actually registered by the method and the corresponding differential quotient dn/dz' which one wishes to obtain. The magnitude of this error can be reduced at will by making $\Delta z' = b_1/r$ sufficiently small. In practice b_1 is fixed and r chosen to optimize sensitivity and accuracy.

The second source of error, inherent in the term $O\ (\psi^2)$, is very small. With suitable dimensioning, $\psi < 10^{-2}$, and the relative error in x will be below 10^{-4}.

APPENDIX H

SUBROUTINE MULTREG

MULTREG is a FORTRAN subroutine, written by J. L. Bartelt (1966), which can be used to obtain a polynomial expression for a number of experimental data points. One particular advantage is its multidimensionality. For example, when provided with a set of measured refractive indices of a substance obtained at various temperatures, concentrations, and wavelengths, the subroutine permits calculation of the coefficients of various powers of the temperature, concentration, wavelength, and cross terms appearing in a prescribed polynomial.

The method consists of a multiple regression analysis, the theory of which is described by Ralston and Wilf (1960). The subroutine can be called from a FORTRAN program by means of the statement

CALL MULTREG (X,W,N,M,NPLUS,A,SIGMA,B,SB,Y,DEV,IPRINT).

The parameters which must be specified are:

(1) N = the number of independent variables plus one dependent variable,

(2) M = the number of data pairs,

(3) NPLUS = N + 1,

(4) W(I) = 1.0, I = 1, ..., M,

(5) X(N,M) = the variables arranged so that X(J,K), J = 1, ..., N - 1, are independent variables, and X(J,K), J = N, are dependent variables.

(6) IPRINT = a parameter equal to zero if printing of intermediate results is not desired and equal to unity if it is.

For example, to obtain a fourth order polynomial expression in terms of temperature for the density of a fluid from 20 data pairs, write

$$X(1,K) = T(K)$$
$$X(2,K) = T^2(K)$$
$$X(3,K) = T^3(K)$$
$$X(4,K) = T^4(K)$$
$$X(5,K) = \rho(K),\ K = 1, \ldots, 20.$$

In this example,

$$N = 5$$
$$M = 20,$$
$$NPLUS = 6.$$

When MULTREG is used, the following dimension statement must appear in the calling program:

```
DIMENSION X(N,M), W(M), A(N + 1, N + 1),
  SIGMA (N + 1), B(N + 1), SB (N + 1), Y(M), DEV(M),
```

where the correct numbers are inserted for the letters. When MULTREG is to be called more than once in the same main program, the two-dimensional arrays, X and A, must be the same size for each calling, i.e., N and M must not change under any one dimension statement.

The output of the subroutine consists of a list of the coefficients of the variables X(J,K), J = 1, ..., N - 1, plus any constant term which appears in the polynomial. Also available are calculated standard errors of each of the coefficients.

Listing of MULTREG

```
 SUBROUTINE MULTREG(X,W,N,M,NPLUS,A,SIGMA,B,SB,Y,DEV,IPRINT)
 DIMENSION X(N,M),W(M),A(NPLUS,NPLUS),SIGMA(NPLUS)
 DIMENSION B(NPLUS),SB(NPLUS),Y(M),DEV(M)
 FORMAT(10X,*CONSTANT*,20X,*VARIABLE*,20X,*COEFFICIENT*,
120X,*STD ERROR OF COEFF*)
 FORMAT(1HO,5X,E14.6)
 FORMAT(36X,I14.16X,E14.6,16X,E14.6)
 FORMAT(1H-,45X,*PREDICTED VS. ACTUAL RESULTS*,/,24X,*OBS. NO.*,18X
1,*ACTUAL*,23X,*PREDICTED*,21X,*DEVIATION*,/)
 FORMAT(26X,I4,16X,E14.6,16X,E14.6,16X,E14.6)
 FORMAT(* VARIABLE LEAVING =*,I3,/,* F LEVEL =*,E14.6)
 FORMAT(* VARIABLE ENTERING =*,I3,/,* F LEVEL =*,E14.6)
 FORMAT(* STANDARD ERROR OF Y =X,E14.6)
 NLES=N-1
 F1=0.0
 F2=0.0
 AMIN=1.0E200
 TOL=0.0001
 DO 1 I=1,NPLUS
 DO 1 J=1,NPLUS
 A(I,J)=0.0
 DO 100 I=1,M
 A(N+1,N+1)=W(I)+A(N+1,N+1)
 DO 100 J=1,N
 A(N+1,J)=A(N+1,J)+/(I)*X(J,I)
 DO 100 K=J,N
 A(J,K)=A(J,K)+W(I)*X(J,I)*X(K,I)
 DO 101 I=1,N
 AN(+1,I)=A(N+1,I)/A(N+1,N+1)
 DO 301 I=1,N
 DO 301 J=I,N
 A(I,J)=A(I,J)=A(N+1,N+1)*A(N+1,I)*A(N+1,J)
 DO 102 I=1,N
 SIGMA(I)=SQRT(A(I,I))
 A(I,I)=1.0
 DO 103 I=1,NLES
 ID=I+1
 DO 103 J=ID,N
 A(I,J)=A(I,J)/(SIGMA(I)*SIGMA(J))
 A(J,I)=A(I,J)
 PHI=A(N+1,N+1)=1.0
 VMIN=1.0E200
 VMAX=0.0
 NMIN=0
 NMAX=0
 A(N,N+1)=SIGMA(N)*SQRT(A(N,N)/PHI)
```

```
PRINT 211,A(N.N+1)
IF(A(N,N+1).LE.AMIN)31.30
F1=FX    + TOL
F2=FX +TOL
GO TO 32
AMIN=A(N,N+1)
DO 104 J=1,NLES
B(J)=0.0
I=1
IF(A(I,I).GT.TOL)7,14
A(I,N+1)=A(I,N)*A'N,I)/A(I,I)
IF(A(I,N+1))11,14,9
IF(A(I,N+1).GT.VMAX)10,14
VMAX=A(I,N+1)
NMAX=I
GO TO 14
B(I)=A(I,N)*SIGMA(N)/SIGMA(I)
SB(I)=A(N,N+1)*SQRT(A(I,I))/SIGMA(I)
IF(ABS(A(I,N+1)).LT.ABS(VMIN))13,14
VMIN=A(I,N+1)
NMIN=I
IF(I.EQ.NLES)16,15
I=I+1
GO TO 6
BO=A(N+1,N)
DO 105 I=1,NLES
BO=BO-B(I)*A(N+1,I)
IF(A(N,N))500.19
FX=ABS(VMIN*PHI/A(N,N)
IF(FX.LE.F2)18,19
K=NMIN
PHI=PHI+1.0
PRINT 209,K,FX
GO TO 21
IF(A(N,N)-VMAX)400,401
FX=VMAX*(PHI-1.0)/(A(N,N)-VMAX)
IF(FX.GT.F1)20,22
IF(PHI-1.0)20,22
K=NMAX
PHI=PHI-1.0
PRINT 210,K,FX
DO 113 I=1,N
DO 113 J=1,N
IF(I.EQ,K.OR,J.EQ,K)GO TO 113
A(I,J)=(A(K,K)*A(I,J)-A(I,K)*A(K,J))/A(K,K)
CONTINUE
DO 313 I=1,N
DO 313 J-1,N
IF(I.NE,K,AND,J,EQ,K)108,109

A(I,K)=-A(I,K)/A(K,K)
IF(I.EQ,K,AND,J.NE,K)110,313
```

```
A(K,J)=A(K,J)/A(K,K)
CONTINUE
A(K,K)=1.0/A(K,K)
GO TO 5
DO 115 J=1,M
Y(J)=BO
DO 114 I=1,NLES
Y(J)=Y(J)+B(I)*X(I,J)
DEV(J)=X(N,J)-Y(J)
PRINT 201
PRINT 202,BO
DO 117 I=1,NLES
IF(A(I,N+1))116,117,117
PRINT 203,I,B(I),SB(I)
CONTINUE
IF(IPRINT.EQ,O)GO TO 1599
PRINT 206
PRINT 207,(I,X(N,I),Y(I),DEV(I),I=1,M)
CONTINUE
RETURN
END
```

APPENDIX I

SUBROUTINE MINIMIZE[†]

The subroutine described herein was written in FORTRAN for use with a CDC3600 digital computer. It is designed to minimize a function of up to ten variables by choosing conjugate search directions. This assures that a quadratic function of n variables will be minimized in at most n steps. (If the number of variables exceeds ten, the program must be redimensioned.) For a theoretical description, see the article by Powell (1964), "An Efficient Method for Finding the Minimum of a Function Without Calculating Derivatives."

There are three considerations for use of the subroutine which must be tailored to the individual purpose.

1. Calling statement. The subroutine may be called from a FORTRAN program by program by means of the following statement:

```
CALL MINIMIZE (X,N,EPS,ENDNORM,ITMAX,IPRINT,SUCCESS).
```

[†]Both the subroutine and this description were written by J. L. Bartelt (1967).

2. Parameters.

   a. X = a linear array dimensioned for the number of variables. The program should be called with a set of initial guesses for the variables stored in X. The solution will be returned in X.

   b. N = the number of variables (less than ten).

   c. EPS = a convergence criterion parameter. The change in each variable from the last step is compared with EPS times the current value, and convergence is assumed if the change is smaller.

   d. ENDNORM = a convergence criterion parameter. The function value at the current point must be less than ENDNORM to obtain convergence.

   e. ITMAX = the maximum desired number of iterations.

   f. IPRINT = an option. If IPRINT equals unity, the program will cause the results to be printed. If IPRINT is zero, no results will be printed.

   g. SUCCESS = a logical variable to indicate convergence. If SUCCESS is unity, the process has converged. If SUCCESS is zero, the method has failed to converge, and a statement will be written to indicate the reason for termination.

3. Required subroutines.

   a. QUADMIN. This is a routine required by MINIMIZE and is furnished with the deck.

b. FNORM. This is a function subroutine where the function to be minimized is placed. It must have the following form:

```
FUNCTION FNORM (X,N)
DIMENSION X(N)
   .
   .
   .
     (any necessary calculations)
   .
   .
   .
   .
   .
   .
FNORM = f(X(1),X(2), ..., X(N))
RETURN
END
```

Where f is the function to be minimized, and X and N have their previous meanings.

For the purpose of analyzing data we choose FNORM to contain a function which is the sum of squares of the deviations of experimental points from some analytical function. The actual FNORM used is shown in the listing of ALPHA in Appendix J.

Listing of MINIMIZE and QUADMIN

```
SUBROUTINE MINIMIZE(X,N,EPS1,EPS2,ITMAX,IPRINT,SUCCESS)
DIMENSION X(N),XO(10),Y(10),P(10,10)
COMMON/MIN/LASTNORM,KOUNT
TYPE REAL NORM, LASTNORM
TYPE LOGICAL SUCCESS
IF(N.GT.10)GO TO 5000
ITER=0
KOUNT=0
DO1 I=1,N
XO(I)=X(I)
P(I,I)=0.1*XO(I)
IF(XO(I).LT.(1.0E-7))P(I,I)=0.01
L=I+1
DO 1 J = L,N
P(I,J)=P(J,I) =0.0
LASTNORM = FNORM(X,N)
KOUNT=KOUNT+1
NM=N-1
IF(IPRINT)PRINT 100,LASTNORM,X
FORMAT(1H1,*THE INITIAL VALUES ARE*,//,5X,*NORM*,10X,*XO
   (1).....XO(N)*,//,
1(N)*,//,9E15.6,/,(15X,8E15.6)
IF(IPRINT)PRINT 110
FORMAT(1H6,*ITER INC*,5X,*NORM*,10X,*X(1).....X(N)*,//)
ITER =ITER+1
IF(ITER.GT.ITMAX)GO TO 3000
DELTA=1.0E-100
M=0
F1=LASTNORM
DO 2000 I=1,N
DO 2 J=1,N
Y(J)=P(J,I)
CALL QUADMIN(X,Y,NORM,N)
IF(IPRINT)PRINT 101,ITER,I,NORM,X
FORMAT(2I5,8E15.6,/,(25X,7#15.6)
IF((LASTNORM-NORM).GE.DELTA)3,4
M=I
DELTA = LASTNORM-NORM
LASTNORM = NORM
CONTINUE
F2=NORM
IF(ITER.GT.N)15,16
IF(NORM.GT.EPS2)16,17
DO 18 I=1,N
IF(ABS(X(I)-XO(I)).GT.ABS(EPS1*X(I)))16,18
CONTINUE
```

```
      GO TO 4000
      DO 5 I=1,N
      Y(I)=2.0*X(I)-XO(I)
    5 F3=FNORM(Y,N)
      KOUNT=KOUNT+1
      IF(F3.GE.F1).OR.(((F1-2.0*F2+F3)*(F1-F2-DELTA)**
     12).GE.(DELTA*((F1-F2)**2)/2.0)))6,7
    6 DO 8 I=1,N
      XO(I)=X(I)
      GO TO 1000
    7 DO 9 I=1,N
    9 Y(I) =X(I)-XO(I)
      CALL QUADMIN(X,Y,NORM,N)
      DO 10 I=1,N
      XO(I)=X(I)
      DO 11 I=M,NM
      DO 11 J=1,N
   11 P(J,I)=P(J,I+1)
      DO 12 I=1,N
   12 P(I,N)=Y(I)
      LASTNORM = NORM
      GO TO 1000
 1000 PRINT 102
  102 FORMAT(1H4,*THE MAXIMUM NUMBER OF ITERATIONS HAS BEEN EXCEEDED*)
      SUCCESS =0
      PRINT 5004,KOUNT
      RETURN
 1001 PRINT 103,ITER
  103 FORMAT(1H4,*THE PROCESS HAS CONVERGED IN*,I6,3X*ITERATIONS*)
      SUCCESS =1
      PRINT 5004,KOUNT
 5004 FORMAT(1H-,*THE NUMBER OF FUNCTIONAL EVALUATIONS WAS*,I10)
      RETURN
 4000 PRINT 5001
 5001 FORMAT(1H4,*MORE THAN 10 VARIABLES, PLEASE REDIMENSION,*)
      SUCCESS=0
      RETURN
      END
      SUBROUTINE QUADMIN(X,P,NORM,N)
      DIMENSION PHI(3),VT(3),X(N),P(N)
      COMMON/MIN/LASTNORM,KOUNT
      TYPE INTEGER UPPER
      TYPE REAL NORM ,LASTT, LASTNORM
      DO 9 I=1,N
    9 X(I) =X(I) +P(I)
      LASTT = 1.0
      T=0.0
      ITER =0
   10 ITER = ITER + 1
      NORM = FNORM(X,N)
```

```
 KOUNT=KOUNT+1
 IF((ABS(T-LASTT).GT.(.01*ABS(T)).AND.ITER.LE.20).OR.(ITER.EQ.2))
111,12
 IF(ITER.EQ.1)13,14
 VT(1)=0.0
 VT(3) =1.0
 PHI(1) =LASTNORM
 PHI(3) =NORM
 IF(PHI(1).GT.PHI(3))1,2
 T=2.0
 LOWER=1
 MID=3
 UPPER=2
 K=2
 GO TO 1000
 T=1.0
 LOWER=2
 MID=1
 UPPER=3
 K=2
 GO TO 1000
 PHI(II)=NORM
 XW =VT(2)-VT(3)
 XX=VT(3)-VT(1)
 XY =VT(1)-VT(2)
 XW =-(PHI(1)*XW+PHI(2)*XX+PHI(3)*XY)/(XW*XX*XY)
 XX=(PHI(1)-PHI(2))/XY-XW*(VT(1)+VT(2))
 LASTT =T
 IF(XW.GT.0.0)15,16
 T=-XX/(2.0*XW)
 GO TO 19
 IF(PHI(UPPER).GT.PHI(LOWER))17,18
 T=3.0*VT(LOWER)-2.0*VT(MID)
 GO TO 19
 T=3.0*VT(UPPER)-2.0*VT(MID)
 IF(T.GT.VT(UPPER))20,21
 I=LOWER
 LOWER =MID
 MID = UPPER
 UPPER =I
 K=UPPER
 GO TO 1000
 IF(T.LT.VT(LOWER))22,23
 I=UPPER
 UPPER =MID
 MID =LOWER
 LOWER=I
 K=LOWER
 GO TO 1000
```

```
23    IF(T.GT.VT(MID))24,25
24    I=LOWER
      LOWER =MID
      MID=I
      K=MID
      GO TO 1000
25    I = UPPER
      UPPER =MID
      MID=I
      K=MID
1000  II=K
      VT(K)=T
      DO 1001 J=1,N
1001  X(J)=X(J)+(T-LASTT)*P(J)
      GO TO 10
12    IF(NORM.LE.LASTNORM)RETURN
      NORM=LASTNORM
      DO 7 I=1,N
7     X(I)=X(I)-LASTT*P(I)
      RETURN
      END
```

APPENDIX J

PROGRAM ALPHA

This program is designed to permit computerized analysis of the raw data from a pure thermal diffusion experiment and calculation of final results. PROGRAM ALPHA consists of three main segments. In the first, measured values of plate temperatures, liquid densities, and interferometric fringe spacings are read and converted to statements of temperature differences, mean temperatures, initial compositions, and apparatus constants.

The second section utilizes SUBROUTINE MINIMIZE to fit a smooth function of three variables to the measured values of fringe position versus time. In the third section, the results of the previous sections are used to calculate values for the thermal diffusion factor and the ordinary diffusion coefficient. A written record is made of all of the information from each experiment. A listing of the program follows.

In addition to what is shown here, the deck must also contain subroutines MINIMIZE and QUADMIN and the following data cards:

(1) a card specifying the number of experiments to to analyzed;

(2) a card for each experiment stating the number of data points in that experiment, the code number of the experiment, the initial liquid density, the fringe spacing, and the final mean temperature;

(3) a card for each experiment containing a set of initial guesses for the three variables which are to be determined by MINIMIZE;

(4) a deck of cards for each experiment, each card containing a measured time and a measured fringe position.

The format for each of the cards is shown in the listing below.

Listing of ALPHA

```
PROGRAM ALPHA
DIMENSION X(3),X0(3),Y(3),P(3,3)
DIMENSION A1(64),D12(64),X11(64)
COMMON/A/D(100),T(100),F(100),L
TYPE REAL NN,MUBYW
TYPE REAL KAPPA
TYPE REAL K1
TYPE LOGICAL SUCCESS
E=2.718281828459
PI=3.1415926536
PI3=2./PI**3
RHOBYT=-.00017
BETA=RHOBYT
BETAP=.714
STHREES=0.
STHREE=0.
AH=0.741
FAC=AH*AH/PI/PI
READ 100,NRUNS
DO 1 I=1,NRUNS
G1=0.
KKOUNT=0
READ 101,NUM,RUN,TH,TC,FZ,R,RHO,TF
L=NUM
W10=1.990136-.01505166*RHO-1.53114/RHO
MUBYW=.03342-.021463*W10*(1.-W10)*(5.369606*W10-3.*4.351411*W10
1*W10+4.*3.018563*W10**3)-.021463*(1.-2.*W10)*(1.+2.694803*W10
```

```
 2 CONTINUE
     XO(2)=1./THETA
     IF(KKOUNT.EQ.0) GO TO 51
52 CONTINUE
     IF(KKOUNT.EQ.1) GO TO 55
     S2=.007/ALPHA1P-1./TM
     SSS=NN/W10/W20+.18/ALPHA1P*PXBYW
     FZERO=-TAU*AH*K1*K1/12.
     FONE=-TAU/AH*K1*2.
     FTWO=K1*K1*TAU/AH
     FTHREE=-K1**3*TAU/AH
     TAF=TAU/AH+FZERO
     SONEINF=-SZERO*(S2*TAF+SSS*SZERO*TAF)
     STWOINF=.5*SZERO*(2./TM*S2*TAF*TAF+S2*FONE)
     PLRDS=-BETA*TAF+BETAP*SZERO*TAF+1./DLIT*(-.201*PXBYW*SZERO*TAF
    1+.0258*TAF)*1.E-5
     G11NF=SZERO*FZERO-AH*AH/24.*(TAF*SONEINF+SZERO*FONE)-AH**4/320.
    1*(TAF*STHREES+STWOINF*FONE+SONEINF*FTWO+SZERO*FTHREE)
     CAPFO=AH/48.*AH*G11NF*PLRDS-AH*AH*W10*W20*PAPLTS
     PIO=DLIT
 51 CONTINUE
     IF(KKOUNT.EQ.0) GO TO 53
     DO 3 J=1.NUM
     EMTOT=E**(-T(J)/THETA)
     GRADW=SZERO*TAU/AH*(1.-4./PI*EMTOT)
     GRAD2W=-4.*SZERO*TAU/AH/AH*BB/PI*EMTOT
     SONE=-SZERO*(S2*TAF+SSS*GRADW)
```

```
2*W10-4.351411*W10**3+3.018563*W10**4)
 READ 102,(X0(J),J=1,3)
 TAU=TH-TC
 TM=(TH+TC)/2.
 TM=TM+273.16
 IF(X0(1).GT.0.0)TM=TF+273.16
 A=-3.11E4*R/1.74
 W20=1.-W10
 X10=W10/W20/(1.96953+W10/W20)
 PXBYW=X10/W10+.96953*X10*X10/W10
 DLIT=(1.484-.201*X10+.0258*(TM-298.16))*1.E-5
 KAPPA=2.47E-4-4.57E-7*(TM-293.16)-8.4E-5*W10
 THETA=FAC/DLIT/60.
 ALPHA1P=-1.82+.18*X10+.007*(TM-298.16)
 PP=-ALPHA1P*TAU/TM
 NN=1.-2.*W10
 AA=TAU*RHOBYT
 PCAP=.5*(AA+PP*NN)
 SP = PP
 V1=1.+E**SP
 BB=.5*(TAU*RHOBYT-SP*(1.-2.*W10))
 W1=BB
 W1P=-PI*PI/AH
 GROUP=PI3*V1*(W1P-SP/AH*W1)*E**(-SP/2.)
 DENOM=W10*(1.-W10)*TAU*GROUP*A*MUBYW
 DO 2 J=1,NUM
 READ 103,T(J),D(J)
```

```
      STWO=.5*SZERO*(2./TM*S2*TAF*TAF+S2*FONE+GRAD2W*(NN/W10/W20
     1+.18/ALPHA1P*PXBYW))
      PAPLTS=TAF/TM*(.18*PXBYW*SZERO*TAF+.007*TAF)+ALPHA1P*FONE
     1/TM-ALPHA1P*TAF/TM/TM
      PLRD=-BETA*TAF+BETAP*GRADW+1./DLIT*(-.201*PXBYW*GRADW
     1+.0258*TAF)*1.E-5
      PAPLT=TAF/TM*(.18*PXBYW*GRADW+.007*TAF)+ALPHA1P*FONE/TM
     1-ALPHA1P*TAF/TM/TM
      P20=-P10*ALPHA1P/TM*TAF*(1.-2.*W10)+.0258E-5*TAF-.201E-5*PXBYW
     1*GRADW+P10*(-BETA*TAF+BETAP*GRADW)
      0=P20
      P30=-P10*(1.-2.*W10)*(PAPLT+ALPHA1P*TAF/TM*PLRD)
      P40=P10*(GRAD2W-ALPHA1P*(1.-2.*W10)*GRADW*TAF/TM-W10*W20*PAPLT
     1+GRADW-ALPHA1P*TAF/TM*W10*W20*PLRD)
      G1=CAPFO/P20*(1./THETA*EMTOT+(1.-EMTOT)*(48.*P10/AH/AH-P30))-P40/O
    3 D(J)=D(J)-G1*A*MUBYW
   5? CONTINUE
      CALL MINIMIZE(X0,3,0.0001,0.5,10,1,SUCCESS)
      DEXP=FAC*X0(2)/60.
      IF(ABSF(DLIT-DEXP).GT.0.06E-5) DEXP=DEXP+0.12E-5
      IF(X0(1).GT.0.)X0(1)=-X0(1)
      ALPHA1=-X0(1)*TM/DENOM
   55 CONTINUE
      IF(KKOUNT.EQ.0) GO TO 60
      K1=1./KAPPA*(-4.57E-7*TAU/AH)
      SZERO=ALPHA1P*W10*W20/TM
      G1INFP=-TAU/AH*SZERO*K1*K1*AH*AH/12.
```

```
      ALPHA1=-AH*TM/W10/W20/TAU*(PI*X0(1)/4./A/MUBYW+G1INFP)
      ALPHA1=-ALPHA1
   60 CONTINUE
      PRINT 302,NUM
      PRINT 301,R
      IT=TM
      TR=IT+.16
      ACORR=ALPHA1-.007*(TM-TR)
      IF(KKOUNT.EQ.1)GO TO 54
      ACOR2=ALPHA1
      ACOR3=ACORR
   54 CONTINUE
      KKOUNT=KKOUNT+1
      IF(KKOUNT.EQ.1) GO TO 52
      PUNCH 741,TM,X10,W10,ACOR2,ACOR3,ALPHA1,ACORR,TAU
      PRINT 201
    1 PRINT 202,RUN,TM,W10,X10,TAU,A,MUBYW,DLIT,DEXP,ACOR2,ACOR3,
     1ALPHA1,ACORR
  100 FORMAT(I2)
  101 FORMAT(I2,3X,A3,3F6.3,F5.3,F7.5,F6.3)
  102 FORMAT(F6.2,F4.3,F5.2)
  103 FORMAT(F7.2,F5.2)
  201 FORMAT(1X,*RUN*,5X,*TM*,8X,*W10*,7X,*X10*,6X,*TAU*,
     18X,*A*,9X,*MUBYW*,5X,*DLIT*,9X,*DEXP*,
     17X,*-ALPHA1*,3X,*-ALPHA2*,3X,*-ALPHA3*,3X,*-ALPHA4*)
  202 FORMAT(1X,A3,3X,F7.3,3X,F7.5,3X,F7.5,2X,F6.3,3X,E10.3,3X,
     1F6.4,3X,E10.3,3X,E10.3,4(3X,F7.4))
```

```
301 FORMAT(1X,E12.5)
302 FORMAT(1X,I5)
741 FORMAT(F7.3,7(F7.5))
    END
    FUNCTION FNORM(X,N)
    DIMENSION X(3),Y(3)
    COMMON/A/D(100),T(100),F(100),L
    E=2.7182818459
    SUMSQ=0.
    DO 1 I=1,L
    SUM=0.
    F(I)=X(1)*E**(-X(2)*T(I))+X(3)
  1 SUMSQ=SUMSQ+(F(I)-D(I))**2
    FNORM=SUMSQ
    RETURN
    END
```